

Under the Paperwork Reduction Act of 1995, no persons are required to respond to a collection of information unless it contains a valid OMB control number.

Application Data Sheet 37 CFR 1.76		Attorney Docket Number	10065-509P01US
		Application Number	
Title of Invention	MECHANICAL ANALYSIS WITH HIGH ACCURACY THREE-DIMENSIONAL FINITE ELEMENTS		
<p>The application data sheet is part of the provisional or nonprovisional application for which it is being submitted. The following form contains the bibliographic data arranged in a format specified by the United States Patent and Trademark Office as outlined in 37 CFR 1.76.</p> <p>This document may be completed electronically and submitted to the Office in electronic format using the Electronic Filing System (EFS) or the document may be printed and included in a paper filed application.</p>			

Secrecy Order 37 CFR 5.2

<input type="checkbox"/>	Portions or all of the application associated with this Application Data Sheet may fall under a Secrecy Order pursuant to 37 CFR 5.2 (Paper filers only. Applications that fall under Secrecy Order may not be filed electronically.)
--------------------------	---

Inventor Information:

Inventor 1					Remove	
Legal Name						
Prefix	Given Name	Middle Name	Family Name	Suffix		
	Gautam		Dasgupta			
Residence Information (Select One) <input checked="" type="radio"/> US Residency <input type="radio"/> Non US Residency <input type="radio"/> Active US Military Service						
City	Briarcliff Mnr.	State/Province	NY	Country of Residence i	US	
Mailing Address of Inventor:						
Address 1		69 Oak Road				
Address 2						
City	Briarcliff Mnr.	State/Province	NY			
Postal Code	10510	Country i	US			
All Inventors Must Be Listed - Additional Inventor Information blocks may be generated within this form by selecting the Add button.						Add

Correspondence Information:

Enter either Customer Number or complete the Correspondence Information section below. For further information see 37 CFR 1.33(a).			
<input type="checkbox"/> An Address is being provided for the correspondence Information of this application.			
Customer Number	97218		
Email Address	hcdocketing@hunter-clark.com	Add Email	Remove Email

Application Information:

Title of the Invention	MECHANICAL ANALYSIS WITH HIGH ACCURACY THREE-DIMENSIONAL FINITE ELEMENTS		
Attorney Docket Number	10065-509P01US	Small Entity Status Claimed	<input checked="" type="checkbox"/>
Application Type	Provisional		
Subject Matter	Utility		
Total Number of Drawing Sheets (if any)		Suggested Figure for Publication (if any)	

Application Data Sheet 37 CFR 1.76		Attorney Docket Number	10065-509P01US
		Application Number	
Title of Invention	MECHANICAL ANALYSIS WITH HIGH ACCURACY THREE-DIMENSIONAL FINITE ELEMENTS		

Publication Information:

<input type="checkbox"/>	Request Early Publication (Fee required at time of Request 37 CFR 1.219)
<input type="checkbox"/>	Request Not to Publish. I hereby request that the attached application not be published under 35 U.S.C. 122(b) and certify that the invention disclosed in the attached application has not and will not be the subject of an application filed in another country, or under a multilateral international agreement, that requires publication at eighteen months after filing.

Representative Information:

<p>Representative information should be provided for all practitioners having a power of attorney in the application. Providing this information in the Application Data Sheet does not constitute a power of attorney in the application (see 37 CFR 1.32). Either enter Customer Number or complete the Representative Name section below. If both sections are completed the customer Number will be used for the Representative Information during processing.</p>			
Please Select One:	<input checked="" type="radio"/> Customer Number	<input type="radio"/> US Patent Practitioner	<input type="radio"/> Limited Recognition (37 CFR 11.9)
Customer Number	97218		

Domestic Benefit/National Stage Information:

This section allows for the applicant to either claim benefit under 35 U.S.C. 119(e), 120, 121, or 365(c) or indicate National Stage entry from a PCT application. Providing this information in the application data sheet constitutes the specific reference required by 35 U.S.C. 119(e) or 120, and 37 CFR 1.78.			
Prior Application Status		Remove	
Application Number	Continuity Type	Prior Application Number	Filing Date (YYYY-MM-DD)
Additional Domestic Benefit/National Stage Data may be generated within this form by selecting the Add button.			Add

Foreign Priority Information:

This section allows for the applicant to claim priority to a foreign application. Providing this information in the application data sheet constitutes the claim for priority as required by 35 U.S.C. 119(b) and 37 CFR 1.55(d). When priority is claimed to a foreign application that is eligible for retrieval under the priority document exchange program (PDX) the information will be used by the Office to automatically attempt retrieval pursuant to 37 CFR 1.55(h)(1) and (2). Under the PDX program, applicant bears the ultimate responsibility for ensuring that a copy of the foreign application is received by the Office from the participating foreign intellectual property office, or a certified copy of the foreign priority application is filed, within the time period specified in 37 CFR 1.55(g)(1).			
Remove			
Application Number	Country ⁱ	Filing Date (YYYY-MM-DD)	Access Code ^j (if applicable)
Additional Foreign Priority Data may be generated within this form by selecting the Add button.			Add

Application Data Sheet 37 CFR 1.76		Attorney Docket Number	10065-509P01US
		Application Number	
Title of Invention	MECHANICAL ANALYSIS WITH HIGH ACCURACY THREE-DIMENSIONAL FINITE ELEMENTS		

Statement under 37 CFR 1.55 or 1.78 for AIA (First Inventor to File) Transition Applications

<input type="checkbox"/> This application (1) claims priority to or the benefit of an application filed before March 16, 2013 and (2) also contains, or contained at any time, a claim to a claimed invention that has an effective filing date on or after March 16, 2013. NOTE: By providing this statement under 37 CFR 1.55 or 1.78, this application, with a filing date on or after March 16, 2013, will be examined under the first inventor to file provisions of the AIA.

Authorization to Permit Access:

<input checked="" type="checkbox"/> Authorization to Permit Access to the Instant Application by the Participating Offices
<p>If checked, the undersigned hereby grants the USPTO authority to provide the European Patent Office (EPO), the Japan Patent Office (JPO), the Korean Intellectual Property Office (KIPO), the World Intellectual Property Office (WIPO), and any other intellectual property offices in which a foreign application claiming priority to the instant patent application is filed access to the instant patent application. See 37 CFR 1.14(c) and (h). This box should not be checked if the applicant does not wish the EPO, JPO, KIPO, WIPO, or other intellectual property office in which a foreign application claiming priority to the instant patent application is filed to have access to the instant patent application.</p> <p>In accordance with 37 CFR 1.14(h)(3), access will be provided to a copy of the instant patent application with respect to: 1) the instant patent application-as-filed; 2) any foreign application to which the instant patent application claims priority under 35 U.S.C. 119(a)-(d) if a copy of the foreign application that satisfies the certified copy requirement of 37 CFR 1.55 has been filed in the instant patent application; and 3) any U.S. application-as-filed from which benefit is sought in the instant patent application.</p> <p>In accordance with 37 CFR 1.14(c), access may be provided to information concerning the date of filing this Authorization.</p>

Applicant Information:

Providing assignment information in this section does not substitute for compliance with any requirement of part 3 of Title 37 of CFR to have an assignment recorded by the Office.

Application Data Sheet 37 CFR 1.76		Attorney Docket Number	10065-509P01US
		Application Number	
Title of Invention	MECHANICAL ANALYSIS WITH HIGH ACCURACY THREE-DIMENSIONAL FINITE ELEMENTS		

Applicant 1			Remove
<p>If the applicant is the inventor (or the remaining joint inventor or inventors under 37 CFR 1.45), this section should not be completed. The information to be provided in this section is the name and address of the legal representative who is the applicant under 37 CFR 1.43; or the name and address of the assignee, person to whom the inventor is under an obligation to assign the invention, or person who otherwise shows sufficient proprietary interest in the matter who is the applicant under 37 CFR 1.46. If the applicant is an applicant under 37 CFR 1.46 (assignee, person to whom the inventor is obligated to assign, or person who otherwise shows sufficient proprietary interest) together with one or more joint inventors, then the joint inventor or inventors who are also the applicant should be identified in this section.</p>			
Clear			
<input type="radio"/> Assignee	<input type="radio"/> Legal Representative under 35 U.S.C. 117	<input type="radio"/> Joint Inventor	
<input type="radio"/> Person to whom the inventor is obligated to assign.		<input type="radio"/> Person who shows sufficient proprietary interest	
If applicant is the legal representative, indicate the authority to file the patent application, the inventor is:			
Name of the Deceased or Legally Incapacitated Inventor : <input type="text"/>			
If the Applicant is an Organization check here. <input type="checkbox"/>			

Prefix	Given Name	Middle Name	Family Name	Suffix
Mailing Address Information:				
Address 1				
Address 2				
City		State/Province		
Country ⁱ		Postal Code		
Phone Number		Fax Number		
Email Address				
Additional Applicant Data may be generated within this form by selecting the Add button. Add				

Assignee Information including Non-Applicant Assignee Information:

<p>Providing assignment information in this section does not substitute for compliance with any requirement of part 3 of Title 37 of CFR to have an assignment recorded by the Office.</p>
Assignee 1
<p>Complete this section if assignee information, including non-applicant assignee information, is desired to be included on the patent application publication. An assignee-applicant identified in the "Applicant Information" section will appear on the patent application publication as an applicant. For an assignee-applicant, complete this section only if identification as an assignee is also desired on the patent application publication.</p>
Remove

Application Data Sheet 37 CFR 1.76		Attorney Docket Number	10065-509P01US
		Application Number	
Title of Invention	MECHANICAL ANALYSIS WITH HIGH ACCURACY THREE-DIMENSIONAL FINITE ELEMENTS		

If the Assignee is an Organization check here. <input type="checkbox"/>				
Prefix	Given Name	Middle Name	Family Name	Suffix
Mailing Address Information:				
Address 1				
Address 2				
City		State/Province		
Country i		Postal Code		
Phone Number		Fax Number		
Email Address				
Additional Assignee Data may be generated within this form by selecting the Add button.				<input type="button" value="Add"/>

Signature:

NOTE: This form must be signed in accordance with 37 CFR 1.33. See 37 CFR 1.4 for signature requirements and certifications					
Signature	/Ido Rabinovitch/			Date (YYYY-MM-DD)	2013-09-11
First Name	Ido	Last Name	Rabinovitch	Registration Number	68434
Additional Signature may be generated within this form by selecting the Add button.					<input type="button" value="Add"/>

This collection of information is required by 37 CFR 1.76. The information is required to obtain or retain a benefit by the public which is to file (and by the USPTO to process) an application. Confidentiality is governed by 35 U.S.C. 122 and 37 CFR 1.14. This collection is estimated to take 23 minutes to complete, including gathering, preparing, and submitting the completed application data sheet form to the USPTO. Time will vary depending upon the individual case. Any comments on the amount of time you require to complete this form and/or suggestions for reducing this burden, should be sent to the Chief Information Officer, U.S. Patent and Trademark Office, U.S. Department of Commerce, P.O. Box 1450, Alexandria, VA 22313-1450. DO NOT SEND FEES OR COMPLETED FORMS TO THIS ADDRESS. **SEND TO: Commissioner for Patents, P.O. Box 1450, Alexandria, VA 22313-1450.**

Privacy Act Statement

The Privacy Act of 1974 (P.L. 93-579) requires that you be given certain information in connection with your submission of the attached form related to a patent application or patent. Accordingly, pursuant to the requirements of the Act, please be advised that: (1) the general authority for the collection of this information is 35 U.S.C. 2(b)(2); (2) furnishing of the information solicited is voluntary; and (3) the principal purpose for which the information is used by the U.S. Patent and Trademark Office is to process and/or examine your submission related to a patent application or patent. If you do not furnish the requested information, the U.S. Patent and Trademark Office may not be able to process and/or examine your submission, which may result in termination of proceedings or abandonment of the application or expiration of the patent.

The information provided by you in this form will be subject to the following routine uses:

1. The information on this form will be treated confidentially to the extent allowed under the Freedom of Information Act (5 U.S.C. 552) and the Privacy Act (5 U.S.C. 552a). Records from this system of records may be disclosed to the Department of Justice to determine whether the Freedom of Information Act requires disclosure of these records.
2. A record from this system of records may be disclosed, as a routine use, in the course of presenting evidence to a court, magistrate, or administrative tribunal, including disclosures to opposing counsel in the course of settlement negotiations.
3. A record in this system of records may be disclosed, as a routine use, to a Member of Congress submitting a request involving an individual, to whom the record pertains, when the individual has requested assistance from the Member with respect to the subject matter of the record.
4. A record in this system of records may be disclosed, as a routine use, to a contractor of the Agency having need for the information in order to perform a contract. Recipients of information shall be required to comply with the requirements of the Privacy Act of 1974, as amended, pursuant to 5 U.S.C. 552a(m).
5. A record related to an International Application filed under the Patent Cooperation Treaty in this system of records may be disclosed, as a routine use, to the International Bureau of the World Intellectual Property Organization, pursuant to the Patent Cooperation Treaty.
6. A record in this system of records may be disclosed, as a routine use, to another federal agency for purposes of National Security review (35 U.S.C. 181) and for review pursuant to the Atomic Energy Act (42 U.S.C. 218(c)).
7. A record from this system of records may be disclosed, as a routine use, to the Administrator, General Services, or his/her designee, during an inspection of records conducted by GSA as part of that agency's responsibility to recommend improvements in records management practices and programs, under authority of 44 U.S.C. 2904 and 2906. Such disclosure shall be made in accordance with the GSA regulations governing inspection of records for this purpose, and any other relevant (i.e., GSA or Commerce) directive. Such disclosure shall not be used to make determinations about individuals.
8. A record from this system of records may be disclosed, as a routine use, to the public after either publication of the application pursuant to 35 U.S.C. 122(b) or issuance of a patent pursuant to 35 U.S.C. 151. Further, a record may be disclosed, subject to the limitations of 37 CFR 1.14, as a routine use, to the public if the record was filed in an application which became abandoned or in which the proceedings were terminated and which application is referenced by either a published application, an application open to public inspections or an issued patent.
9. A record from this system of records may be disclosed, as a routine use, to a Federal, State, or local law enforcement agency, if the USPTO becomes aware of a violation or potential violation of law or regulation.

MECHANICAL ANALYSIS WITH HIGH ACCURACY THREE-DIMENSIONAL FINITE ELEMENTS

BACKGROUND

[0001] From a computational mechanics perspective, Courant (as described, for example, in R. Courant, "Variational methods for the solution of problems of equilibrium and vibration," Bulletin of the American Mathematical Society, 49:1–29, 1943, the content of which is incorporated by reference herein in its entirety) pioneered the technique of approximating continuous solutions of mathematical physics with finite number of scalar variables to calculate shear stresses on a multiply connected non-circular prismatic shaft subjected to end torques. With that technique, two-dimensional cross sections were triangulated and introduced piecewise linear interpolants on those "triangular" elements. The unknown weights were then calculated from the Ritz formulation (as described, for example, in W. Ritz, "Über eine neue methode zur lösung gewisser variationalprobleme der mathematischen physic," Journal Reine Angew, Math., 135:1– 61, 1908, the content of which is incorporated by reference herein in its entirety).

[0002] Motivated by the structural mechanics applications, Clough (as described, for example, in Ray W. Clough, "The finite element method in plane stress analysis," In Proceedings, 2nd Conference on Electronic Computation, A.S.C.E. Structural Division, pages 345 – 378, Pittsburgh, PA, September 8 and 9, 1960, the content of which is incorporated by reference herein in its entirety) introduced an analogous technique, which is closely related to the Courant's methodology mentioned above, namely, the finite element technique. Under this technique, various important practical problems were solved by assuming piecewise linear displacement profiles. Therein, the principle of virtual work played the role of the Ritz functional. The strain energy density function remained constant within each triangulated zone. Hence, the exact integration was possible leading to computationally trustworthy element stiffness matrices. A weak version of equilibrium and compatibility, which were enforced only at the discrete vertices of Courant's triangles, led to unconditional convergence in all cases. However, for flexures – beams, plates and shell bending problems, due to the imposition of

constant stress fields – unacceptably high stiffness was encountered even within considerably fine “triangular” meshes.

DESCRIPTION

[0003] The present disclosure builds on the discussion in Columbia University’s U.S. Patent No. 6,101,450 to Gautam Dasgupta, entitled “Stress Analysis Using a Defect-Free Four Node Finite Element Technique,” the content of which is incorporated by reference herein in its entirety, to provide solutions for its three-dimensional counterpart. Applications to locking-free solid, plate and shell elements can be developed that are devoid of errors from element shape distortion and Poisson’s effect. For example, in order to construct locking-free, three-dimensional brick elements, cubic polynomials, which depend upon Poisson’s ratio(s), in the physical (x, y, z) coordinates are derived for twenty four Rayleigh modes. Their linear combinations yield twenty four shape functions that are associated with the degrees-of-freedom located on the vertices.

[0004] To maintain the high accuracy consistently, especially the locking-free features, numerical quadrature has been avoided in evaluating the stiffness-like system matrices. This analytical strategy, which is based on the divergence theorem, is computationally more efficient than any quadrature scheme.

[0005] The locking-free interpolants (for an eight node hexahedral brick element) in the physical (x, y, z) co-ordinates are cubic functions, hence the linear elastic stresses are quadratic in (x, y, z) . Hence, the energy density expressions comprise of the terms in the expanded expression of $(1 + x + y + z)^4$. Each term, within a brick, can be exactly integrated (e.g., by a computer application) without resorting to any numerical quadrature.

[0006] Restrictions of convex elements do not apply and concavity, as it develops during elastoplastic deformation, can be considered. For general vector field problems, e.g., those of continuum mechanics, computer algebra systems can be incorporated seamlessly within, for example, a UNIX environment. The Modelica Language can achieve the same for all platforms.

Therein, general numerics can be optimized for efficiency and accuracy by utilizing, for example, C++ routines.

[0007] Thus, disclosed herein are methods, procedures, systems, devices, products, and other implementations, including a computer-implemented method that includes performing three-dimensional mechanical analysis for finite element analysis based on indefinite integral determined algebraically and based on Poisson's ratio dependent shape functions satisfying equilibrium throughout a finite element. In some embodiments, the finite element includes a three-dimensional brick element.

[0008] In some embodiments, for the three-dimensional brick element, a test function – displacement vector in the physical (x, y, z) coordinates – includes three full cubic polynomials in x, y and z, with sixty coefficients. The twelve coefficients pertaining to the constant and linear terms lead to six rigid body modes and five uniform deviatoric strains. The dilatation is zero and non-zero for incompressible and compressible solids, respectively. For quadratic terms, point-wise equilibrium and shear free bending requirements remove twelve coefficients out of eighteen, and thus completely effaces shear and Poisson locking. To obtain point-wise equilibrium, the coefficients for compressible solids are functions of the Poisson's ratio(s). For the cubic terms, equilibrium requirement eliminates nine out of thirty coefficients. Selection of bending under a constant shear force eliminates another set of fifteen coefficients. All other operations are generally similar to their two-dimensional counterparts (as more particularly described in U.S. patent No. 6,101,450).

[0009] Further details regarding the methods, procedures, systems, apparatus, devices, products and other implementations described herein are provided below in "Locking-free 'brick' interpolants – a 'high accuracy' finite element" (also identified as "[a] Rayleigh mode acquiescence to Single element test") by Gautam Dasgupta, and in "High Accuracy three-dimensional Finite Elements" by Gautam Dasgupta, the contents of all of which are incorporated by reference herein in their entireties.

[0010] Performing the various operations described herein may be facilitated by a processor-based computing system. Particularly, various devices / systems / units used in various

embodiments may be implemented, at least in part, using one or more processor-based devices. With reference to FIG. 1, provided below, a schematic diagram of a generic computing system 100 is shown.

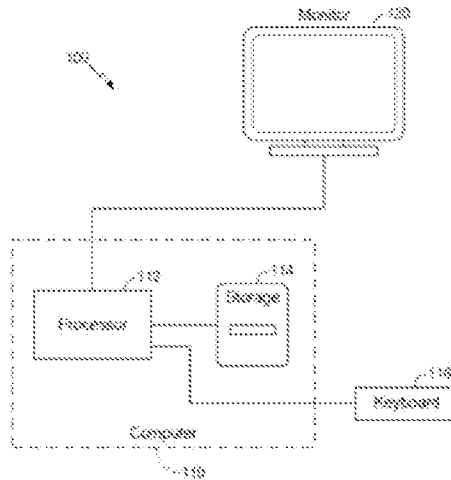


FIG. 1

[0011] The computing system 100 includes a processor-based device 110 such as a personal computer, a specialized computing device, and so forth, that typically includes a central processor unit 112. In addition to the CPU 112, the system includes main memory, cache memory and bus interface circuits (not shown in FIG. 1). The processor-based device 110 may include a mass storage element 114, such as a hard drive or flash drive associated with the computer system. The computing system 100 may further include a keyboard, or keypad, or some other user input interface 116, and a monitor 120, e.g., a CRT (cathode ray tube) or LCD (liquid crystal display) monitor, that may be placed where a user can access them.

[0012] The processor-based device 110 is configured to perform at least some of the operations / procedures described herein. The storage device 114 may thus include a computer program product that when executed on the processor-based device 110 causes the processor-based device to perform operations/procedures described herein. The processor-based device may further include peripheral devices to enable input/output functionality. Such peripheral devices may

include, for example, a CD-ROM drive and/or flash drive (e.g., a removable flash drive), or a network connection (e.g., implemented using a USB port and/or a wireless transceiver), for downloading related content to the connected system. Such peripheral devices may also be used for downloading software containing computer instructions to enable general operation of the respective system/device. Alternatively and/or additionally, in some embodiments, special purpose logic circuitry, e.g., an FPGA (field programmable gate array), an ASIC (application-specific integrated circuit), a DSP processor, etc., may be used in the implementation of the system 100. Other modules that may be included with the processor-based device 110 are speakers, a sound card, a pointing device, e.g., a mouse or a trackball, by which the user can provide input to the computing system 100. The processor-based device 110 may include an operating system, e.g., Windows XP® Microsoft Corporation operating system, Ubuntu operating system, etc.

[0013] Computer programs (also known as programs, software, software applications or code) include machine instructions for a programmable processor, and may be implemented in a high-level procedural and/or object-oriented programming language, and/or in assembly/machine language. As used herein, the term “machine-readable medium” refers to any non-transitory computer program product, apparatus and/or device (e.g., magnetic discs, optical disks, memory, Programmable Logic Devices (PLDs)) used to provide machine instructions and/or data to a programmable processor, including a non-transitory machine-readable medium that receives machine instructions as a machine-readable signal.

[0014] Some or all of the subject matter described herein may be implemented in a computing system that includes a back-end component (e.g., as a data server), or that includes a middleware component (e.g., an application server), or that includes a front-end component (e.g., a client computer having a graphical user interface or a Web browser through which a user may interact with an embodiment of the subject matter described herein), or any combination of such back-end, middleware, or front-end components. The components of the system may be interconnected by any form or medium of digital data communication (e.g., a communication network). Examples of communication networks include a local area network (“LAN”), a wide area network (“WAN”), and the Internet.

[0015] The computing system may include clients and servers. A client and server are generally remote from each other and typically interact through a communication network. The relationship of client and server generally arises by virtue of computer programs running on the respective computers and having a client-server relationship to each other.

[0016] In some embodiments, any suitable computer readable media can be used for storing instructions for performing the processes / operations / procedures described herein. For example, in some embodiments computer readable media can be transitory or non-transitory. For example, non-transitory computer readable media can include media such as magnetic media (such as hard disks, floppy disks, etc.), optical media (such as compact discs, digital video discs, Blu-ray discs, etc.), semiconductor media (such as flash memory, electrically programmable read only memory (EPROM), electrically erasable programmable read only Memory (EEPROM), etc.), any suitable media that is not fleeting or not devoid of any semblance of permanence during transmission, and/or any suitable tangible media. As another example, transitory computer readable media can include signals on networks, in wires, conductors, optical fibers, circuits, any suitable media that is fleeting and devoid of any semblance of permanence during transmission, and/or any suitable intangible media.

[0017] Although particular embodiments have been disclosed herein in detail, this has been done by way of example for purposes of illustration only, and is not intended to be limiting with respect to the scope of the appended claims, which follow. Some other aspects, advantages, and modifications are considered to be within the scope of the claims provided below. The claims presented are representative of at least some of the embodiments and features disclosed herein. Other unclaimed embodiments and features are also contemplated.

*Locking-free ‘brick’ interpolants
a ‘high accuracy’ finite element*

Gautam Dasgupta
Columbia University
New York, NY, USA
E-mail: dasgupta@columbia.edu

Received: date / Accepted: date

Abstract

‘High accuracy’ finite elements reproduce *point-wise* a set of stipulated continuum mechanics responses *exactly*. It addresses incompressibility as a kinematic constraint; therein, the element pressure and the Rayleigh (displacement) modal participation factors constitute the local degrees-of-freedom. The single element (*patch*) test suffices because all spatial integrations are carried out *analytically*. The demanded stress profiles beyond linear interpolants must be *tensorially invariant*. Needs to capturing outgoing waves in unbounded media, and to simulating viscoplastic responses in (fiber-reinforced, bio- and nano-) composites motivated the research. The details, in here, will enable incorporation into existing computer programs these ‘high accuracy’ elements — *including concavity*, since generating shape functions from the Rayleigh modes completely eliminates *mesh distortional* locking.

For the three-dimensional brick element, a test function — displacement vector in the physical (x, y, z) coordinates — consists of three *full* cubic polynomials in x, y and z , with all sixty coefficients. The twelve coefficients pertaining to the constant and linear terms lead to six rigid body modes and five uniform deviatoric strains. The dilatation is zero and non-zero for incompressible and compressible solids, respectively. For quadratic terms, *point-wise* equilibrium and shear free bending requirements annihilate twelve coefficients out of eighteen, and thus completely effaces *shear* and *Poisson* locking. To guarantee *point-wise* equilibrium, the coefficients for *compressible* solids are necessarily functions of the *Poisson’s ratio(s)*. For the cubic terms, equilibrium requirement eliminates nine out of thirty coefficients. Selection of bending under a constant shear force eliminates another set of fifteen coefficients. All other steps are identical to their two-dimensional counterparts.

Department of Civil Engineering and Engineering Mechanics
School of Engineering and Applied Sciences
Waseda University, Tokyo, JAPAN, Tsunoda Senior Exchange Researcher from January to August 2013

Keywords brick element · concave element · cubic interpolants · eight node element · exact integration · hexahedral element · high accuracy element · locking free · patch test · Poisson ratio dependent shape functions · Rayleigh modes · single element test · symbolic computation · three dimensional finite element

Author's note:

The Appendix is intended for the electronic version unless the reviewers want that to be a part of the printed pages.

Sufficient familiarity with the 2-D version, *vide* reference[17], will permit the paper to be shortened by about 30% and most of the footnotes and many repetitions can also be eliminated.

1 Introduction

From the computational mechanics perspective, Courant[8] pioneered the technique of approximating continuous solutions of mathematical physics with *finite* number of scalar variables to calculating shear stresses on a multiply connected non-circular prismatic shaft subjected to end torques. He triangulated the two-dimensional cross section and introduced piecewise linear interpolants on those “triangular” *elements* [41]. He then calculated the unknown weights from the Ritz formulation [42].

Motivated by the structural mechanics applications, Clough [7] christened an analogous technique, which is closely related to the Courant’s methodology mentioned above, *finite element*. He solved various important practical problems by assuming piecewise linear displacement profiles. Therein, the principle of *virtual work* played the role of the Ritz functional. The strain energy density function remained constant within each triangulated zone. Hence, the *exact* integration was possible leading to computationally trustworthy element stiffness matrices. A *weak* version of equilibrium and compatibility, which were enforced only at the discrete vertices of Courant’s triangles, led to unconditional convergence in all cases. However, for flexures — beams, plates and shell bending problems, due to the imposition of constant stress fields — unacceptably high stiffness was encountered even within considerably fine “triangular” meshes.

To alleviate the shortcoming, which originated from linear interpolants, and specifically, to capturing spatial gradients in stress distributions — Taig [47] introduced four-node plane “quadrilateral” elements. This formulation, which indeed revolutionized the finite element industry — as commented by Wilson [60], proved effective in a large variety of problems including three-dimensional elastic deformations [33,28] and of course in plates and shells [20,2]. In Taig’s original formulation, the kernel test functions were bi-linear functions — rather than *full* quadratic maps — on a square, hence, equilibrium was satisfied only in a limited number of cases. The strain energy density functions are quadratics in the computational (not physical) domains and their integrations on arbitrary quadrilaterals necessarily invoked numerical quadratures. To assess the ambiguity so encountered, Irons introduced the *patch test* to examine both the theoretical and programming accuracies in any new formulation by judging its capabilities to reproducing known basic continuum mechanics solutions [29,31].

Departure from any analytical solution, caused failure in the *patch test* [37]. An element manifested *locking* — a concept originated by observing, under pure bending, finite element *non-zero* shear stresses that was termed *shear locking*. MacNeal [36] furnished a theorem, after closely examining all possible responses with four node *isoparametric*¹ finite elements. He conclu-

¹ *vide* [30], *iso* — the same — *parameteric* representation is advocated to interpolating the displacement functions $u(x, y, z)$, $v(x, y, z)$, $w(x, y, z)$ as well as physical x, y coordinates from the computational unit square in the η, ξ frame— Taig himself did *not* use the term *isoparametric* in his seminal publication, *vide* [47]

sively identified the inherent deficiency — the *locking* phenomenon — in Taig’s formulation.

The single element *patch test*, *vide* [44,43,51], can assess the *locking-free* criteria, because it essentially verifies the quality of the shape functions and necessary characteristics of element stiffness matrices. Symbolic² and numeric treatment of test cases have been proved to be effective.

The main obstacle in seeking any alternative to Taig’s computational domain approach with functions in the physical (x, y, z) frame, *e.g.*, the polynomials in (x, y, z) , Wachspress coordinates [56,26,38] with Padé interpolants [40], can be traced to be the difficulty originating from integrating strain energy densities within a finite element³ of an arbitrary shape. With the recent availability of *exact* integration — based on the divergence theorem — within arbitrary polyhedra, a 3D ‘brick’ can be completely diagnosed to be *locking-free* via the single element test.

1.1 Exact volume integration

In a generic brick element, in **Fig. 1**, vertices 1, 2, 3 and 6 were supplied and nodes 4, 5, 7 and 8 in equation (1) were so generated by employing a random number generator that *all* faces come out to be flat.

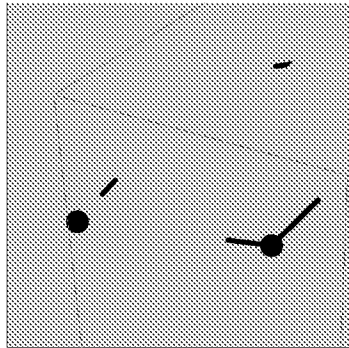


Fig. 1 A hexahedral finite element

² *vide* lecture notes in:

<http://www.colorado.edu/engineering/CAS/courses.d/AFEM.d/AFEM.Ch15.d>

³ concavity was out of question in the isoparametric formulation

node:	1	2	3	4	5	6	7	8
x	0	0	1	1.20272	0	0	1.21608	1.59793
y	1	0	0	1.31422	1.36807	0	0	1.90818
z	0	0	0	0	1.30599	1	1.23926	1.74118

(1)

Table 1 nodal values for a brick element

The individual polynomial terms — needed to *exactly* integrating the energy density expressions in the element stiffness matrix for any convex or concave ‘brick’ element — appear in equation (2) alongside their *exact* values⁴ pertaining to **Fig. 1**:

$$\begin{pmatrix} 1 & x & x^2 & x^3 & x^4 \\ y & xy & x^2y & x^3y & y^2 \\ xy^2 & x^2y^2 & y^3 & xy^3 & y^4 \\ z & xz & x^2z & x^3z & yz \\ xyz & x^2yz & y^2z & xy^2z & y^3z \\ z^2 & xz^2 & x^2z^2 & yz^2 & xyz^2 \\ y^2z^2 & z^3 & xz^3 & yz^3 & z^4 \end{pmatrix} \rightarrow \begin{pmatrix} 2.22344 & 1.53912 & 1.37624 & 1.37572 & 1.46922 \\ 1.71844 & 1.29807 & 1.23539 & 1.30083 & 1.73422 \\ 1.39974 & 1.39106 & 1.97293 & 1.68464 & 2.4153 \\ 1.63007 & 1.22254 & 1.15959 & 1.21846 & 1.39539 \\ 1.13712 & 1.14255 & 1.5175 & 1.31454 & 1.83679 \\ 1.54731 & 1.23191 & 1.21622 & 1.42495 & 1.22679 \\ 1.62714 & 1.64678 & 1.37935 & 1.61085 & 1.87798 \end{pmatrix} \quad (2)$$

1.2 Computer algebra implementation

The capability of analytically integrating the energy density function played a decisive role in this research that essentially circumvented the isoparametric mythology. In the physical (x, y, z) frame, the formulation was carried out within *Mathematica*. For general anisotropic solids, with twenty one Poisson’s ratio parameters, use of computer algebra will be advantageous.

Concept development is indeed formidable with any numerically oriented language but resulting *Mathematica* expressions can be translated into **FORTRAN** or \mathbf{C}^{++} with *MathCode* [21], rather effortlessly. Multi-domain modeling tools, *e.g.*, *Modelica* [22], have emerged to accept physical description of an engineering problem in terms of partial differential field equations and generate numerically efficient \mathbf{C}^{++} codes.

Using *Mathematica*, the author obtained the algebraic expressions for the Rayleigh modes — as functions of the Poisson’s ratio, for isotropic solids. Especially to eliminating constants in the polynomial expressions — on the physical basis of satisfying equilibrium and all other tensorial prescriptions *point-wise* — one needs special equation solving capabilities that cannot be found in matrix calculation procedures[25,39].

⁴ A paper on exact integration of an arbitrary function within arbitrary polyhedra is under review [15] — if the exact integration fails then any predetermined amount of error can be prescribed — along the line of $\epsilon-\delta$ argument for convergence; for polynomials *always* the *exact* integration is attainable

In this paper, all equations, figures and tables have been generated and exported by *Mathematica* as EPS, PDF and T_EX outputs to a L^AT_EX file for typesetting.

1.3 The *locking-free* ‘brick’ : a 3-D extension of four-node compressible/incompressible and convex/concave finite elements

This ‘brick’ formulation is the third paper in the sequel of implementing the Rayleigh modal construction that leads to algebraic expressions of element shape functions. For two-dimensional four node elements, not restricted to convex geometry, the author published [16, 17] for the isochoric and compressible cases.

Here, all equilibrium equations are satisfied *point-wise*⁵, thus no *variational crime* is committed. Subsequently, the energy density integrals, for the element stiffness matrix, are calculated *analytically*, hence, all controversies pertaining to numerical quadrature approximations have been averted.

This paper starts with a (coupled) triplet of cubic polynomials in the physical x, y, z frame. There are 60 unknown coefficients⁶. In order to comply with the *patch test* the displacement vector is taxonomized as follows⁷:

- (i) constant and linear terms: 12 coefficients — 6 rigid body modes and 6 constant strain modes — equilibrium is satisfied *identically*
- (ii) quadratic terms: 18 coefficients — equilibrium condition reduces to 15 unknowns — pure bending conditions eliminates shear and 9 terms and reduces to 6 unknowns: correspond to two orthogonal bending in each direction
- (iii) cubic terms: 30 coefficients — equilibrium condition reduces to 21 unknowns — 6 conditions are selected by setting axial stress σ_{xx} to $x * y$ and $x * z$; σ_{yy} to $y * z$ and $y * x$, and σ_{zz} to $z * x$ and $z * y$. These were identified from a cantilever beam under an end loading case.

For compressible solids, from the above three categories, twenty four Rayleigh modes are evaluated. Their linear combinations led to the shape functions.

For incompressible cases, the 60 coefficients of the cubic triplet reduce to 50. There are 11 linear terms, and as before 6 shear free pure bending cases and 6 ‘cantilever beam’ terms led to Rayleigh modes with a *constant element pressure*.

⁵ in the *strong* not in an error minimization nor variational sense

⁶ each *full* cubic polynomial has 20 terms

⁷ In equation (12), combinations of constant and linear terms yield the simplex modes, viz., the rigid body and constant strain profiles while the quadratic terms are associated with (shear free) pure bending modes. In addition, the cubic terms in equation (12) depict the parabolic shear stress profiles that is observed in a beam with a constant shear force.

1.4 Field equations

1.4.1 Tensors and lists

In order to avoid confusion the term ‘vector’ will be restricted to denoting a single rank tensor, *e.g.*, displacement ϖ . In general, a tensor quantity will be indicated with a bold face symbol, *e.g.*, $\varpi, \Delta\epsilon, \mathbf{C}_{ijkl}$. In the traditional literature, a column matrix is also called a vector and a row matrix is often referred to be a row vector. These do not imply any tensorial sense because they are not abide by the coordinate transformation rules when viewed as a whole. In this paper, the author adopts the computer algebra terminology, consequently, terms a single row or column matrix to be (just) a *list*. However, a rectangular array will be called a matrix even though technically⁸ it is also a *list* — list of lists.

1.4.2 The body force vector

In order to conduct the *patch test* in the presence of zero *body force*, each shape function is designed to satisfy the equilibrium equation *unconditionally*. This guarantees the element against any locking due to its original geometrical shape⁹ as well as Poisson’s ratio(s)¹⁰. Furthermore, not to incur shear locking, only shear-free displacement fields pertaining to bending modes are selected.

Since the shape functions are constructed as linear combinations of Rayleigh modes, it is crucial to undertake the tensor treatment of elasticity field equations. To emphasize, the Cartesian coordinates and the associated displacement components are indicated as vectors:

$$\mathbf{x} = \begin{Bmatrix} x \\ y \\ z \end{Bmatrix}; \quad \varpi(x, y, z) = \begin{Bmatrix} u(x, y, z) \\ v(x, y, z) \\ w(x, y, z) \end{Bmatrix} \quad (3)$$

The six — three axial and three shear strain γ and stress τ — components are then:

$$\gamma_{ij} = \frac{1}{2} \left(\frac{\partial \varpi_i}{\partial x_j} + \frac{\partial \varpi_j}{\partial x_i} \right) \quad (4)$$

$$\{\tau\} = [\mathcal{D}]\{\gamma\}; \quad [\mathcal{D}] : \text{constitutive matrix, in general with 21 constants} \quad (5)$$

In this static case the *body force* vector \mathbf{f} is:

$$\mathbf{f}_i = \frac{\partial \tau_{ij}}{\partial x_j} \quad \text{— summation is implied over repeated indices} \quad (6)$$

In some places of this paper, for clarity, the axial stresses and strains are indicated by σ, ϵ respectively, for example:

$$\sigma_{xx} = \tau_{xx}; \quad \epsilon_{xx} = \gamma_{xx}; \quad \text{— no sum over repeated indices} \quad (7)$$

⁸ *list* of lists is also a *list*

⁹ “distortion” [32,46]

¹⁰ “dilatation or Poisson locking” [1]

1.5 Rayleigh modal vis-à-vis the *isoparametric* formulation

For the deformed element, boundaries should not be constrained to piecewise linear functions¹¹. because, this will impart additional stiffness in the system.

The *patch test* should be conducted in the absence of the *body force* vector. This demands that the shape functions necessarily satisfy equilibrium equations. From equation (6):

$$\mathbf{f}_i = 0 \text{ for } \forall (x, y, z) \quad (8)$$

that is not met by the *isoparametric* formulation, hence a *locking-free* solution field becomes unavoidable. Each Rayleigh displacement vector complies with the equilibrium condition, equation (8), *exactly*. The multi-linear¹² isoparametric shape functions, which is oblivious to Poisson's ratio — the non-dimensional parameter responsible for coupling directional displacements into a vector, can never satisfy equilibrium *pointwise* in the physical x, y, z -frame. Furthermore, *isoparametric* representations decouple displacement vector. The elasticity displacement solutions are always coupled vector fields.

The incompressibility issue is traected separately in the 'high accuracy' formulation. The *isoparametric* maps cannot reproduce zero dilatation *pointwise*. Hence the *Poisson locking* is inevitable.

Ubiquitously, quadrature is destined to fetch numerical contamination into the stiffness matrix, hence, the strain energy in the element is not captured correctly. The nodal forces must always, without exception, be calculated as virtual work quantities, *vide* Clough [6], rather than simply lumping the applied traction only on the segment of application. The latter in *patch tests* miscalculates the total strain energy in an element.

1.5.1 Unconditional possibility of analytical integration

For the isoparametric transformation, integration of the energy density functions poses a formidable task when a quadrilateral finite element Ω_i departs from parallelograms. Even though Taig, *vide* page-15, equation 35) of [47], researched on analytical integration and derived *closed-form* integrals of trapezoidal elements, numerical quadrature [24] still captures the center stage even when closed form expressions are available [13] for **Fortran** and **C++** coding. With *lower order* interpolants a hypercube in \mathfrak{R}^m will have the following

¹¹ straight line and plane for two and three dimensions respectively

¹² bilinear and trilinear for 2-D and 3-D cases respectively

element stiffness matrix \mathcal{K} expression:

$$\mathcal{K}^{(i)} = \int_{\Omega_i} \mathcal{B}^T \mathcal{D} \mathcal{B} d\Omega \quad (9)$$

for the element i of domain Ω_i with 2^m nodes and

m degrees-of-freedom per node

\mathcal{B} : strain-displacement matrix — \wp^{n-1}

\mathcal{D} : stress-strain matrix — constant

\wp^m : polynomial of degree m

m : spatial dimension of $\Omega \subset \Re^m$ — (x_1, x_2, \dots, x_m)

Each Rayleigh mode is \wp^m in (x_1, x_2, \dots, x_m) and their linear combinations are the element shape functions. *Exact* integration[17]¹³ within a ‘brick’ element, for quartic polynomial terms then suffices for equation (9). Since incompatible displacement models [59, 61, 27] are unavoidable for *locking-free* finite elements, the Rayleigh modes are equally suitable for any finite element in \Re^m that has 2^m nodes with m number of degrees-of-freedom per node.

In particular, the present derivation is *not* dependent on the orientation nor the location of the (x, y, z) frame. Hence, the question of curved elements only arises while *analytically* integrating the energy density functions in stiffness matrices and nodal loads (as virtual work quantities).

1.6 Rayleigh modes with cubic (x, y, z) polynomials

Each i^{th} . Rayleigh mode $\psi_i(x, y, z)$ is in the following vector form:

$$\psi_i(x, y, z) = \begin{Bmatrix} \psi_i^{(x)}(x, y, z) \\ \psi_i^{(y)}(x, y, z) \\ \psi_i^{(z)}(x, y, z) \end{Bmatrix} : \text{satisfies tensor transformation rules} \quad (10)$$

In any arbitrary direction α the component of $\psi_i(x, y, z)$ is $\psi_i^{(\alpha)}(x, y, z)$ and

$$\psi_i(x, y, z) \text{ satisfies equilibrium } \textit{point-wise} \quad (11)$$

For every Rayleigh mode, equation (10) is calculated from:

$$\begin{Bmatrix} \wp_x^3(x, y, z) \\ \wp_y^3(x, y, z) \\ \wp_z^3(x, y, z) \end{Bmatrix}; \quad \wp^3(x, y, z) : \text{cubic polynomial in } x, y, z \text{ such that} \quad (12)$$

the triplet satisfies equilibrium *point-wise*

¹³ the paper: ‘exact integration within polyhedra’ is currently under review, for analogous two-dimensional problems, *vide* [14, 12].

1.6.1 Incompressible cases

For two-dimensional problems, *vide* [16] seven pairs of shape functions, each yielding zero dilatation, were obtained from quadratic polynomials. For each element there are seven modal participation factors and a uniform pressure constituted the eight unknowns. Since a nodal displacement is not a degree-of-freedom¹⁴, consequently, no attempt was made to assemble the stiffness matrix is assembled. Instead, explicit equations of *nodal* equilibrium and compatibility were solved simultaneously. It is important to recognize that all nodal forces are computed as virtual work quantities with respect to the Rayleigh modal degrees-of-freedom then they are transformed into equivalent nodal loads according to the virtual work relations between the Rayleigh modal and element nodal descriptions. Reference [16] contains all details of four node elements — convex, concave and triangle with a side node.

The idea is seamlessly extended to three-dimensional brick elements. Twenty three triplets of shape functions, each yielding zero dilatation, are obtained from cubic polynomials. For each element, the associated modal participation factors and a uniform ‘element pressure’ are solved from explicit equations of *nodal* equilibrium and compatibility. Algebraic details of [16] are not repeated here.

1.7 Shape functions from Rayleigh modes: compressible solid $\nu \neq \frac{1}{2}$

In conformity with the modal displacement vectors, $\boldsymbol{\psi}_i(x, y, z)$ in equation (10), the finite element shape function, which is associated with the nodal degrees-of-freedom j , $\phi_j(x, y, z)$ has the following vector structure with components:

$$\phi_j(x, y, z) = \begin{Bmatrix} \phi_j^{(x)}(x, y, z) \\ \phi_j^{(y)}(x, y, z) \\ \phi_j^{(z)}(x, y, z) \end{Bmatrix} : \text{satisfies equilibrium } \textit{point-wise} \quad (13)$$

this is a linear combinations of Rayleigh mode vectors $\boldsymbol{\psi}_i(x, y, z)$ of equation (10) :

$$\phi_j(x, y, z) = \lambda_{ji} \boldsymbol{\psi}_i(x, y, z); \quad (14)$$

$$[\lambda] : \text{modal contribution to shape function} \quad (15)$$

¹⁴ because independent values will cause dilatation

The relationship between ϕ_j and ψ_i is dictated by the Klocker condition ¹⁵:

$$\text{with } c_m = (x_m, y_m, z_m) : \text{nodal coordinate for node number } m \quad (16)$$

$$\phi_j^{(x)}(x_m, y_m, z_m) = \delta_{j,(3m-2)}$$

$$\text{leads to : } \phi_j^{(y)}(x_m, y_m, z_m) = \delta_{j,(3m-1)} \quad (17)$$

$$\phi_j^{(z)}(x_m, y_m, z_m) = \delta_{j,(3m)}$$

$$\text{where the Kronecker symbol: } \delta_{m,n} = \begin{cases} 1, & \text{if } m = n \\ 0, & \text{if } m \neq n \end{cases} \quad (18)$$

Details for two-dimensional plane stress/strain problems can be found in [17].

1.7.1 Finite elements from Rayleigh modes

Finite element nodal and the Rayleigh modal variables are:

$$\{r\} : \text{list of nodal displacements; } \{R\} : \text{list of nodal forces} \quad (19)$$

$$\{q\} : \text{list of modal participation factors;} \quad (20)$$

$$\{Q\} : \text{list of modal generalized forces: conjugate of } \{q\} \quad (21)$$

The matrix $[G_{rq}]$, without any ambiguity $[G]$, transformations $\{q\}$ to $\{r\}$:

$$\{r\} = [G_{rq}] \{q\} \text{ or } \{r\} = [G] \{q\} \rightarrow \{q\} = [G]^{-1} \{r\} \quad (22)$$

For this brick finite element there are twenty four nodal degrees-of-freedom and equal number of Rayleigh modes. For this square $[G]$ the inversion is assumed to exist at the least in the generalized Moore-Penrose sense. Concavity in the brick geometry is inconsequential.

1.7.2 Relationship between **modal** and nodal strain-displacement matrices

The physical strains are independent of the choice of modal or nodal perspective, hence:

$$\begin{aligned} \{\epsilon_{xx} \ \epsilon_{yy} \ \epsilon_{zz} \ \gamma_{xy} \ \gamma_{yz} \ \gamma_{zx}\} &= \{q\}^T [b_q]^T = \{r\}^T [b_r]^T = \{q\}^T [G]^T [b_r]^T \\ &\rightarrow [b_r] = [b_q][G]^{-1} \text{ or } [b_r]^T = [G^T]^{-1}[b_q^T] \end{aligned} \quad (23)$$

¹⁵ in the vector form for \mathbb{R}^3

1.7.3 Relationship between **modal** and nodal element stiffness matrices

From the energy balance principle:

$$\{R\}^T \{r\} = \{Q\}^T \{q\} \rightarrow \{R\} = [G^T]^{-1} \{Q\} \quad (24)$$

Now the *modal* stiffness matrix $[\mathcal{K}_{qq}]$ for an arbitrary polyhedron Ω can be obtained from:

$$[\mathcal{K}_{qq}] = \int_{\Omega} [b_q]^T [d] [b_q] d\Omega \quad (25)$$

$$: \text{exactly without any numerical scheme} \quad (26)$$

It is important to emphasize that the integrand in equation (25) comprises of polynomial terms of the form: $x^{\alpha_1} y^{\alpha_2} z^{\alpha_3}$ as in equation (2), hence, analytical integration within an arbitrary polyhedra is possible, *vide* [15].

Finally, the conventional finite element (nodal) stiffness matrix $[\mathcal{K}_{rr}]$ or simply $[\mathcal{K}]$ can be calculated from:

$$[\mathcal{K}_{rr}] = [\mathcal{K}] = [G^T]^{-1} [\mathcal{K}_{qq}] [G]^{-1} \quad (27)$$

for more details *vide* [17].

The *modal* strain displacement transformation matrix $[b_q]$ is through by:

$$\text{the row list : } \{\epsilon_{xx} \ \epsilon_{yy} \ \epsilon_{zz} \ \gamma_{xy} \ \gamma_{yz} \ \gamma_{zx}\} = \{q\}^T [b_q]^T \quad (28)$$

1.7.4 General elements admitting volume change

Interpolant polynomials are considered according to the degrees of their parts. First, the constant and the linear terms are selected to reproduce the *twelve*¹⁶ modes akin to tetrahedrons. This accounts for the *six* rigid body displacements and *six* constant stress distributions. Secondly, the quadratic terms reproduce *six* pure bending cases where zero shear condition is explicitly enforce to discard any shear locking whatsoever. It is important to recognize, for isotropic elastic continua, that for these pure bending modes the Poisson's ratio appear in the polynomial coefficients. Finally, the cubic terms a subjective judgement is made in this paper. Parabolic shear stress distributions, which appear in analytical solutions for a beam with constant shear force, are reproduced *exactly*. Since for each directional spanning of a beam there could be two orthogonal bending there are then *six* (cantilever beam) modes. These *twenty four* Rayleigh modes yield *twenty four* shape functions via linear combinations¹⁷ using the definition in equation (17).

¹⁶ for incompressible solids, the dilatational mode is eliminated; therein, eleven displacement mode and a constant pressure may constitute the twelve degrees-of-freedom (in the general sense)

¹⁷ Merely from geometrical considerations the Rayleigh modes are related to the nodal displacements (via the $[G]$ matrix — references [16,17] describe in detail)

The stiffness matrix \mathcal{K} in equation (9) has to be evaluated from equation (12). The strain displacement matrix \mathcal{B} is a quadratic function in x, y, z . All that is needed for \mathcal{K} are the fourth order polynomial terms presented in the left hand side of equation (2), its right hand side shows the exact integral values for a test hexahedral element shown in **Fig. 1**.

1.8 Poisson's ratio(s): a *persistent* nondimensional system parameter(s) to enforce *point-wise* the zero body force requirement in a *patch test*

Locking-free finite elements cannot be achieved without explicitly involving the Poisson's ratio in the shape functions. This is evidenced by the requirement of satisfying the equilibrium equation *pointwise*:

$$\mathbf{f}(x, y, z) = 0, \forall(x, y, z); \quad \text{vide equation (6)} \quad (29)$$

For the two dimensional case detailed analysis can be found in [17]. Those arguments are indeed valid for this three-dimensional formulation, hence not repeated here. A solid with twenty one Poisson's ratios poses no problem whatsoever¹⁸. This paper furnishes all derivations in a tensorial sense, hence the following treatment of Poisson's ratios in the invariant form is warranted.

1.8.1 Poisson's ratios for the generalized case

The stress σ and strain ϵ tensors are related through the fourth rank compliance tensor \mathbf{C} in the following incremental form:

$$\Delta\epsilon = \mathbf{C} \cdot \Delta\sigma \text{ or } \Delta\epsilon_{ij} = \mathbf{C}_{ijkl} \sigma_{kl} \quad (30)$$

For two orthogonal directions \mathbf{m} and \mathbf{n} , the corresponding Poisson's ratio $\nu_{\beta\alpha}$ is given by:

$$\nu_{\beta\alpha} = \nu_{\alpha\beta} = -\frac{\alpha_i \alpha_j \beta_k \beta_l \mathbf{C}_{ijkl}}{\beta_i \beta_j \beta_k \beta_l \mathbf{C}_{ijkl}} \quad (31)$$

The proposed methodology can be extended¹⁹ to encompass the generalized stress strain relation equations (30) and (31).

1.8.2 Isotropic constitutive equation: an important special case

For the spacial case of isotropy:

$$\sigma_{ij} = \lambda_o \epsilon_{kk} + 2\mu \epsilon_{ij}; \quad \text{for } i \neq j : \gamma_{ij} = 2\epsilon_{ij} \quad (32)$$

¹⁸ can be incorporated in equation (5)

¹⁹ the symbolic algebraic computer code does *not* need any modification to accept the general stress-strain relation in terms of \mathbf{C}_{ijkl}

will be used here. The Lamé constants λ_o ²⁰, and μ are connected via the single poisson's ratio ν :

$$\lambda_o = \frac{2 \mu \nu}{1 - 2\nu} \quad (33)$$

For incompressible cases, such as $\nu = \frac{1}{2}$ the nodal displacements are *not* independent variables. For constant pressure elements, the entire analysis, *i.e.*, enforcement of nodal equilibrium and compatibility, is to be carried out with the modal participation factors and a uniform pressure — to be the element level independent variable — as in two-dimensional [16] problems.

2 Derivation of Rayleigh modes

Modeling with both compressible and incompressible solids are addressed here. For three-dimensional cases, from equation (9), the lower order cube element will admit cubic polynomial, as a natural extension to Taig [47]. Hence the same is selected here.

The ‘high accuracy’ formulation generates Rayleigh modes independent of convexities in the element.

2.1 Cubic interpolants in the physical (x, y, z) frame

The full cubic polynomial displacement expressions are in the following form:

$$\begin{aligned} u(x, y, z) = & a(1) + x * a(2) + y * a(3) + z * a(4) \\ & + x^2 * a(5) + x * y * a(6) + y^2 * a(7) \\ & + x * z * a(8) + y * z * a(9) + z^2 * a(10) \\ & + x^3 * a(11) + x^2 * y * a(12) + x * y^2 * a(13) + y^3 * a(14) \\ & + x^2 * z * a(15) + x * y * z * a(16) + y^2 * z * a(17) \\ & + x * z^2 * a(18) + y * z^2 * a(19) + z^3 * a(20) \end{aligned} \quad (34)$$

In order to emphasize the polynomial terms, as those appeared in the left hand side of equation (2), the notation with post-fix coefficients is employed in equation (34). Multiplication is explicitly indicated by *.

The other two displacement components v, w along y, z respectively, are obtained by cyclic replacement; to obtain v from u replace a by b and then x by y , y by z and z by x . Similarly, w is obtained from v with coefficient

²⁰ in order to avoid conflict of notation with the modal participation factor λ in equation (15), here the isotropic Lamé constant is indicated with a subscript of zero

$c(i)$:

$$\begin{aligned}
v(x, y, z) = & b(1) + y * b(2) + z * b(3) + x * b(4) \\
& + y^2 * b(5) + y * z * b(6) + z^2 * b(7) \\
& + x * y * b(8) + x * z * b(9) + x^2 * b(10) \\
& + y^3 * b(11) + y^2 * z * b(12) + y * z^2 * b(13) + z^3 * b(14) \\
& + x * y^2 * b(15) + x * y * z * b(16) + x * z^2 * b(17) \\
& + x^2 * y * b(18) + x^2 * z * b(19) + x^3 * b(20)
\end{aligned} \tag{35}$$

$$\begin{aligned}
w(x, y, z) = & c(1) + z * c(2) + x * c(3) + y * c(4) \\
& + z^2 * c(5) + x * z * c(6) + x^2 * c(7) \\
& + y * z * c(8) + x * y * c(9) + y^2 * c(10) \\
& + z^3 * c(11) + x * z^2 * c(12) + x^2 * z * c(13) + x^3 * c(14) \\
& + y * z^2 * c(15) + x * y * z * c(16) + x^2 * y * c(17) \\
& + y^2 * z * c(18) + x * y^2 * c(19) + y^3 * c(20)
\end{aligned} \tag{36}$$

To emphasize the tensorial invariant characteristic of the displacement function the vector $\varpi(x, y, z)$ is introduced in equation (3). It is conceptually convenient to treating each degree of polynomial with the following physical interpretation:

$$\varpi(x, y, z) = \varpi^{(1)}(x, y, z) + \varpi^{(2)}(x, y, z) + \varpi^{(3)}(x, y, z) \tag{37}$$

— full cubic polynomial vector with 30 unknown coefficients

$$\varpi^{(1)}(x, y, z) : \text{linear terms for simplex modes} \tag{38}$$

— Courant interpolants in a tetrahedron (pyramid)

$$\varpi^{(2)}(x, y, z) : \text{quadratic terms for flexural modes} \tag{39}$$

— admitted in a 6 node pentahedron, triangular prism

$$\varpi^{(3)}(x, y, z) : \text{cubic terms for quadratic stress modes} \tag{40}$$

— appears in a brick

All *elliptic* partial differential equations of mathematical physics are of even order, $2n$, starting with two, $n = 1$. Hence one way to select Ritz test function is to deploy polynomials of order n . Hence, the first order polynomials will satisfy the field equations in the *strong* sense. Courant [8] employed linear test functions in his development of potentials and steady vibrations that are governed by elliptic partial differential equations. This is the principal reason why Courant's formulation will always satisfy the *patch tests*²¹.

²¹ within the context of this paper, rigid body motions and linear stress distributions are exactly reproduced in *single element tests*

2.2 Compressible elements: Poisson's ratio $\nu \neq \frac{1}{2}$

Here twenty four Rayleigh modes are derived in order to generating twenty four shape functions.

2.2.1 Extension of Courant's triangulation

The twelve parameters, $a[1] \dots a[4], b[1] \dots b[4], c[1] \dots c[4]$, are assigned unit value, at a time, with others set to zero. Thus the twelve Rayleigh modes, which pertain to tetrahedrons, are obtained as the following twelve vectors:

$$\begin{array}{c} 1 \left| \begin{array}{c} x \\ 0 \\ 0 \end{array} \right| y \left| \begin{array}{c} z \\ 0 \\ 0 \end{array} \right| 0 \left| \begin{array}{c} 0 \\ 1 \\ 0 \end{array} \right| 0 \left| \begin{array}{c} 0 \\ y \\ 0 \end{array} \right| 0 \left| \begin{array}{c} 0 \\ z \\ 0 \end{array} \right| 0 \left| \begin{array}{c} 0 \\ x \\ 1 \end{array} \right| 0 \left| \begin{array}{c} 0 \\ 0 \\ z \end{array} \right| 0 \left| \begin{array}{c} 0 \\ 0 \\ x \end{array} \right| 0 \left| \begin{array}{c} 0 \\ 0 \\ y \end{array} \right| \end{array} \quad (41)$$

each column represents the (x, y, z) components of one Rayleigh mode

It can be readily observed that *all* rigid body modes and linear stress distribution cases are included in equation (41).

2.2.2 Rejection of shear locking modes

The quadratic terms enter into the shape functions for triangular prisms. Arbitrary selection of eighteen parameters, $a[5] \dots a[10], b[5] \dots b[10], c[5] \dots c[10]$, will violate equilibrium, $\mathbf{f} \neq 0$, *vide* equation (8). Types of the following expression is obtained *by satisfying* equation (8):

$$\begin{aligned} u = & a(5)x^2 + a(7)y^2 + a(9)yz + a(10)z^2 + 4b(5)\nu xy + 4b(7)\nu xy + \\ & 4b(10)\nu xy - 4b(5)xy - 2b(7)xy - 2b(10)xy - b(6)xz - c(8)xy + \\ & 4c(5)\nu xz + 4c(7)\nu xz + 4c(10)\nu xz - 4c(5)xz - 2c(7)xz - 2c(10)xz \end{aligned} \quad (42)$$

that *without exception* should involve the Poisson's ratio ν , are essential. The associated v, w expressions, to satisfy pointwise equilibrium, are:

$$\begin{aligned} v = & 4a(5)\nu xy + 4a(7)\nu xy + 4a(10)\nu xy - 4a(5)xy - 2a(7)xy - 2a(10)xy \\ & + b(10)x^2 + b(9)xz + b(5)y^2 + b(6)yz + b(7)z^2 - c(6)xy \end{aligned} \quad (43)$$

$$w = c(7)x^2 + c(9)xy + c(6)xz + c(10)y^2 + c(8)yz + c(5)z^2 \quad (44)$$

To forsake shear locking, one selects only those parts of $\{u, v, w\}$ that lead to zero shear strains. The results are:

$$u(x, y, z) = a(5)x^2 + \frac{a(5)y^2}{\nu} - a(5)y^2 - a(10)y^2 + a(10)z^2 - \frac{2b(5)xy}{\nu} + 2b(5)xy + 2b(7)xy - \frac{2c(5)xz}{\nu} + 2c(5)xz + 2c(10)xz \quad (45)$$

$$v(x, y, z) = -\frac{2a(5)xy}{\nu} + 2a(5)xy + 2a(10)xy + \frac{b(5)x^2}{\nu} - b(5)x^2 - b(7)x^2 + b(5)y^2 + b(7)z^2 - 2c(10)yz \quad (46)$$

$$w(x, y, z) = -2a(10)xz - 2b(7)yz + \frac{c(5)x^2}{\nu} - c(5)x^2 - c(10)x^2 + c(10)y^2 + c(5)z^2 \quad (47)$$

The coupled (quadratic polynomial) vector field $\varpi^{(2)} = \{u, v, w\}$ has six undetermined parameters:

$$a(5), a(10), b(5), b(7), c(5) \text{ and } c(10) \quad (48)$$

Each is assigned unit value, in turn, with others set to zero leading to the six shear-free flexure modes that are associated with pure bending cases:

$$\left(\begin{array}{c|c|c} u(x, y, z) & v(x, y, z) & w(x, y, z) \\ \hline x^2 - \frac{y^2(\nu-1)}{\nu} & \frac{2xy(\nu-1)}{\nu} & 0 \\ z^2 - y^2 & 2xy & -2xz \\ \frac{2xy(\nu-1)}{\nu} & \left(\frac{1}{\nu} - 1\right)x^2 + y^2 & 0 \\ 2xy & z^2 - x^2 & -2yz \\ \frac{2xz(\nu-1)}{\nu} & 0 & \left(\frac{1}{\nu} - 1\right)x^2 + z^2 \\ 2xz & -2yz & y^2 - x^2 \end{array} \right) \quad (49)$$

In the appendix the Rayleigh modal responses are arranged in columns. However, for clarity the polynomial quadratic modes in equation (49) are presented as rows.²²

²² Each row in equation (49) represents a displacement vector in equilibrium without body force. This poses an insignificant inconsistency, *vide* equation (41) where each column represents a distinct Rayleigh mode, however no ambiguity is encountered.

To facilitate verification, the author did *not* replace $\nu - 1$ by $-(1 - \nu)$ in equation (49) — the original output from *Mathematica* had to be changed by adding a custom tailored function. For the general anisotropic case the output becomes too lengthy due to 21 Poisson's ratios. However, any computer algebra system will handle such expressions symbolically without any user intervention.

2.2.3 The three-dimensional element — additional stipulated modes

The cubic terms in the displacement vector $\varpi(x, y, z)$, *vide* equation (3), yields quadratic stress fields. Out of 30 constants, 9 are eliminated to ensure equilibrium. The candidate displacements are:

$$\begin{aligned}
u &= \frac{x^3(a(13)(1-2\nu) + a(18)(1-2\nu) + b(18) + c(13))}{6(\nu-1)} \\
&\quad + \frac{1}{3}y^3(-a(12) - a(19) + b(15) + b(17) + 3b(20)) \\
&\quad + y^2z(-a(15) - 3a(20) + c(12) + 3c(14) + c(19)) + a(12)x^2y \\
&\quad + a(15)x^2z + a(13)xy^2 + a(18)xz^2 + a(19)yz^2 \\
&\quad + a(20)z^3 - 2xyz(b(12) - 2c(15)(\nu-1) - (c(17) + 3c(20))(2\nu-1)) \\
v &= \frac{y^3(a(13) + b(13)(1-2\nu) - 2b(18)\nu + b(18) + c(18))}{6(\nu-1)} \\
&\quad - 2xyz(a(15) - 2c(12)(\nu-1) - (3c(14) + c(19))(2\nu-1)) \\
&\quad + \frac{1}{3}z^3(-b(12) - b(19) + c(15) + c(17) + 3c(20)) \\
&\quad + b(20)x^3 + b(18)x^2y + b(19)x^2z + b(15)xy^2 \\
&\quad + b(17)xz^2 + b(12)y^2z + b(13)yz^2 \\
w &= \frac{z^3(a(18) + b(13) - (c(13) + c(18))(2\nu-1))}{6(\nu-1)} \\
&\quad - 2xyz(a(12) - 2b(15)(\nu-1) - (b(17) + 3b(20))(2\nu-1)) \\
&\quad + c(14)x^3 + c(17)x^2y + c(13)x^2z + c(19)xy^2 + c(12)xz^2 \\
&\quad + c(20)y^3 + c(18)y^2z + c(15)yz^2
\end{aligned} \tag{50}$$

Expressions in equation (50) are *not* unique, but always 21 constants survive.

Different finite element applications with different purposes can select tensorially invariant statement to determine the 21 coefficients in equation (50). Now, the displacement profile in a cantilever beam with an end force is selected ²³. The following two displacement vectors are solved to reproduce

²³ without referring to any coordinate system one can state that the selected axial stress in any arbitrary direction is proportional to the product of the location in that direction and in a transverse one, this in turn breaks into two statements that the two orthogonal other direction will guarantee the tensor requirement

$\sigma_{xx} = x * y$ and $x * z$:

$$\sigma_{xx} = x * y \rightarrow \varpi(x, y, z) = \begin{Bmatrix} \frac{x^2 y}{4} - \frac{y^3}{12} \\ 0 \\ -\frac{1}{2}xyz \end{Bmatrix} \quad \text{and} \quad (51)$$

$$\sigma_{xx} = x * z \rightarrow \varpi(x, y, z) = \begin{Bmatrix} \frac{x^2 z}{4} - \frac{z^3}{12} \\ -\frac{1}{2}xyz \\ 0 \end{Bmatrix} \quad (52)$$

Similarly, four other Rayleigh modes are selected by interchanging x, y, z of equations (51) and (52), in the cyclic order, leading to the following 6 cubic displacement profiles:

$$\left(\begin{array}{c|c|c} \text{from } \sigma_{xx} & \text{from } \sigma_{yy} & \text{from } \sigma_{zz} \\ \hline \text{from equation (51)} : & \begin{Bmatrix} \frac{x^2 y}{4} - \frac{y^3}{12} \\ 0 \\ -\frac{1}{2}xyz \end{Bmatrix} & \begin{Bmatrix} -\frac{1}{2}xyz \\ \frac{y^2 z}{4} - \frac{z^3}{12} \\ 0 \end{Bmatrix} & \begin{Bmatrix} 0 \\ -\frac{1}{2}xyz \\ \frac{xz^2}{4} - \frac{x^3}{12} \end{Bmatrix} \\ \hline \text{from equation (52)} : & \begin{Bmatrix} \frac{x^2 z}{4} - \frac{z^3}{12} \\ -\frac{1}{2}xyz \\ 0 \end{Bmatrix} & \begin{Bmatrix} 0 \\ \frac{xy^2}{4} - \frac{x^3}{12} \\ -\frac{1}{2}xyz \end{Bmatrix} & \begin{Bmatrix} -\frac{1}{2}xyz \\ 0 \\ \frac{yz^2}{4} - \frac{y^3}{12} \end{Bmatrix} \end{array} \right) \quad (53)$$

2.2.4 The **modal** strain-displacement transformation matrix

In the interest of clarity $[b_q]$ is partitioned into four 6x6 matrices in the following form:

$$[b_q] = [[b_q^{(1)}], [b_q^{(2)}], [b_q^{(3)}], [b_q^{(4)}]] \quad \text{and thereby:} \quad (54)$$

$$[b_q^{(1)}] = \begin{bmatrix} 0 & 1 & 0 & 0 & 0 & 0 \\ 0 & 0 & 0 & 0 & 0 & 1 \\ 0 & 0 & 0 & 0 & 0 & 0 \\ 0 & 0 & 1 & 0 & 0 & 0 \\ 0 & 0 & 0 & 0 & 0 & 0 \\ 0 & 0 & 0 & 1 & 0 & 0 \end{bmatrix}; \quad [b_q^{(2)}] = \begin{bmatrix} 0 & 0 & 0 & 0 & 0 & 0 \\ 0 & 0 & 0 & 0 & 0 & 0 \\ 0 & 0 & 0 & 1 & 0 & 0 \\ 0 & 1 & 0 & 0 & 0 & 0 \\ 1 & 0 & 0 & 0 & 0 & 1 \\ 0 & 0 & 0 & 0 & 1 & 0 \end{bmatrix} \quad (55)$$

are the rigid-body and uniform strain modes that are mandatory, and are always necessary and sufficient for simplex (in this case tetrahedron) elements. From the point of view of Iron's *patch tests*, which caution of shear-locking, the quadratic displacement fields that yield linear strains (and stresses for the

homogeneous constitutive case with constant elements in the $[d]$ matrix) led to the following component of the element strain-displacement matrix:

$$[b_q^{(3)}] = \begin{bmatrix} 2x & 0 & \frac{2y(\nu-1)}{\nu} & 2y & \frac{2z(\nu-1)}{\nu} & 2z \\ \frac{2x(\nu-1)}{\nu} & 2x & 2y & 0 & 0 & -2z \\ 0 & -2x & 0 & -2y & 2z & 0 \\ 0 & 0 & 0 & 0 & 0 & 0 \\ 0 & 0 & 0 & 0 & 0 & 0 \\ 0 & 0 & 0 & 0 & 0 & 0 \end{bmatrix} \quad (56)$$

For three-dimensional cases, the cubic terms in the (coupled) displacement fields permit quadratic stress distributions. Here the structural mechanics results of stress distribution in a cantilever beam with end load have been captured:

$$[b_q^{(4)}] = \quad (57)$$

$$\begin{bmatrix} \frac{xy}{2} & \frac{xz}{2} & -\frac{yz}{2} & 0 & 0 & -\frac{yz}{2} \\ 0 & -\frac{xz}{2} & \frac{yz}{2} & \frac{xy}{2} & -\frac{xz}{2} & 0 \\ -\frac{xy}{2} & 0 & 0 & -\frac{xy}{2} & \frac{xz}{2} & \frac{yz}{2} \\ \frac{1}{4}(x^2 - y^2) & -\frac{yz}{2} & -\frac{xz}{2} & \frac{1}{4}(y^2 - x^2) & -\frac{yz}{2} & -\frac{xz}{2} \\ -\frac{xz}{2} & -\frac{xy}{2} & \frac{1}{4}(y^2 - z^2) & -\frac{xz}{2} & -\frac{xy}{2} & \frac{1}{4}(z^2 - y^2) \\ -\frac{yz}{2} & \frac{1}{4}(x^2 - z^2) & -\frac{xy}{2} & -\frac{yz}{2} & \frac{1}{4}(z^2 - x^2) & -\frac{xy}{2} \end{bmatrix}$$

Since the elastic response fields do not uniformly converge as $\nu \rightarrow \frac{1}{2}$ the incompressible modes *cannot* be obtained from equations (56) and (57). An independent derivation for the Rayleigh modes follows.

2.3 Incompressible solids

Starting with the form of equation (34), there are 60 unknown parameters in the vector-valued shape function $\varpi(x, y, z) = \{u(x, y, z), v(x, y, z), w(x, y, z)\}$:

$$a[1] \dots a[20], b[1] \dots b[20], c[1] \dots c[20] \quad (58)$$

Incompressibility demands:

$$\frac{\partial u}{\partial x} + \frac{\partial v}{\partial y} + \frac{\partial w}{\partial z} = 0, \quad \text{for all } x, y, z \quad (59)$$

that leads to the following possible interrelations between the parameters:

$$\begin{aligned} a[2] &\rightarrow -b[2] - c[2], a[8] \rightarrow -b[6] - 2c[5], a[5] \rightarrow -\frac{b[8]}{2} - \frac{c[6]}{2}, \\ a[6] &\rightarrow -2b[5] - c[8], a[18] \rightarrow -b[13] - 3c[11], a[15] \rightarrow -\frac{b[16]}{2} - c[12], \\ a[11] &\rightarrow -\frac{b[18]}{3} - \frac{c[13]}{3}, a[16] \rightarrow -2b[12] - 2c[15], \\ a[12] &\rightarrow -b[15] - \frac{c[16]}{2}, a[13] \rightarrow -3b[11] - c[18] \end{aligned} \quad (60)$$

These ten substitutions make the incompressible vector-valued shape function $\varpi^o(x, y, z)$ to contain 50 constants, in the following three parts:

$$\varpi^o(x, y, z) = \varpi_1^o(x, y, z) + \varpi_2^o(x, y, z) + \varpi_3^o(x, y, z) \quad (61)$$

$$\varpi_1^o(x, y, z) : \text{“triangulation” modes} \quad (62)$$

$$\varpi_2^o(x, y, z) : \text{“flexural” modes} \quad (63)$$

$$\varpi_3^o(x, y, z) : \text{“quadratic stress” modes} \quad (64)$$

in particular:

$$\varpi_1^o(x, y, z) = \begin{Bmatrix} a(3)y + a(4)z + a(1) + x(-b(2) - c(2)) \\ b(4)x + b(2)y + b(3)z + b(1) \\ c(3)x + c(4)y + c(2)z + c(1) \end{Bmatrix} \quad (65)$$

therein, the 11 parameters are associated with 6 rigid body modes and 5 deviatoric modes. These eleven modes are evaluated by setting one parameter to unity and rest to zero, at a time leading to:

$$\begin{array}{c|c|c|c|c|c|c|c|c|c|c|c} 1 & y & z & 0 & -x & 0 & 0 & 0 & -x & 0 & 0 \\ 0 & 0 & 0 & 1 & y & z & x & 0 & 0 & 0 & 0 \\ 0 & 0 & 0 & 0 & 0 & 0 & 0 & 1 & z & x & y \end{array} \quad (66)$$

The flexural modes contain quadratic terms in x, y, z and free from shear strains:

$$0 = \frac{\partial u}{\partial y} + \frac{\partial v}{\partial x} = \frac{\partial v}{\partial z} + \frac{\partial w}{\partial y} = \frac{\partial w}{\partial x} + \frac{\partial u}{\partial z}, \quad \text{for all } x, y, z \quad (67)$$

and yields the following possible interrelations between the parameters:

$$\begin{aligned} a[7] &\rightarrow -(b[8]/2), a[9] \rightarrow 0, b[9] \rightarrow 0, a[10] \rightarrow -(c[6]/2), \\ b[6] &\rightarrow -2c[10], c[5] \rightarrow c[7] + c[10], b[5] \rightarrow b[7] + b[10], \\ c[8] &\rightarrow -2b[7], c[9] \rightarrow 0 \end{aligned} \quad (68)$$

the six (independent) terms:

$$b(7), b(8), b(10), c(6), c(7), c(10) \quad (69)$$

are responsible for pure bending in two orthogonal planes on each of three orthogonal directions. Thus the three incompressible flexural modes are:

$$\begin{array}{c|c|c|c|c|c} 0 & -\frac{x^2}{2} - \frac{y^2}{2} & -2xy & -\frac{x^2}{2} - \frac{z^2}{2} & -2xz & 0 \\ y^2 + z^2 & xy & x^2 + y^2 & 0 & 0 & -2yz \\ -2yz & 0 & 0 & xz & x^2 + z^2 & y^2 + z^2 \end{array} \quad (70)$$

Following the steps to deriving equation (53) the Rayleigh modes due to cubic displacement profiles are obtained as:

$$\left(\begin{array}{c} \text{from: } \sigma_{xx} \\ \left(\begin{array}{c} \frac{x^2 y}{4} - \frac{y^3}{12} \\ \frac{1}{2} x \left(\frac{z^2}{2} - \frac{y^2}{2} \right) \\ 0 \\ \frac{x^2 z}{4} - \frac{z^3}{12} \\ 0 \\ \frac{1}{2} x \left(\frac{y^2}{2} - \frac{z^2}{2} \right) \end{array} \right) \end{array} \middle| \begin{array}{c} \text{from: } \sigma_{yy} \\ \left(\begin{array}{c} 0 \\ \frac{y^2 z}{4} - \frac{z^3}{12} \\ \frac{1}{2} y \left(\frac{x^2}{2} - \frac{z^2}{2} \right) \\ \frac{1}{2} y \left(\frac{z^2}{2} - \frac{x^2}{2} \right) \\ \frac{x y^2}{4} - \frac{x^3}{12} \\ 0 \end{array} \right) \end{array} \middle| \begin{array}{c} \text{from: } \sigma_{zz} \\ \left(\begin{array}{c} \frac{1}{2} z \left(\frac{y^2}{2} - \frac{x^2}{2} \right) \\ 0 \\ \frac{x z^2}{4} - \frac{x^3}{12} \\ 0 \\ \frac{1}{2} z \left(\frac{x^2}{2} - \frac{y^2}{2} \right) \\ \frac{y z^2}{4} - \frac{y^3}{12} \end{array} \right) \end{array} \right) \quad (71)$$

3 Closed-form development: compressible isotropic solid

The constitutive matrix $[d]$ relates the stress and strain distributions:

$$[d] = \mu \left(\begin{array}{ccc|ccc} \frac{2(\nu-1)}{2\nu-1} & \frac{2\nu}{1-2\nu} & \frac{2\nu}{1-2\nu} & 0 & 0 & 0 \\ \frac{2\nu}{1-2\nu} & \frac{2(\nu-1)}{2\nu-1} & \frac{2\nu}{1-2\nu} & 0 & 0 & 0 \\ \frac{2\nu}{1-2\nu} & \frac{2\nu}{1-2\nu} & \frac{2(\nu-1)}{2\nu-1} & 0 & 0 & 0 \\ \hline 0 & 0 & 0 & 1 & 0 & 0 \\ 0 & 0 & 0 & 0 & 1 & 0 \\ 0 & 0 & 0 & 0 & 0 & 1 \end{array} \right); \quad [d] = \overbrace{\begin{pmatrix} 3 & 1 & 1 & 0 & 0 & 0 \\ 1 & 3 & 1 & 0 & 0 & 0 \\ 1 & 1 & 3 & 0 & 0 & 0 \\ 0 & 0 & 0 & 1 & 0 & 0 \\ 0 & 0 & 0 & 0 & 1 & 0 \\ 0 & 0 & 0 & 0 & 0 & 1 \end{pmatrix}}^{\mu=1 \text{ and } \nu=\frac{1}{4}} \quad (72)$$

now, energy density matrix: $[b_\psi]^T [d] [b_\psi]$ can be calculated from equations (54) through (72).

3.1 Numerical Example: $\mu = 1, \nu = \frac{1}{4}$

A generic brick element with nodal coordinates furnished in equation (1) is shown in **Fig. 1**. The modal stiffness matrix is calculated from the *closed-form* integration results in equation (2) using equations (54) through (57)²⁴. The determinant of $[G]$ is $\frac{109362}{1123}$. The modal and the element stiffness matrices, *vide* equation (27) are presented in the Appendix.

²⁴ the eigenvalues are: 46.716, 67.7913, 18.304, 9.52665, 2.88408, 2.29533, 2.19528, 2.0452, 1.08073, 0.795941, 0.510553, 0.504974, 0.389806, 0.148966, 0.132988, 0.0728463, 0.0619707, 0.0514826 and 0,0,0,0,0

3.1.1 The $[G]$ Matrix

The Rayleigh modes beyond *Courant's triangulation*²⁵ are developed in equations (49) and (53). The modal to nodal transformation matrix $[G]$ is now used to convert the *closed-form* integral of equation (25). The 24 by 24 $[G]$ has been obtained by using the element nodal coordinates of equation (1)²⁶. For convenience of presentation the following form is selected:

$$[G] = \begin{bmatrix} G_{11} & G_{12} & G_{13} \\ G_{21} & G_{22} & G_{23} \\ G_{31} & G_{32} & G_{33} \end{bmatrix} \quad (73)$$

The numerical values of the submatrices in equation (73) are furnished in equations (84) through (87).

4 Conclusions: what is a ‘high accuracy’ finite element

MacNeal, in [36,35], systematically described the limitations of isoparametric formulations, especially with plane stress/strain four node quadrilaterals. He elaborated the *locking-phenomena* due to *shear*, *Poisson's effect* and *shape distortion*. He conclusively proved the deficiency inspite of various innovative numerical integration schemes that led to stiffness matrices. In the three-dimensional isoparametric formulation:

$$\begin{Bmatrix} u(\eta, \xi, \zeta) \\ v(\eta, \xi, \zeta) \\ w(\eta, \xi, \zeta) \end{Bmatrix} = \begin{bmatrix} N_1 * [I], N_2 * [I], \dots, N_i * [I], \dots, N_8 * [I] \end{bmatrix} \{r\} \quad (74)$$

$$[I] : \text{identity matrix; } * : \text{multiplication operator} \quad (75)$$

$$N_i(\eta, \xi, \zeta) : \text{eight scalar tri-linear functions of coordinates alone} \quad (76)$$

the diagonal structure of the identity matrix $[I]$ decouples the displacement components $\{u(x, y, z), v(x, y, z), w(x, y, z)\}$. In essence, equation (74) forces zero displacements in y and z directions when nodal displacements associated with only the x -degrees-of-freedom are applied. This is contrary to the Poisson effect that cannot be resolved by any means, *e.g.*, application of variational principle, nor by avoiding exact integration to yield the element stiffness matrix. In addition, the isoparametric map constrains all straight edges to remain straight after pure bending. This is true only for sections normal to the neutral axis and not in an arbitrary eight-node (convex) ‘brick’ element. Here, following the successes in two-dimensional problems [19,16,17], where *point-wise* locking-free criteria were met, all numerical quadratures and ‘variational crimes’ are circumvented for the ‘high accuracy’ ‘brick’ element. For problems of mathematical physics where a (positive definite) scalar, *e.g.*, the Eulerian

²⁵ tetrahedrons in this three-dimensional counterpart

²⁶ the procedure does not depend on the spatial dimensionality, hence, the computer program for the two-dimensional case, [17], has been used

or the Dirichlet energy, exists the structural mechanics principle of *virtual work* is synonymous with the Ritz formulation. Clough in [6] elegantly states to identify the finite element nodal forces as virtual work quantities that are identical with the duals of the Ritz coordinates from the variational principle. By no means, utilization of the virtual work principle could be misconstrued to be ‘variational crimes.’ Numerical integration on the computational square brings in the limitation of negative Jacobian for concave elements. Even for scalar problems, the extension of the isoparametric idea for polygonal finite elements with Wachspress coordinates, [55,57,54], which are founded on projective geometry [9], can be challenging. Wilson, in chapter 6 of [60], provides an exposé of numerical integration associated with improved isoparametric formulations but [13,14] completely resolve all such issues.

Point-wise equilibrium *cannot* be achieved when the Buckingham *II*-theorem [4] is ignored by discarding the Poisson’s ratio(s)²⁷ in test functions. Here, *vide* equation (56), the coupled representation of $\{u, v, w\}$ contains the Poisson’s ratio, and no minimization was necessary.

Finally, MacNeal’s theorem [36] whose three-dimensional extension is obvious, conclusively supports searching for alternatives — not to mention the incapability of those methods to model concavities that are germane to large, especially plastic, deformations. The central question of integrating the energy density functions within arbitrary polyhedra persisted. The author in [15] demonstrates the use of divergence theorem to calculate such integrals *analytically*.

4.1 The single element test and limitations of the present formulation

Extensive *patch tests* as in [16,17], have *not* been carried out here. The *Single Element Test* [44] deemed to be adequate with special attention to Clough’s assertion [6] to accounting for the nodal loads on a *patch* as virtual work quantities that are consistent with the Ritz formulation [42].

Using shape functions of the lowest possible order *only* the local convergence can be addressed. Incompatibility on the interface is not addressed within this single element test technic. According to the Ritz formulation [42], nodal compatibility and equilibrium should be adequate. With the fixed number of nodal degree-of-freedom there is no scope to introducing more or higher order interpolants for the brick finite element. Thus only mesh refinement can improve accuracy.

²⁷ Even Poisson himself conjectured that Poisson’s ratio was 1/4 for all isotropic materials (in the *uniconstant theory*)! Assuming an atomic model, with the atoms as point particles, a centrosymmetric lattice [58] interacted by central forces that depended only on the distance. Consequently, the Cauchy relations led the tensorial elastic constants of an anisotropic solid to a Poisson’s ratio of $\frac{1}{4}$ for all materials. After Born [3] two elastic constants μ, ν are universally accepted for isotropy.

4.2 Embellishing existing finite element programs

The major motivation of this research was to improve the response prediction for real-world design engineering problems, for example, difficulties outlined in [45] may be completely eliminated with the proposed ‘high accuracy’ finite elements. In a generic finite element code, *e.g.*, **FEAP** [48], subroutines of ‘high accuracy’ elements can be easily incorporated. Notably, *Mathematica* can automatically generate **FORTRAN** and **C++** modules, moreover, *Modelica* [22, 52] can seamlessly implement the ‘high accuracy’ formulation alongside any existing commercial finite element code.

4.3 Sommerfeld problems motivated ‘high accuracy’ finite elements

For unboundrd domains, *e.g.*, soil foundations, the damping radiation due to outgoing waves must be estimated correctly. To cover the semi-infinite domains, isoparametric finite elements are forsaken in favor of Poisson’s ratio dependent influence coefficients [5, 18]. The cloning algorithm [10] demands defect-free finite elements [37], in identifying the incoming and outgoing waves as two complex conjugate roots of the matrix quadratic equation [11].

4.4 Incompressibility and concavity

In plasticity [34] incompressibility and the formation of concavity cannot be ignored. The ‘high accuracy’ formulation accepts concave, *i.e.*, *dented* brick element, and to enforce incompressibility the procedure of [16] is recommended²⁸ the element stiffness matrix matrix does *not* exist in the conventional sense²⁹. The twenty three Rayleigh modes³⁰ are separately calculated since the right-sided limit of Poisson’s ratio, as $\nu \rightarrow \frac{1}{2}+$, is not permitted in continuum mechanics. Taylor [50] conclusively established the existence of the left-hand limit as $\nu \rightarrow \frac{1}{2}-$, *vide* [49]. The author addresses the $\nu = \frac{1}{2}$ case separately, since incompressibility is a deformation constraint rather than a parameterized statement $\left(e.g., \nu \rightarrow \frac{1}{2}\right)$. The limiting value of the the compressible Rayleigh

²⁸ in fact the same computer program, which was written in *Mathematica*, can be used to forming the equations of nodal equilibrium and compatibility in terms of Rayleigh modal participation factors and uniform element pressures, and subsequently generating finite element solutions for any prescribed boundary value problem

²⁹ the nodal displacements of an incompressible element do not constitute degrees-of-freedom an arbitrary displacement can cause volume change

³⁰ with zero dilatation

modes, equations (49) and (53), will *not* converge to their incompressible counterparts, equations (70) and (71)³¹.

4.5 Generalization for *linear* partial differential equations

The three *coupled* response component $\{\varpi(x, y, z)\}$ for a linear vector field elliptic³² problem³³ of mathematical physics is governed by:

$$\mathcal{L} = \begin{bmatrix} \mathcal{L}_{11} & \mathcal{L}_{12} & \mathcal{L}_{13} \\ \mathcal{L}_{21} & \mathcal{L}_{22} & \mathcal{L}_{23} \\ \mathcal{L}_{31} & \mathcal{L}_{32} & \mathcal{L}_{33} \end{bmatrix}; \quad \mathcal{L}^T \left[[\mathcal{C}\mathcal{L}] \{ \varpi(x, y, z) \} \right] = \{ f(x, y, z) \} \quad (77)$$

$$\mathcal{L}_{ij} : \text{linear partial differential operators} \quad (78)$$

$$\mathcal{C} : \text{is the constitutive matrix — a *positive definite* operator} \quad (79)$$

To capture a stress profile $\{g(x, y, z)\}$ *alongside* the rigid body modes ϖ_o , the the *locking-free* Rayleigh vectors are particular solutions of :

$$\mathcal{C}\mathcal{L} \left[\{ \varpi_i(x, y, z) \} \right] = \{ g(x, y, z) \}; \text{ with} \quad (80)$$

$$\mathcal{L} \left[\{ \varpi_o(x, y, z) \} \right] = \{ 0 \} \quad (81)$$

4.6 Generalization for structural elements

Characteristic non-dimensional parameters (*e.g.*, the Poisson's ratio) intrinsic in the constitutive operator \mathcal{C} in equations (77) and (79) *most likely* will enter into the algebraic expressions of $\{\varpi_i(x, y, z)\}$ in equation (80) but never in $\{\varpi_o(x, y, z)\}$ *vide* equation (81). Structural mechanics problems of plates and shells and via the geometric stiffness matrix stability of structural elements are governed by equation (77). Polynomial test functions provide a systematic way to build up elements with increasing nodes. Since splines are integrable in *closed-form*, they can substitute polynomial series as test functions. *Mathematica* can carry out operations with Wachspress' coordinates [56], which are rational polynomials — Padé approximants, and rational splines [53]. A minor modification of the *Mathematica* code in [15] will permit curved surfaces as demanded in designing shell elements in bio- and nano-technology applications. A suitable multi-domain application, *e.g.*, *Modelica*, will facilitate accurate and efficient 'high accuracy' finite element formulation.

³¹ due to the lack of uniform convergence criterion for the Poisson's ratio around $\frac{1}{2}$. This is the reason why an independent computation was undertaken for the incompressible elements by enforcing zero dilatation in equation (67)

³² Courant captured the essence to be problems of potentials in static equilibrium and steady vibrations [8]

³³ for a scalar response field $\varpi(x, y, z)$, \mathcal{L} is a column matrix

Appendix

This section is provided to aiding code verification during development and incorporating this ‘high accuracy’ element into any existing finite element computer program.

Only the *isotropic* homogeneous properties with the Poisson’s ratio ν and the shear modulus $\mu = 1$ are used. General anisotropic case will not require any more computer programing to carry out steps of equations (42) through (71). Specifically, the numerical examples are carried out with $\nu = \frac{1}{4}$.

In the interest of saving pages the smaller fonts are selected in some tables. The pages, especially for **Fig. 5** should be viewed as PDF with magnification suitable for reading. However, an OCR³⁴ tool can generate an ASCII file³⁵, which should be suitable for inputting in *Mathematica* or a **FORTRAN** program segment, from a printed page.

Efficient codes from *Mathematica* can be effortlessly generated by *MathCode* [23] in **FORTRAN** and **C++**, for example.

Rayleigh modes

The application development steps are as follows³⁶:

1. Isotropic case: *problem independent* ‘brick’ element data with $\mu = 1$:
The physical coordinates are named x, y, z , and the Poisson’s ratio ν .
(a) Compressible, $\nu \neq \frac{1}{2}$, Rayleigh modes:
The three components of the conventional *shear-locking free* modes are in equations (41) and (49).
If the shear force loading on a cantilever beam is selected as the case for which *exact analytical* results are to be reproduced in a *patch test*, then the modes in equation (53) can be used. For other cases the cubic polynomial terms, starting with equation (50) must be determined.
2. Anisotropic solid: compressible and incompressible cases:
The 21 Poisson’s ratios in 6 by 6 \mathbf{C}_{ijkl} , *vide* equation (30), is to be used.
The computer program for the counterpart of equations (53) and (49), equation (30), equations (70) and (71) are to be written by the developer.
3. Element geometry and *closed-form* integration A computer program to execute the steps described in [15] need to be used. Since the *closed-form* indefinite integrals of quartic terms are easy to write even in **FORTRAN**, this step can be generated by *MathCode* [23].

³⁴ Optical Character Recognizing

³⁵ e.g., the author uses: <http://www.irislink.com>

³⁶ Complete symbolic code: In the interest of further research and development the author has prepared a paper³⁷ for ‘The *Mathematica* Journal’ that is currently under review

The Rayleigh modes

displacements	mode II-1	mode II-2	mode II-3	mode II-4	mode II-5	mode II-6	mode II-7	mode II-8	mode II-9	mode II-10	mode II-11	mode II-12
u	1	x	y	z	0	0	0	0	0	0	0	0
v	0	0	0	0	1	y	z	x	0	0	0	0
w	0	0	0	0	0	0	0	0	1	z	x	y

Fig. 2 Modes 1 through 12: Simplex modes

displacements	mode II-13	mode II-14	mode II-15	mode II-16	mode II-17	mode II-18
u	$x^2 - \frac{(\nu-1)y^2}{\nu}$	$z^2 - y^2$	$\frac{2(\nu-1)xy}{\nu}$	$2xy$	$\frac{2(\nu-1)xz}{\nu}$	$2xz$
v	$\frac{2(\nu-1)xy}{\nu}$	$2xy$	$\left(\frac{1}{\nu} - 1\right)x^2 + y^2$	$z^2 - x^2$	0	$-2yz$
w	0	$-2xz$	0	$-2yz$	$\left(\frac{1}{\nu} - 1\right)x^2 + z^2$	$y^2 - x^2$

Fig. 3 Modes 13 through 18: shear-free flexure modes

displacements	mode H-19	mode H-20	mode H-21	mode H-22	mode H-23	mode H-24
u	$-\frac{1}{12}y(y^2-3x^2)$	$-\frac{1}{12}z(z^2-3x^2)$	$-\frac{1}{2}xyz$	0	0	$-\frac{1}{2}xyz$
v	0	$-\frac{1}{2}xyz$	$-\frac{1}{12}z(z^2-3y^2)$	$-\frac{1}{12}x(x^2-3y^2)$	$-\frac{1}{2}xyz$	0
w	$-\frac{1}{2}xyz$	0	0	$-\frac{1}{2}xyz$	$-\frac{1}{12}x(x^2-3z^2)$	$-\frac{1}{12}y(y^2-3z^2)$

Fig. 4 Modes 19 through 24: shear-free flexure modes

Modal to nodal transformation matrix: $[G]$

These matrices must be read as a PDF with needful magnification. These figures are provided for direct input to an OCR application.

The numerical value of $[G]$ is included in the main part, in equations (84) through (87).

1	0	1	0	0	0	0	0	0	0	0	0	3	-1	0	0	0	0	$-\frac{1}{12}$	0	0	0	0	0	0
1	0	0	0	1	1	0	0	0	0	0	0	0	0	1	0	0	0	0	0	0	0	0	0	0
0	0	0	0	0	0	0	0	1	0	0	1	0	0	0	0	0	1	0	0	0	0	0	$-\frac{1}{12}$	0
1	0	0	0	0	0	0	0	0	0	0	0	0	0	0	0	0	0	0	0	0	0	0	0	0
0	0	0	0	1	0	0	0	0	0	0	0	0	0	0	0	0	0	0	0	0	0	0	0	0
0	0	0	0	0	0	0	0	1	0	0	0	0	0	0	0	0	0	0	0	0	0	0	0	0
1	1	0	0	0	0	0	0	0	0	0	0	1	0	0	0	0	0	0	0	0	0	0	0	0
0	0	0	0	1	0	0	1	0	0	0	0	0	0	3	-1	0	0	0	0	0	$-\frac{1}{12}$	0	0	0
0	0	0	0	0	0	0	0	1	0	1	0	0	0	0	0	3	-1	0	0	0	0	$-\frac{1}{12}$	0	0
1	$\frac{65}{54}$	$\frac{46}{35}$	0	0	0	0	0	0	0	0	$\frac{232}{35}$	$\frac{19}{11}$	$-\frac{294}{31}$	$\frac{98}{31}$	0	0	$\frac{2}{7}$	0	0	0	0	0	0	0
0	0	0	0	1	$\frac{46}{35}$	0	$\frac{65}{54}$	0	0	0	$-\frac{294}{31}$	$\frac{98}{31}$	$\frac{91}{15}$	$-\frac{55}{38}$	0	0	0	0	0	0	$\frac{3}{8}$	0	0	0
0	0	0	0	0	0	0	0	1	0	$\frac{65}{54}$	$\frac{46}{35}$	0	0	0	0	$\frac{204}{47}$	$\frac{7}{25}$	0	0	0	0	$-\frac{7}{48}$	$\frac{7}{37}$	
1	0	$\frac{26}{19}$	$\frac{47}{36}$	0	0	0	0	0	0	0	$\frac{73}{13}$	$-\frac{1}{6}$	0	0	0	0	$-\frac{3}{14}$	$-\frac{5}{27}$	0	0	0	0	0	0
0	0	0	0	1	$\frac{26}{19}$	$\frac{47}{36}$	0	0	0	0	0	0	$\frac{58}{31}$	$\frac{29}{17}$	0	$-\frac{193}{54}$	0	0	$\frac{17}{40}$	0	0	0	0	0
0	0	0	0	0	0	0	0	1	$\frac{47}{36}$	0	$\frac{26}{19}$	0	0	0	$-\frac{193}{54}$	$\frac{29}{17}$	$\frac{58}{31}$	0	0	0	0	0	$\frac{10}{27}$	0
1	0	0	1	0	0	0	0	0	0	0	0	0	1	0	0	0	0	0	$-\frac{1}{12}$	0	0	0	0	0
0	0	0	0	1	0	1	0	0	0	0	0	0	0	0	1	0	0	0	0	$-\frac{1}{12}$	0	0	0	0
0	0	0	0	0	0	0	0	1	1	0	0	0	0	0	0	0	0	0	0	0	0	0	0	0
1	$\frac{45}{37}$	0	$\frac{31}{25}$	0	0	0	0	0	0	0	0	$\frac{34}{23}$	$\frac{43}{28}$	0	0	$-\frac{217}{24}$	$\frac{214}{71}$	0	$\frac{3}{10}$	0	0	0	0	0
0	0	0	0	1	0	$\frac{31}{25}$	$\frac{45}{37}$	0	0	0	0	0	0	$\frac{71}{16}$	$\frac{2}{35}$	0	0	0	0	$-\frac{3}{19}$	$-\frac{3}{20}$	0	0	0
0	0	0	0	0	0	0	0	1	$\frac{31}{25}$	$\frac{45}{37}$	0	0	$\frac{214}{71}$	0	$\frac{209}{35}$	$\frac{34}{23}$	0	0	0	0	0	$\frac{13}{41}$	0	0
1	$\frac{107}{67}$	$\frac{21}{11}$	$\frac{47}{27}$	0	0	0	0	0	0	0	$\frac{283}{21}$	$\frac{14}{23}$	$\frac{311}{17}$	$\frac{250}{41}$	$\frac{601}{36}$	$\frac{128}{23}$	$\frac{16}{25}$	$\frac{39}{58}$	$\frac{69}{26}$	0	0	$-\frac{69}{26}$	0	$-\frac{69}{26}$
0	0	0	0	1	$\frac{21}{11}$	$\frac{47}{27}$	$\frac{107}{67}$	0	0	0	$-\frac{311}{17}$	$\frac{250}{41}$	$\frac{599}{53}$	$\frac{11}{23}$	0	$-\frac{206}{31}$	0	$\frac{69}{26}$	$\frac{55}{48}$	$\frac{29}{26}$	$\frac{69}{26}$	0	0	$-\frac{69}{26}$
0	0	0	0	0	0	0	0	1	$\frac{47}{27}$	$\frac{107}{67}$	$\frac{21}{11}$	0	$\frac{128}{23}$	0	$\frac{206}{31}$	$\frac{139}{13}$	$\frac{25}{23}$	$-\frac{69}{26}$	0	0	$-\frac{69}{26}$	$\frac{27}{31}$	$\frac{13}{15}$	0

Fig. 5 G-Matrix

The calculated determinant of $[G]$ is 97.3838. Here is just the evidence that the $[G]^{-1}$ matrix exists: In shape function and stiffness matrix calcula-

Fig. 6 G-inverse matrix

tions, *vide* equations (89) and (27) respectively, $[G]^{-1}$ is encountered. The LU decomposition³⁸ (with partial pivoting) has been used in stress calculations. equation (15): $\phi_j(x, y, z) = \lambda_{ji} \psi_i(x, y, z)$ here $[\lambda]$ is related to $[G]$. Here, Ψ is a 3 by 24 matrix, for each nodal coordinate c_m in equation (16), the column $[\Psi(c_m)]$ is then 24 by 24 and by definition from equation (22):

$$\{r\} = [G] \{q\} \text{ also } \{r\} = [\Psi(c_m)] \{q\}; \quad \therefore [\Psi(c_m)] = [G] \text{ but} \quad (82)$$

$$[G] [\lambda] = [I]: \text{ the identity matrix } \therefore \Phi = \Psi \odot [\lambda] \therefore \Phi^T = [G^T]^{-1} \Psi^T \quad (83)$$

Here the *dot product* is explicitly indicated with \odot .

³⁸ in *Mathematica* the condition number is also returned alongside the L and U and the the permutation matrix

Up to a round-off error of 10^{-3} the submatrices in equation (73) are ³⁹:

$$\begin{aligned} & \overbrace{\begin{pmatrix} 1 & 0 & 0 & 1 & 0 & 0 & 1 & 0 \\ 0 & 0 & 0 & 0 & 0 & 0 & 0 & 0 \\ 0 & 0 & 0 & 0 & 0 & 0 & 0 & 0 \\ 0 & 0 & 0 & 0 & 0 & 0 & 0 & 0 \\ 3 & 0 & 0 & 0 & 0 & 0 & 1 & 0 \\ 0 & 0 & 0 & 0 & 0 & 0 & 0 & -1 \\ -\frac{1}{12} & 0 & 0 & 0 & 0 & 0 & 0 & 0 \\ 0 & 0 & 0 & 0 & 0 & 0 & 0 & -\frac{1}{12} \end{pmatrix}}^{[G_{11}]} ; \quad \overbrace{\begin{pmatrix} 0 & 0 & 0 & 0 & 0 & 0 & 1 & 0 \\ 0 & 1 & 0 & 0 & 1 & 0 & 0 & 1 \\ 0 & 0 & 0 & 0 & 0 & 0 & 0 & 1 \\ 0 & 0 & 0 & 0 & 0 & 0 & 0 & 0 \\ -1 & 0 & 0 & 0 & 0 & 0 & 0 & 0 \\ 0 & 0 & 0 & 0 & 0 & 0 & 0 & 0 \\ 0 & 0 & 0 & 0 & 0 & 0 & 0 & 0 \\ 0 & 0 & 0 & 0 & 0 & 0 & 0 & 0 \end{pmatrix}}^{[G_{12}]} ; \quad \overbrace{\begin{pmatrix} 1 & 0 & 0 & 0 & 0 & 0 & 0 & 0 \\ 0 & 1 & 0 & 0 & 0 & 0 & 0 & 0 \\ 0 & 0 & 1 & 0 & 0 & 1 & 0 & 0 \\ 0 & 0 & 1 & 0 & 0 & 0 & 0 & 0 \\ 0 & 1 & 0 & 0 & 0 & 0 & 0 & 3 \\ 0 & 0 & 1 & 0 & 0 & 0 & 0 & 0 \\ 0 & 0 & 0 & 0 & 0 & 0 & 0 & 0 \\ 0 & 0 & -\frac{1}{12} & 0 & 0 & 0 & 0 & 0 \end{pmatrix}}^{[G_{13}]} \quad (84) \end{aligned}$$

$$\begin{aligned} & \overbrace{\begin{pmatrix} 0 & 1 & 0 & 0 & 1 & 0 & 0 & 1 \\ 0 & 0 & 0 & 0 & \frac{47}{36} & 0 & 0 & 1 \\ 0 & 0 & 0 & 0 & 0 & \frac{47}{36} & 0 & 0 \\ 0 & 0 & 0 & 0 & 0 & 0 & \frac{47}{36} & 0 \\ 0 & \frac{232}{35} & -\frac{294}{31} & 0 & \frac{73}{13} & 0 & 0 & 0 \\ 0 & \frac{98}{31} & -\frac{55}{38} & 0 & 0 & \frac{29}{17} & -\frac{193}{54} & 0 \\ 0 & \frac{2}{7} & 0 & 0 & -\frac{3}{14} & 0 & 0 & 0 \\ 0 & 0 & \frac{3}{8} & 0 & 0 & 0 & 0 & 0 \end{pmatrix}}^{[G_{21}]} ; \quad \overbrace{\begin{pmatrix} 0 & \frac{65}{54} & 0 & 0 & 0 & 0 & 0 & 0 \\ 0 & 0 & 1 & 0 & 0 & 1 & 0 & 0 \\ 0 & 0 & \frac{65}{54} & 0 & 0 & 0 & 0 & 0 \\ 1 & 0 & 0 & \frac{65}{54} & 0 & 0 & 0 & 0 \\ 0 & -\frac{19}{11} & \frac{98}{31} & 0 & -\frac{1}{6} & 0 & 0 & 1 \\ 3 & 0 & 0 & \frac{204}{47} & 0 & 0 & \frac{29}{17} & 0 \\ 0 & 0 & 0 & 0 & -\frac{5}{27} & 0 & 0 & -\frac{1}{12} \\ -\frac{1}{12} & 0 & 0 & -\frac{7}{48} & 0 & 0 & 0 & 0 \end{pmatrix}}^{[G_{22}]} \quad (85) \end{aligned}$$

$$\begin{aligned} & \overbrace{\begin{pmatrix} 0 & 0 & 1 & 0 & 0 & 1 & 0 & 0 \\ 0 & 0 & \frac{31}{25} & 0 & 0 & \frac{47}{27} & 0 & 0 \\ 1 & 0 & 0 & \frac{31}{25} & 0 & 0 & \frac{47}{27} & 0 \\ 0 & 1 & 0 & 0 & \frac{31}{25} & 0 & 0 & \frac{47}{27} \\ 0 & 0 & \frac{34}{23} & 0 & 0 & \frac{283}{21} & -\frac{311}{17} & 0 \\ 1 & 0 & 0 & \frac{2}{35} & 0 & \frac{250}{41} & \frac{11}{23} & -\frac{206}{31} \\ 0 & 0 & 0 & 0 & 0 & \frac{16}{25} & 0 & -\frac{69}{25} \\ 0 & 0 & 0 & -\frac{3}{20} & 0 & 0 & \frac{29}{26} & -\frac{69}{25} \end{pmatrix}}^{[G_{31}]} ; \quad \overbrace{\begin{pmatrix} 0 & 0 & \frac{45}{37} & 0 & 0 & \frac{107}{67} & 0 & 0 \\ 1 & 0 & 0 & 1 & 0 & 0 & 1 & 0 \\ 0 & 0 & 0 & \frac{45}{37} & 0 & 0 & \frac{107}{67} & 0 \\ 0 & 0 & 0 & 0 & \frac{45}{37} & 0 & 0 & \frac{107}{67} \\ 0 & 0 & \frac{43}{28} & 0 & -\frac{214}{71} & -\frac{14}{23} & \frac{250}{41} & -\frac{128}{23} \\ 0 & 1 & -\frac{217}{24} & 0 & \frac{209}{35} & -\frac{601}{36} & 0 & \frac{139}{13} \\ 0 & 0 & \frac{3}{10} & 0 & 0 & \frac{39}{58} & -\frac{69}{26} & 0 \\ 0 & 0 & 0 & 0 & \frac{13}{41} & 0 & -\frac{69}{26} & \frac{27}{31} \end{pmatrix}}^{[G_{32}]} \quad (86) \end{aligned}$$

$$\begin{aligned} & \overbrace{\begin{pmatrix} 0 & \frac{46}{35} & 0 & 0 & \frac{26}{19} & 0 & 0 & 0 \\ 0 & 0 & \frac{46}{35} & 0 & 0 & \frac{26}{19} & 0 & 0 \\ 1 & 0 & 0 & 1 & 0 & 0 & 1 & 0 \\ 0 & 0 & 0 & \frac{46}{35} & 0 & 0 & \frac{26}{19} & 0 \\ 0 & -\frac{294}{31} & \frac{91}{15} & 0 & 0 & \frac{58}{31} & 0 & 0 \\ -1 & 0 & 0 & \frac{7}{25} & 0 & -\frac{193}{54} & \frac{58}{31} & 0 \\ 0 & 0 & 0 & 0 & 0 & \frac{17}{40} & 0 & 0 \\ 0 & 0 & 0 & -\frac{7}{37} & 0 & 0 & \frac{10}{27} & 0 \end{pmatrix}}^{[G_{23}]} ; \quad \overbrace{\begin{pmatrix} 0 & 0 & 0 & 0 & 0 & \frac{21}{11} & 0 & 0 \\ 0 & 0 & 0 & 0 & 0 & 0 & \frac{21}{11} & 0 \\ 0 & 1 & 0 & 0 & 1 & 0 & 0 & 1 \\ 0 & 0 & 0 & 0 & 0 & 0 & 0 & \frac{21}{11} \\ 0 & 0 & 0 & \frac{71}{16} & 0 & -\frac{311}{17} & \frac{599}{53} & 0 \\ 0 & 0 & \frac{214}{71} & 0 & -\frac{34}{23} & \frac{128}{23} & -\frac{206}{31} & \frac{25}{23} \\ -\frac{1}{12} & 0 & 0 & -\frac{3}{19} & 0 & -\frac{69}{26} & \frac{55}{48} & 0 \\ 0 & 0 & 0 & 0 & 0 & -\frac{69}{26} & 0 & \frac{13}{15} \end{pmatrix}}^{[G_{33}]} \quad (87) \end{aligned}$$

³⁹ this page should be read as PDF with suitable magnification

Element shape functions

The element shape functions are displacement vectors that are governed by tensor transformation rules. Here, in this ‘high accuracy’ formulation, shape functions :

$$\phi_i(x, y, z) = \begin{Bmatrix} \phi_i^{(x)}(x, y, z) \\ \phi_i^{(y)}(x, y, z) \\ \phi_i^{(z)}(x, y, z) \end{Bmatrix} : \text{are housed in } \Phi = \{\phi_1, \phi_2, \dots\} \quad (88)$$

and Φ is calculated from the corresponding Rayleigh mode collection Ψ :

$$\Psi = \{\psi_1, \psi_2, \dots\}; \quad \Phi^T = ([G]^T)^{-1} \Psi^T \text{ from equation (83)} \quad (89)$$

using matrix-tensor operators in *Mathematica*. The tabulated expressions in **Figs. 7** through **12** should be viewed as PDF with sufficient magnification⁴⁰.

A *Mathematica* function: Calculation for a given Poisson’s ratio ν

To aid symbolic computation the following *Mathematica* ‘one-liner’ function is included here. The Rayleigh mode shapes from **Figs. 2** through **4** are to be evaluated for the numerical ν and stored in a variable `mode`. The instruction, along with the *Mathematica* code, to generate the shape functions follows:

```
fromModesToShapeFunctions::usage = "
fromModesToShapeFunctions[modes,{x,y,z},nodes]
  generates element shape functions from modes
  in x,y,z variables for an eight node 3-d element.
Each Rayleigh response vector is stored as one column in modes."

fromModesToShapeFunctions[modes_, {x_, y_, z_}, nodes_] :=
  LinearSolve[
    Flatten /@ Thread[modes /. Thread[
      {x, y, z} -> #] &
      /@ nodes], modes]

testKronecker[mode_, {x_, y_, z_}, nodes_] := Round[Table[
  Chop[
    Flatten[(mode[[i]] /. Thread[
      {x, y, z} -> #] & /@ nodes)]]],
{i, Length[nodes // Flatten]]] ==
  IdentityMatrix[Length[nodes // Flatten]]
```

⁴⁰ The author uses 200% in the Acrobat Pro reader

The vector form of the Kronecker condition of equation (17) can be tested to yield **True** with the above *Mathematica* function. In the large scale computation a **C⁺⁺** program generated the factors of the the inverse for $[G]$ in **Fig. 5**, and used in many places, such as generating the element stiffness matrix, the strain calculations.

Shape functions	Shape-1	Shape-2	Shape-3	Shape-4
u	$ \begin{aligned} &5.44934xy(y^2 - 3x^2) - \\ &1.15747(x^2 + 3y^2) - \\ &7.97817z(x^2 - 3x^2) - 6.58780xyz + \\ &13.5179xy - 23.9522xz + \\ &1.5747x - 11.8802(z^2 - y^2) - \\ &12.8371y + 19.8384z \end{aligned} $	$ \begin{aligned} &1.00779y(y^2 - 3x^2) - \\ &0.210348(x^2 + 3y^2) - \\ &2.64269z(x^2 - 3x^2) - 0.319104xyz + \\ &4.99444xy - 7.69673xz + \\ &0.210248y - 4.08996(z^2 - y^2) - \\ &5.40096y + 6.73664z \end{aligned} $	$ \begin{aligned} &8.22911y(y^2 - 3x^2) - \\ &1.03601(x^2 + 3y^2) - \\ &10.7155z(x^2 - 3x^2) - 1.13090xyz + \\ &21.8407xy - 31.0801xz + \\ &1.05604x - 15.0478(z^2 - y^2) - \\ &21.0889y - 36.6639z \end{aligned} $	$ \begin{aligned} &-7.2779y(y^2 - 3x^2) - \\ &1.49667(x^2 + 3y^2) + \\ &10.6682z(x^2 - 3x^2) + 0.712079xyz - \\ &18.4418xy - 31.8977xz - \\ &2.40467x + 15.8764(z^2 - y^2) + \\ &17.7861y - 37.5743z + 1 \end{aligned} $
v	$ \begin{aligned} &-4.96896x(x^2 - 3y^2) - \\ &0.170219(3x^2 + y^2) + \\ &6.24829(z^2 - x^2) - 0.913557xyz - \\ &16.8155xy + 11.7279xz + \\ &4.24276z(x^2 - 3y^2) + \\ &13.8753yz + 0.170219y - 10.491z \end{aligned} $	$ \begin{aligned} &-1.7971x(x^2 - 3y^2) - \\ &0.0554876(3x^2 + y^2) + \\ &2.33126(z^2 - x^2) + 0.257113xyz - \\ &6.90643xy + 4.20482xz + \\ &1.32402z(x^2 - 3y^2) + \\ &4.1959yz + 1.05349y - 3.88487z \end{aligned} $	$ \begin{aligned} &-7.57585x(x^2 - 3y^2) - \\ &0.284072(3x^2 + y^2) + \\ &9.91812(z^2 - x^2) - 1.38451xyz - \\ &25.5594xy + 18.3462xz + \\ &6.4779z(x^2 - 3y^2) + 21.1072yz + \\ &0.284072y - 16.399z \end{aligned} $	$ \begin{aligned} &6.73603x(x^2 - 3y^2) + \\ &0.296002(3x^2 + y^2) - \\ &8.48289(z^2 - x^2) + 1.22279xyz + \\ &22.7847xy - 15.9575xz - \\ &5.76957z(x^2 - 3y^2) - 18.8757yz - \\ &0.246002y + 14.2525z \end{aligned} $
w	$ \begin{aligned} &-6.93764(y^2 - x^2) + \\ &7.82591x(x^2 - 3y^2) + \\ &1.52949(3x^2 + y^2) + \\ &2.8823xyz + 73.7604xz - \\ &19.332x - 4.34068y(y^2 - 3x^2) - \\ &12.4966yz + 11.2783y - 1.52949z \end{aligned} $	$ \begin{aligned} &-2.09795(y^2 - x^2) + \\ &2.68258x(x^2 - 3y^2) + \\ &0.573472(3x^2 + y^2) + \\ &0.913888xyz + 8.16792xz - \\ &6.5039x - 1.5768y(y^2 - 3x^2) - \\ &4.86251yz + 3.67475y - 0.573472z \end{aligned} $	$ \begin{aligned} &-10.55746(y^2 - x^2) + \\ &10.4847x(x^2 - 3y^2) + \\ &1.65715(3x^2 + y^2) + \\ &3.91948xyz + 31.8956xz - \\ &26.0098x - 6.6678y(y^2 - 3x^2) - \\ &19.8465yz + 18.2214y - 1.65715z \end{aligned} $	$ \begin{aligned} &9.43784(y^2 - x^2) - \\ &10.4944x(x^2 - 3y^2) - \\ &2.17034(3x^2 + y^2) - \\ &3.82239xyz - 31.7527xz + \\ &26.4437x + 5.88825y(y^2 - 3x^2) + \\ &16.9658yz - 15.3261y + 2.17034z \end{aligned} $

Fig. 7 Shape functions # 1 to 4

Shape functions	Shape-5	Shape-6	Shape-7	Shape-8
w	$-14.0934(x^2 - 3y^2) +$ $1.70772(x^3 - 3y^3) +$ $18.5991z(x^2 - 3y^2) + 2.64271xyz -$ $36.7896xy + 53.7727xz -$ $1.70772x + 27.4358(z^2 - y^2) +$ $36.4311y - 45.9749z$	$-10.3489y(z^2 - 3y^2) +$ $1.23838(x^2 - 3y^2) +$ $13.586z(x^2 - 3y^2) + 1.98665xyz -$ $27.0998xy + 39.4811xz -$ $1.73858x + 19.7327(z^2 - y^2) +$ $26.3658y - 33.5187z$	$1.69577y(z^2 - 3y^2) -$ $0.196366(x^2 + 3y^2) +$ $2.1599z(x^2 - 3y^2) + 0.317847xyz +$ $3.55693xy - 7.08129xz +$ $1.19099x - 3.48414(z^2 - y^2) -$ $4.21815y + 5.31404z$	$10.8593y(z^2 - 3y^2) -$ $1.77861(x^2 + 3y^2) +$ $14.0037z(x^2 - 3y^2) - 1.54617xyz +$ $27.7808xy - 46.8266xz +$ $1.27861x - 20.6896(z^2 - y^2) -$ $27.4901y + 34.6063z$
v	$13.0014x(x^2 - 3y^2) +$ $1.19372(3x^2 + y^2) -$ $14.7987(z^2 - x^2) + 2.65062xyz +$ $44.6553xy - 32.3812xz -$ $9.8766z(x^2 - 3y^2) - 31.331yz -$ $2.19372y + 23.6753z + 1.$	$9.49739x(x^2 - 3y^2) +$ $0.362578(3x^2 + y^2) -$ $12.4572(z^2 - x^2) + 1.72984xyz +$ $32.034xy - 23.0423xz -$ $8.12743z(x^2 - 3y^2) - 26.4806yz -$ $0.363578y + 20.3846z$	$-1.50952x(x^2 - 3y^2) -$ $0.0129558(3x^2 + y^2) +$ $1.7146(z^2 - x^2) - 0.310599xyz -$ $5.16477xy + 3.26289xz +$ $1.25222z(x^2 - 3y^2) + 4.11565yz +$ $0.0129558y - 2.96682z$	$-0.89603x(x^2 - 3y^2) -$ $0.965798(3x^2 + y^2) +$ $10.9779(z^2 - x^2) - 2.15899xyz -$ $35.7015xy + 24.6822xz +$ $7.35868z(x^2 - 3y^2) + 24.2209yz +$ $0.965798y - 18.3566z$
u	$15.7655(y^2 - x^2) -$ $18.0973x(x^2 - 3y^2) -$ $3.70696(3x^2 + y^2) -$ $6.55186xyz - 54.8717xz +$ $44.9827x + 10.2171y(y^2 - 3x^2) +$ $29.5973yz - 25.9825y + 3.70696z$	$13.2403(y^2 - x^2) -$ $13.2977x(x^2 - 3y^2) -$ $2.16675(3x^2 + y^2) - 5.10877xyz -$ $39.4634xz + 32.0382xz +$ $8.37821y(y^2 - 3x^2) - 24.9144yz -$ $22.6155y + 1.16673z + 1.$	$-2.05683(y^2 - x^2) +$ $2.10813x(x^2 - 3y^2) +$ $0.494624(3x^2 + y^2) +$ $0.757474xyz + 6.30628xz -$ $5.64885x - 1.19924y(z^2 - 3x^2) -$ $3.42319yz + 3.25607y - 0.494624z$	$-12.1115(y^2 - x^2) +$ $13.6439x(x^2 - 3y^2) +$ $2.73395(3x^2 + y^2) +$ $4.99456xyz + 41.3732xz -$ $35.9373x - 7.61638y(y^2 - 3x^2) -$ $21.9558yz + 19.7278y - 2.73395z$

Fig. 8 Shape functions # 5 to 8

Shape functions	Shape-9	Shape-10	Shape-11	Shape-12
u	$ \begin{aligned} & 7.13698 y (y^2 - 3 y^3) - \\ & 0.842862 (x^2 - 3 x^3) - 1.63172 x y z + \\ & 9.37637 z (z^2 - 3 z^3) - 27.2594 x z + \\ & 18.6652 x y - 27.2594 x z + \\ & 0.842862 x - 13.5783 (z^2 - z^3) - \\ & 18.1787 y + 22.9428 z \end{aligned} $	$ \begin{aligned} & -0.818062 x (z^2 - 3 z^3) + \\ & 0.0978334 (y^2 - 3 y^3) - \\ & 1.07167 z (z^2 - 3 z^3) - 0.244058 x y z - \\ & 1.8064 x y + 3.12634 x z - \\ & 0.697854 x + 1.89138 (z^2 - y^2) + \\ & 2.11586 y - 2.46993 z \end{aligned} $	$ \begin{aligned} & -0.672097 (z^2 - 3 z^3) + \\ & 0.0333338 (y^2 - 3 y^3) - \\ & 0.449689 z (z^2 - 3 z^3) + 0.120415 x y z - \\ & 1.67482 x y + 2.79666 x z - \\ & 0.0333336 x + 1.81486 (z^2 - y^2) - \\ & 2.03087 y - 3.66129 z \end{aligned} $	$ \begin{aligned} & -5.98327 y (z^2 - 3 z^3) + \\ & 0.604083 (x^2 - 3 x^3) - \\ & 7.02194 z (z^2 - 3 z^3) + 0.746312 x y z - \\ & 14.1126 x y + 20.3456 x z - \\ & 0.694083 x + 10.4728 (z^2 - y^2) + \\ & 13.7836 y - 17.4947 z \end{aligned} $
v	$ \begin{aligned} & -6.53504 x (z^2 - 3 y^2) - \\ & 0.315288 (3 x^2 + y^2) + \\ & 8.38523 (z^2 - x^2) - 1.11461 x y z - \\ & 22.0954 x y + 15.886 x + \\ & 5.69749 z (z^2 - 3 y^2) + 18.6584 y z + \\ & 0.315258 y - 14.0877 z \end{aligned} $	$ \begin{aligned} & 0.7515 x (z^2 - 3 y^2) - \\ & 0.0435084 (3 x^2 + y^2) - \\ & 0.793726 (z^2 - x^2) + 0.174317 x y z + \\ & 2.59564 x y - 1.5017 x - \\ & 0.601362 z (z^2 - 3 y^2) - 1.97704 y z + \\ & 0.0143084 y + 1.39529 z \end{aligned} $	$ \begin{aligned} & 0.610742 x (x^2 - 3 y^2) + \\ & 0.019395 (3 x^2 + y^2) - \\ & 0.778625 (z^2 - x^2) - \\ & 0.249230 x y z + 2.607 x y - \\ & 1.44763 x - 0.518929 z (z^2 - 3 y^2) - \\ & 1.69351 y z - 0.019395 y + 1.29755 z \end{aligned} $	$ \begin{aligned} & 4.97608 x (x^2 - 3 y^2) + \\ & 0.236718 (3 x^2 + y^2) - \\ & 6.34682 (z^2 - x^2) + 0.848267 x y z + \\ & 16.7811 x y - 12.0339 x - \\ & 4.32374 z (z^2 - 3 y^2) - 14.1606 y z - \\ & 0.236718 y + 10.6706 z \end{aligned} $
w	$ \begin{aligned} & -9.32919 (y^2 - x^2) + \\ & 9.19008 x (x^2 - 3 z^2) + \\ & 1.43343 (3 x^2 + z^2) + \\ & 3.45567 x y z + 27.1525 x z - \\ & 21.8203 x - 5.86944 y (y^2 - 3 z^2) - \\ & 16.7795 y z + 15.1986 y - 1.43343 z \end{aligned} $	$ \begin{aligned} & 0.988522 (y^2 - x^2) - \\ & 1.04852 x (x^2 - 3 z^2) - \\ & 0.19155 (3 x^2 + z^2) - 0.399254 x y z - \\ & 3.18276 x z + 2.61169 x + \\ & 0.560589 y (y^2 - 3 z^2) + \\ & 1.58745 y z - 1.54941 y + 0.19155 z \end{aligned} $	$ \begin{aligned} & 0.846754 (y^2 - x^2) - \\ & 0.991229 x (x^2 - 3 z^2) - \\ & 0.174192 (3 x^2 + z^2) - \\ & 0.37095 x y z - 3.02912 x z + \\ & 2.36056 x + 0.540498 y (y^2 - 3 z^2) + \\ & 1.55725 y z - 1.38725 y + 0.174192 z \end{aligned} $	$ \begin{aligned} & 7.03128 (y^2 - x^2) - \\ & 6.88057 x (x^2 - 3 z^2) - \\ & 1.03001 (3 x^2 + z^2) - \\ & 2.49778 x y z - 20.9456 x z + \\ & 17.0519 x + 4.44812 y (y^2 - 3 z^2) + \\ & 12.6936 y z - 11.5394 y + 1.03001 z \end{aligned} $

Fig. 9 Shape functions # 9 to 12

Shape functions	shape-13	shape-13	shape-13	shape-15
w	$-3.21775(x^2 - 3y^2) +$ $0.737104(x^3 + 3y^3) +$ $3.81847(x^2 - 3y^2)(x^2 - 3y^2) + 0.4624yz -$ $9.49567xy - 13.8068xz -$ $0.757104x + 7.16491(x^2 - y^2) +$ $8.14086y - 12.0134z$	$-0.800266(x^2 - 3y^2) +$ $0.119913(x^3 + 3y^3) +$ $1.02203(x^2 - 3y^2)(x^2 - 3y^2) + 0.101096xyz -$ $2.09492xy + 2.94108xz -$ $0.118915x + 1.60002(x^2 - y^2) +$ $2.05354y - 2.55103z$	$-0.861849(x^2 - 3y^2) +$ $0.178899(x^3 + 3y^3) +$ $1.12122(x^2 - 3y^2)(x^2 - 3y^2) + 0.108896xyz -$ $2.33477xy + 3.24977xz -$ $0.125899x + 1.65841(x^2 - y^2) +$ $2.15768y - 3.73463z$	$4.86443y(x^2 - 3y^2) -$ $1.06383(x^3 + 3y^3) -$ $7.17145(x^2 - 3y^2)(x^2 - 3y^2) - 0.521468xyz +$ $12.8231xy - 21.844xz +$ $1.06265x - 10.6571(x^2 - y^2) -$ $12.3339y + 18.2283z$
v	$2.92623x(x^2 - 3y^2) +$ $0.155442(3x^2 - 3y^2) -$ $3.78651(x^2 - 3y^2)(x^2 - 3y^2) + 0.483541xyz +$ $9.84719xy - 7.17307x -$ $2.55899z(x^2 - 3y^2) -$ $8.38697yz - 0.155442y + 6.3393z$	$0.741774x(x^2 - 3y^2) +$ $0.0234642(3x^2 - 3y^2) -$ $0.972717(x^2 - 3y^2)(x^2 - 3y^2) - 0.211103xyz +$ $2.50454xy - 1.78918x -$ $0.630799z(x^2 - 3y^2) -$ $1.49115yz - 0.0234642y + 1.564z$	$0.757956x(x^2 - 3y^2) -$ $0.00348796(3x^2 - 3y^2) -$ $1.17785(x^2 - 3y^2)(x^2 - 3y^2) + 0.181165xyz +$ $2.55167xy - 1.92534x -$ $0.600794z(x^2 - 3y^2) - 1.89148yz +$ $0.00348796y + 1.77864z$	$-4.43756x(x^2 - 3y^2) -$ $0.232609(3x^2 - 3y^2) +$ $5.71573(x^2 - 3y^2)(x^2 - 3y^2) - 0.735726xyz -$ $14.9382xy + 10.8481x +$ $3.87792z(x^2 - 3y^2) - 3y^3 + 12.7032yz +$ $0.232609y - 9.59194z$
w	$4.19048(y^2 - x^2) -$ $4.73488x(x^2 - 3y^2 - 3z^2) -$ $0.921285(3x^2 + 3y^2 + 3z^2) -$ $1.74617xyz - 14.3898xz +$ $11.6921x + 2.62399y(x^2 - 3y^2) +$ $7.56102yz - 6.81847y + 0.921283z$	$0.748575(x^2 - x^2) -$ $1.05722x(x^2 - 3y^2 - 3z^2) -$ $0.24165(3x^2 + 3y^2 + 3z^2) - 0.350955xyz -$ $3.21803xz + 2.52774x +$ $0.647119y(x^2 - 3y^2 - 3z^2) +$ $1.04743yz - 1.35266y + 0.24165z$	$0.943739(x^2 - x^2) -$ $1.09103x(x^2 - 3y^2 - 3z^2) -$ $0.226299(3x^2 + 3y^2 + 3z^2) -$ $0.743361xyz - 3.30687xz +$ $2.71565x + 0.618943y(x^2 - 3y^2 - 3z^2) +$ $2.3557yz - 1.56468y + 0.226299z$	$-6.35161(y^2 - x^2) +$ $7.04883x(x^2 - 3y^2 + 3z^2) +$ $1.47346(3x^2 + 3y^2 + 3z^2) - 2.5612xyz +$ $21.3141xz - 17.8708x -$ $3.96482y(x^2 - 3y^2 - 3z^2) -$ $11.4275yz + 10.3184y - 1.47346z$

Fig. 10 Shape functions # 13 to 16

$\frac{1}{2} \log \frac{1+\nu}{1-\nu} \frac{1+\nu}{1-\nu}$	$\frac{1}{2} \log \frac{1+\nu}{1-\nu}$	$\frac{1}{2} \log \frac{1+\nu}{1-\nu}$
ν	$-0.35477 \times (\nu^4 - 3\nu^3) + 0.046037 (\nu^4 + 3\nu^3) +$ $0.131027 \nu^2 - 3\nu^2 - 0.006773 \nu^2 -$ $1.03075 \times (\nu^2 - 3\nu) + 0.061048 \nu^2 +$ $1.03075 (\nu^2 - 3\nu) + 1.03075 \nu^2 - 1.03075 \nu$	$-0.10509 (\nu^2 - 3\nu^2) + 0.030403 (\nu^2 - 3\nu^2) +$ $1.03075 \nu^2 - 3\nu^2 + 1.03075 \nu^2 - 2.03075 \nu^2 + 2.03075 \nu^2 -$ $1.03075 \nu^2 - 3\nu^2 - 2.03075 \nu^2 - 2.03075 \nu^2$
ν	$0.25131 \times (\nu^4 - 3\nu^3) + 0.0410947 (\nu^4 + 3\nu^3) +$ $0.460207 \nu^2 - 3\nu^2 - 0.006773 \nu^2 -$ $0.460207 \nu^2 - 3\nu^2 - 0.006773 \nu^2 -$ $0.460207 \nu^2 - 3\nu^2 - 0.006773 \nu^2 -$	$0.27744 (\nu^4 - 3\nu^3) + 0.77744 (\nu^4 + 3\nu^3) +$ $0.27744 (\nu^4 - 3\nu^3) + 0.77744 (\nu^4 + 3\nu^3) +$ $0.27744 (\nu^4 - 3\nu^3) + 0.77744 (\nu^4 + 3\nu^3) +$
ν	$0.77744 (\nu^4 - 3\nu^3) + 0.77744 (\nu^4 + 3\nu^3) +$ $0.77744 (\nu^4 - 3\nu^3) + 0.77744 (\nu^4 + 3\nu^3) +$ $0.77744 (\nu^4 - 3\nu^3) + 0.77744 (\nu^4 + 3\nu^3) +$	$0.77744 (\nu^4 - 3\nu^3) + 0.77744 (\nu^4 + 3\nu^3) +$ $0.77744 (\nu^4 - 3\nu^3) + 0.77744 (\nu^4 + 3\nu^3) +$ $0.77744 (\nu^4 - 3\nu^3) + 0.77744 (\nu^4 + 3\nu^3) +$

Fig. 11 Shape functions # 17 to 20

	0.049e-21	0.049e-22	0.049e-23	0.049e-24
x	$-0.573858 x (y^2 - 3 x^2) +$ $0.0361433 (x^3 + 3 y^3) -$ $0.497604 z (z^2 - 3 x^2) + 0.103678 x y z -$ $1.53643 x y + 2.38871 x z -$ $0.0261423 x + 0.889788 (z^2 - y^2) +$ $1.85615 y - 1.65766 z$	$0.0145377 x (y^2 - 3 x^2) -$ $0.0036140 (x^3 + 3 y^3) -$ $0.0127088 z (z^2 - 3 x^2) +$ $0.137768 x y z + 0.0397146 x y -$ $0.044356 x z + 0.0036140 x -$ $0.0284777 (z^2 - y^2) -$ $0.0313907 y + 0.0441863 z$	$0.0135632 x (y^2 - 3 x^2) -$ $0.0131967 (x^3 + 3 y^3) -$ $0.00180635 z (z^2 - 3 x^2) +$ $0.00666112 x y z + 0.0374641 x y +$ $0.00733268 x z + 0.0131661 x -$ $0.0364639 (z^2 - y^2) -$ $0.0301339 y + 0.0363380 z$	$0.03443871 x (y^2 - 3 x^2) -$ $0.0146438 (x^3 + 3 y^3) -$ $0.0231935 z (z^2 - 3 x^2) +$ $0.00393616 x y z + 0.103969 x y -$ $0.007975 x z + 0.0146439 x -$ $0.0307138 (z^2 - y^2) -$ $0.0303716 y + 0.0632113 z$
y	$0.469329 x (z^2 - 3 y^2) +$ $0.0404491 (3 x^3 + y^3) -$ $0.641869 (z^2 - x^2) + 0.0625726 x y z +$ $1.80265 x y - 1.23258 x -$ $0.427048 z (z^2 - 3 y^2) - 1.40077 y z -$ $0.0404491 y + 1.06892 z$	$-0.011505 x (z^2 - 3 y^2) -$ $0.0122468 (3 x^3 + y^3) -$ $0.0173822 (z^2 - x^2) + 0.0120277 x y z -$ $0.035659 x y + 0.0308623 x +$ $0.0235142 z (z^2 - 3 y^2) +$ $0.0088951 y z +$ $0.0122468 y - 0.00813202 z$	$-0.0101519 x (z^2 - 3 y^2) -$ $0.0020231 (3 x^3 + y^3) +$ $0.0128477 (z^2 - x^2) + 0.183266 x y z -$ $0.0337453 x y + 0.0290473 x +$ $0.0108126 z (z^2 - 3 y^2) + 0.06543 y z +$ $0.0029281 y - 0.0234603 z$	$-0.000906071 x (z^2 - 3 y^2) -$ $0.0116608 (3 x^3 + y^3) +$ $0.017996 (z^2 - x^2) + 0.0114953 x y z +$ $0.00763104 x y + 0.0559806 x +$ $0.0138068 z (z^2 - 3 y^2) +$ $0.0489067 y z +$ $0.01156628 y - 0.0318028 z$
xy	$0.700133 (y^2 - x^2) -$ $0.787475 x (z^2 - 3 x^2) -$ $0.16424 (3 x^2 + z^2) - 0.632093 x y z -$ $1.71952 x z + 1.98033 x +$ $0.44327 y (y^2 - 3 x^2) +$ $1.28374 y z - 1.14468 y + 0.16124 z$	$-0.0494476 (y^2 - x^2) +$ $0.0177134 x (z^2 - 3 x^2) -$ $0.00912328 (3 x^2 + z^2) +$ $0.0163063 x y z +$ $0.0569553 x z - 0.0397912 x +$ $0.0037991 y (z^2 - 3 x^2) +$ $0.0347694 y z -$ $0.0436676 y + 0.00912326 z$	$-0.0182715 (y^2 - x^2) +$ $0.0332741 x (z^2 - 3 x^2) -$ $0.00731159 (3 x^2 + z^2) +$ $0.0176873 x y z +$ $0.117976 x z - 0.0296108 x -$ $0.00989099 x (z^2 - 3 x^2) -$ $0.0232953 x z +$ $0.028106 y + 0.00731159 z$	$-0.0246033 (y^2 - x^2) +$ $0.0264114 x (z^2 - 3 x^2) +$ $0.00319472 (3 x^2 + z^2) +$ $0.190146 x y z +$ $0.0814316 x z - 0.0603988 x -$ $0.0139683 y (z^2 - 3 x^2) - 0.034992 y z +$ $0.0373718 y - 0.00319472 z$

Fig. 12 Shape functions # 21 to 24

Modal and nodal *element stiffness* matrices

These pages must be read as a PDF with magnification, however, an OCR should be able to read and generate ASCII file for comparison.

Modal *element stiffness* matrix: \mathcal{K}_{qq}

In the interest of printing the following partitioning is used:

$$[\mathcal{K}_{qq}] = \begin{bmatrix} [\mathcal{K}_{qq}^{(1,1)}] & [\mathcal{K}_{qq}^{(1,2)}] \\ [\mathcal{K}_{qq}^{(2,1)}] & [\mathcal{K}_{qq}^{(2,2)}] \end{bmatrix} \quad (90)$$

0	0	0	0	0	0	0	0	0	0	0	0
0	3	0	0	0	1	0	0	0	1	0	0
0	0	1	0	0	0	0	1	0	0	0	0
0	0	0	1	0	0	0	0	0	0	1	0
0	0	0	0	0	0	0	0	0	0	0	0
0	1	0	0	0	3	0	0	0	1	0	0
0	0	0	0	0	0	1	0	0	0	0	1
0	0	1	0	0	0	0	1	0	0	0	0
0	0	0	0	0	0	0	0	0	0	0	0
0	1	0	0	0	1	0	0	0	3	0	0
0	0	0	1	0	0	0	0	0	0	1	0
0	0	0	0	0	0	1	0	0	0	0	1

Fig. 13 $[\mathcal{K}_{qq}^{(1,1)}]$: Modal element stiffness matrix

0	0	0	0	0	0	0	0	0	0	0	0
0	0	$-\frac{371}{36}$	$-\frac{34}{11}$	$-\frac{305}{26}$	$-\frac{44}{15}$	$-\frac{7}{12}$	$-\frac{11}{20}$	$-\frac{22}{35}$	0	0	$-\frac{22}{35}$
0	0	0	0	0	0	$-\frac{1}{25}$	$-\frac{11}{35}$	$-\frac{8}{29}$	$-\frac{1}{25}$	$-\frac{11}{35}$	$-\frac{8}{29}$
0	0	0	0	0	0	$-\frac{11}{35}$	$-\frac{1}{51}$	$-\frac{7}{24}$	$-\frac{11}{35}$	$-\frac{1}{51}$	$-\frac{7}{24}$
0	0	0	0	0	0	0	0	0	0	0	0
$-\frac{443}{40}$	$-\frac{36}{13}$	0	0	$-\frac{44}{15}$	$-\frac{44}{15}$	0	$-\frac{11}{20}$	$-\frac{22}{35}$	$-\frac{7}{12}$	$-\frac{11}{20}$	0
0	0	0	0	0	0	$-\frac{8}{29}$	$-\frac{7}{24}$	$-\frac{1}{47}$	$-\frac{8}{29}$	$-\frac{7}{24}$	$-\frac{1}{47}$
0	0	0	0	0	0	$-\frac{1}{25}$	$-\frac{11}{35}$	$-\frac{8}{29}$	$-\frac{1}{25}$	$-\frac{11}{35}$	$-\frac{8}{29}$
0	0	0	0	0	0	0	0	0	0	0	0
$-\frac{36}{13}$	$-\frac{36}{13}$	$-\frac{34}{11}$	$-\frac{34}{11}$	0	0	$-\frac{7}{12}$	0	0	$-\frac{7}{12}$	$-\frac{11}{20}$	$-\frac{22}{35}$
0	0	0	0	0	0	$-\frac{11}{35}$	$-\frac{1}{51}$	$-\frac{7}{24}$	$-\frac{11}{35}$	$-\frac{1}{51}$	$-\frac{7}{24}$
0	0	0	0	0	0	$-\frac{8}{29}$	$-\frac{7}{24}$	$-\frac{1}{47}$	$-\frac{8}{29}$	$-\frac{7}{24}$	$-\frac{1}{47}$

Fig. 14 $[\mathcal{K}_{qq}^{(1,2)}]$: Modal element stiffness matrix

$\frac{1129}{19}$	$\frac{921}{62}$	$\frac{411}{22}$	$\frac{327}{76}$	$\frac{541}{123}$	$\frac{651}{37}$	$\frac{10}{9}$	$\frac{121}{29}$	$\frac{45}{11}$	$\frac{10}{3}$	$\frac{97}{31}$	$\frac{44}{43}$
$\frac{921}{62}$	$\frac{307}{31}$	$\frac{327}{70}$	$\frac{327}{70}$	$\frac{541}{123}$	$\frac{541}{123}$	$\frac{10}{9}$	$\frac{24}{23}$	$\frac{44}{43}$	$\frac{20}{9}$	$\frac{48}{23}$	$\frac{44}{43}$
$\frac{411}{22}$	$\frac{327}{70}$	$\frac{3070}{41}$	$\frac{468}{25}$	$\frac{1215}{22}$	$\frac{241}{12}$	$\frac{34}{9}$	$\frac{45}{11}$	$\frac{202}{37}$	$\frac{34}{27}$	$\frac{44}{43}$	$\frac{86}{21}$
$\frac{327}{70}$	$\frac{327}{70}$	$\frac{468}{25}$	$\frac{312}{25}$	$\frac{241}{12}$	$\frac{241}{48}$	$\frac{68}{27}$	$\frac{44}{43}$	$\frac{56}{41}$	$\frac{34}{27}$	$\frac{44}{43}$	$\frac{71}{26}$
$\frac{541}{123}$	$\frac{541}{123}$	$\frac{1215}{22}$	$\frac{241}{12}$	$\frac{1737}{26}$	$\frac{618}{37}$	$\frac{45}{11}$	$\frac{113}{34}$	$\frac{50}{13}$	$\frac{44}{43}$	$\frac{31}{28}$	$\frac{241}{47}$
$\frac{651}{37}$	$\frac{541}{123}$	$\frac{241}{12}$	$\frac{241}{48}$	$\frac{618}{37}$	$\frac{412}{37}$	$\frac{44}{43}$	$\frac{82}{37}$	$\frac{100}{39}$	$\frac{44}{43}$	$\frac{31}{28}$	$\frac{41}{32}$
$\frac{10}{9}$	$\frac{10}{9}$	$\frac{34}{9}$	$\frac{68}{27}$	$\frac{45}{11}$	$\frac{44}{43}$	$\frac{40}{41}$	$\frac{9}{20}$	$\frac{4}{29}$	$\frac{50}{83}$	$\frac{3}{26}$	$\frac{15}{34}$
$\frac{121}{29}$	$\frac{24}{23}$	$\frac{45}{11}$	$\frac{44}{43}$	$\frac{113}{34}$	$\frac{82}{37}$	$\frac{9}{20}$	$\frac{21}{23}$	$\frac{4}{9}$	$\frac{9}{64}$	$\frac{17}{29}$	$\frac{3}{26}$
$\frac{45}{11}$	$\frac{44}{43}$	$\frac{202}{37}$	$\frac{56}{41}$	$\frac{50}{13}$	$\frac{100}{39}$	$\frac{4}{29}$	$\frac{4}{9}$	$\frac{39}{37}$	$\frac{15}{34}$	$\frac{4}{25}$	$\frac{17}{27}$
$\frac{10}{3}$	$\frac{20}{9}$	$\frac{34}{27}$	$\frac{34}{27}$	$\frac{44}{43}$	$\frac{44}{43}$	$\frac{50}{83}$	$\frac{9}{64}$	$\frac{15}{34}$	$\frac{40}{41}$	$\frac{9}{20}$	$\frac{5}{32}$
$\frac{97}{31}$	$\frac{48}{23}$	$\frac{34}{43}$	$\frac{44}{43}$	$\frac{31}{28}$	$\frac{31}{28}$	$\frac{3}{26}$	$\frac{17}{29}$	$\frac{4}{25}$	$\frac{9}{20}$	$\frac{21}{23}$	$\frac{4}{9}$
$\frac{44}{43}$	$\frac{44}{43}$	$\frac{86}{21}$	$\frac{71}{26}$	$\frac{241}{47}$	$\frac{41}{32}$	$\frac{15}{34}$	$\frac{3}{26}$	$\frac{17}{27}$	$\frac{5}{32}$	$\frac{4}{9}$	$\frac{39}{37}$

Fig. 15 $[\mathcal{K}_{qq}^{(2,2)}]$: Modal element stiffness matrix

$\frac{7776}{53}$	$\frac{1627}{24}$	$\frac{421}{23}$	$\frac{181}{19}$	$\frac{75}{26}$	$\frac{62}{27}$
$\frac{79}{36}$	$\frac{45}{22}$	$\frac{27}{25}$	$\frac{35}{44}$	$\frac{23}{45}$	$\frac{43}{85}$
$\frac{7}{18}$	$\frac{4}{27}$	$\frac{2}{15}$	$\frac{3}{41}$	$\frac{1}{16}$	$\frac{2}{39}$
0	0	0	0	0	0

Fig. 16 Eigenvalues of modal stiffness matrix

Nodal element stiffness matrix: \mathcal{K}_{rr}

Here the matrix is partitioned according to:

$$[\mathcal{K}_{rr}] = \begin{bmatrix} [\mathcal{K}_{rr}^{(1,1)}] & [\mathcal{K}_{rr}^{(1,2)}] \\ [\mathcal{K}_{rr}^{(2,1)}] & [\mathcal{K}_{rr}^{(2,2)}] \end{bmatrix} \quad (91)$$

$\frac{132\,104}{65}$	$\frac{3544}{5}$	$\frac{69\,259}{24}$	$\frac{99\,131}{36}$	$\frac{175\,799}{36}$	$\frac{47\,374}{13}$	$\frac{10\,902}{19}$	$\frac{224\,343}{61}$	$\frac{58\,055}{23}$	$\frac{6847}{24}$	$\frac{503}{2}$	$\frac{81\,661}{43}$
$\frac{3544}{5}$	$\frac{1726}{7}$	$\frac{21\,074}{21}$	$\frac{47\,683}{50}$	$\frac{59\,363}{35}$	$\frac{27\,873}{22}$	$\frac{3784}{29}$	$\frac{48\,523}{36}$	$\frac{22\,819}{26}$	$\frac{2577}{26}$	$\frac{3574}{41}$	$\frac{19\,159}{29}$
$\frac{69\,259}{24}$	$\frac{21\,074}{21}$	$\frac{49\,219}{12}$	$\frac{143\,688}{37}$	$\frac{394\,067}{57}$	$\frac{124\,231}{24}$	$\frac{22\,761}{28}$	$\frac{114\,501}{22}$	$\frac{107\,593}{30}$	$\frac{14\,936}{37}$	$\frac{3193}{9}$	$\frac{124\,259}{46}$
$\frac{99\,131}{36}$	$\frac{47\,683}{50}$	$\frac{143\,688}{37}$	$\frac{118\,533}{32}$	$\frac{151\,078}{23}$	$\frac{93\,180}{19}$	$\frac{6950}{9}$	$\frac{103\,879}{21}$	$\frac{78\,133}{23}$	$\frac{10\,354}{27}$	$\frac{9606}{29}$	$\frac{122\,689}{48}$
$\frac{175\,799}{36}$	$\frac{59\,363}{35}$	$\frac{394\,067}{57}$	$\frac{151\,078}{23}$	$\frac{164\,071}{89}$	$\frac{321\,621}{38}$	$\frac{21\,989}{16}$	$\frac{326\,276}{37}$	$\frac{114\,818}{19}$	$\frac{9573}{14}$	$\frac{25\,213}{42}$	$\frac{122\,822}{27}$
$\frac{47\,374}{13}$	$\frac{27\,873}{22}$	$\frac{124\,231}{24}$	$\frac{93\,180}{19}$	$\frac{331\,621}{36}$	$\frac{45\,737}{7}$	$\frac{26\,679}{26}$	$\frac{236\,515}{36}$	$\frac{104\,117}{23}$	$\frac{18\,857}{37}$	$\frac{12\,094}{27}$	$\frac{115\,919}{34}$
$\frac{10\,902}{19}$	$\frac{3784}{29}$	$\frac{22\,761}{28}$	$\frac{6950}{9}$	$\frac{21\,989}{16}$	$\frac{26\,679}{26}$	$\frac{1781}{11}$	$\frac{21\,731}{21}$	$\frac{5683}{8}$	$\frac{503}{10}$	$\frac{5507}{78}$	$\frac{16\,051}{50}$
$\frac{224\,343}{61}$	$\frac{48\,523}{36}$	$\frac{114\,501}{22}$	$\frac{103\,879}{21}$	$\frac{326\,276}{37}$	$\frac{236\,515}{36}$	$\frac{21\,731}{21}$	$\frac{245\,763}{37}$	$\frac{200\,171}{44}$	$\frac{7211}{14}$	$\frac{51\,104}{113}$	$\frac{75\,335}{22}$
$\frac{58\,055}{23}$	$\frac{22\,819}{26}$	$\frac{107\,593}{30}$	$\frac{78\,133}{23}$	$\frac{114\,818}{19}$	$\frac{104\,117}{23}$	$\frac{5683}{8}$	$\frac{200\,171}{44}$	$\frac{34\,508}{11}$	$\frac{8471}{24}$	$\frac{7135}{23}$	$\frac{75\,599}{32}$
$\frac{6847}{24}$	$\frac{2577}{26}$	$\frac{14\,936}{37}$	$\frac{10\,354}{27}$	$\frac{9573}{14}$	$\frac{18\,857}{37}$	$\frac{803}{10}$	$\frac{7211}{14}$	$\frac{8471}{24}$	$\frac{1657}{41}$	$\frac{917}{26}$	$\frac{12\,475}{47}$
$\frac{503}{2}$	$\frac{3574}{41}$	$\frac{3193}{9}$	$\frac{9606}{29}$	$\frac{25\,213}{42}$	$\frac{12\,094}{27}$	$\frac{5507}{78}$	$\frac{51\,104}{113}$	$\frac{7135}{23}$	$\frac{917}{26}$	$\frac{4387}{140}$	$\frac{7230}{31}$
$\frac{81\,661}{43}$	$\frac{19\,159}{29}$	$\frac{124\,259}{46}$	$\frac{122\,689}{48}$	$\frac{122\,822}{27}$	$\frac{115\,919}{34}$	$\frac{16\,051}{30}$	$\frac{75\,335}{22}$	$\frac{75\,599}{32}$	$\frac{12\,475}{47}$	$\frac{7230}{31}$	$\frac{140\,633}{79}$

Fig. 17 $[\mathcal{K}_{rr}^{(1,1)}]$: Nodal element stiffness matrix

$\frac{106858}{87}$	$\frac{8844}{31}$	$\frac{11402}{39}$	$\frac{68002}{37}$	$\frac{140904}{37}$	$\frac{21912}{35}$	$\frac{3362}{17}$	$\frac{72273}{26}$	$\frac{5136}{25}$	$\frac{204}{37}$	$\frac{190}{37}$	$\frac{157}{31}$
$\frac{15720}{37}$	$\frac{4098}{41}$	$\frac{2845}{28}$	$\frac{15909}{25}$	$\frac{6614}{5}$	$\frac{2809}{12}$	$\frac{2131}{31}$	$\frac{17381}{18}$	$\frac{2064}{29}$	$\frac{87}{49}$	$\frac{52}{29}$	$\frac{79}{44}$
$\frac{29391}{17}$	$\frac{10940}{27}$	$\frac{5797}{14}$	$\frac{75141}{29}$	$\frac{102479}{19}$	$\frac{28341}{32}$	$\frac{13757}{49}$	$\frac{350260}{89}$	$\frac{6955}{24}$	$\frac{191}{27}$	$\frac{122}{17}$	$\frac{233}{30}$
$\frac{41301}{25}$	$\frac{8828}{23}$	$\frac{5899}{15}$	$\frac{91469}{37}$	$\frac{46105}{9}$	$\frac{12632}{15}$	$\frac{8240}{31}$	$\frac{149567}{40}$	$\frac{11597}{42}$	$\frac{292}{39}$	$\frac{242}{35}$	$\frac{111}{16}$
$\frac{93593}{32}$	$\frac{25971}{38}$	$\frac{701}{1}$	$\frac{144571}{35}$	$\frac{357981}{37}$	$\frac{53433}{27}$	$\frac{17515}{37}$	$\frac{140057}{21}$	$\frac{49091}{100}$	$\frac{2111}{176}$	$\frac{218}{17}$	$\frac{83}{7}$
$\frac{69875}{32}$	$\frac{23008}{45}$	$\frac{16197}{31}$	$\frac{78535}{24}$	$\frac{319977}{47}$	$\frac{25723}{23}$	$\frac{16646}{47}$	$\frac{183810}{37}$	$\frac{9807}{26}$	$\frac{281}{31}$	$\frac{109}{12}$	$\frac{227}{23}$
$\frac{15131}{44}$	$\frac{884}{11}$	$\frac{3375}{41}$	$\frac{13329}{26}$	$\frac{68617}{64}$	$\frac{3523}{20}$	$\frac{1615}{29}$	$\frac{14869}{19}$	$\frac{2018}{35}$	$\frac{36}{25}$	$\frac{16}{11}$	$\frac{16}{11}$
$\frac{147568}{67}$	$\frac{13898}{27}$	$\frac{6865}{13}$	$\frac{69286}{21}$	$\frac{233913}{34}$	$\frac{12411}{11}$	$\frac{2493}{7}$	$\frac{236099}{47}$	$\frac{24722}{67}$	$\frac{667}{74}$	$\frac{77}{8}$	$\frac{244}{27}$
$\frac{561137}{371}$	$\frac{21969}{62}$	$\frac{50317}{139}$	$\frac{47606}{21}$	$\frac{141427}{30}$	$\frac{19067}{13}$	$\frac{8345}{34}$	$\frac{58477}{17}$	$\frac{10645}{42}$	$\frac{157}{25}$	$\frac{242}{39}$	$\frac{41}{6}$
$\frac{14152}{83}$	$\frac{6999}{175}$	$\frac{1399}{34}$	$\frac{12287}{48}$	$\frac{11206}{21}$	$\frac{1663}{19}$	$\frac{807}{29}$	$\frac{15379}{40}$	$\frac{629}{24}$	$\frac{21}{32}$	$\frac{18}{25}$	$\frac{28}{59}$
$\frac{4070}{27}$	$\frac{1725}{49}$	$\frac{1153}{32}$	$\frac{5871}{26}$	$\frac{10305}{22}$	$\frac{2617}{34}$	$\frac{683}{28}$	$\frac{6490}{19}$	$\frac{432}{17}$	$\frac{19}{30}$	$\frac{3}{5}$	$\frac{32}{51}$
$\frac{133147}{117}$	$\frac{7735}{29}$	$\frac{4082}{15}$	$\frac{54573}{32}$	$\frac{85169}{24}$	$\frac{29734}{31}$	$\frac{739}{4}$	$\frac{51789}{20}$	$\frac{6853}{36}$	$\frac{159}{34}$	$\frac{103}{22}$	$\frac{58}{11}$

Fig. 18 $[\mathcal{K}_{rr}^{(1,2)}]$: Nodal element stiffness matrix

$\frac{19183}{26}$	$\frac{4950}{29}$	$\frac{1749}{10}$	$\frac{51833}{47}$	$\frac{84384}{37}$	$\frac{37892}{101}$	$\frac{4134}{35}$	$\frac{44951}{27}$	$\frac{7263}{59}$	$\frac{451}{129}$	$\frac{73}{24}$	$\frac{58}{19}$
$\frac{4950}{29}$	$\frac{1051}{26}$	$\frac{329}{8}$	$\frac{7958}{31}$	$\frac{1609}{3}$	$\frac{3329}{38}$	$\frac{949}{34}$	$\frac{13223}{34}$	$\frac{718}{25}$	$\frac{19}{27}$	$\frac{9}{13}$	$\frac{19}{26}$
$\frac{1749}{10}$	$\frac{329}{8}$	$\frac{1314}{31}$	$\frac{9707}{37}$	$\frac{90254}{165}$	$\frac{2333}{26}$	$\frac{1109}{39}$	$\frac{16769}{42}$	$\frac{1858}{63}$	$\frac{13}{18}$	$\frac{14}{19}$	$\frac{19}{27}$
$\frac{51833}{47}$	$\frac{7958}{31}$	$\frac{9707}{37}$	$\frac{23109}{14}$	$\frac{454394}{133}$	$\frac{21347}{38}$	$\frac{4261}{24}$	$\frac{72315}{29}$	$\frac{4978}{27}$	$\frac{584}{117}$	$\frac{77}{17}$	$\frac{139}{30}$
$\frac{84384}{37}$	$\frac{1609}{3}$	$\frac{90254}{165}$	$\frac{434394}{133}$	$\frac{477528}{67}$	$\frac{26878}{23}$	$\frac{10709}{29}$	$\frac{119681}{23}$	$\frac{37838}{99}$	$\frac{453}{49}$	$\frac{388}{39}$	$\frac{293}{31}$
$\frac{37892}{101}$	$\frac{3329}{38}$	$\frac{2333}{26}$	$\frac{21347}{38}$	$\frac{26878}{23}$	$\frac{7502}{39}$	$\frac{425}{7}$	$\frac{7678}{9}$	$\frac{1257}{20}$	$\frac{69}{44}$	$\frac{30}{19}$	$\frac{35}{22}$
$\frac{4134}{35}$	$\frac{949}{34}$	$\frac{1109}{39}$	$\frac{4261}{24}$	$\frac{10709}{29}$	$\frac{425}{7}$	$\frac{315}{16}$	$\frac{6193}{23}$	$\frac{742}{37}$	$\frac{7}{16}$	$\frac{66}{133}$	$\frac{1}{2}$
$\frac{44951}{27}$	$\frac{13223}{34}$	$\frac{16769}{42}$	$\frac{72315}{29}$	$\frac{119681}{23}$	$\frac{7678}{9}$	$\frac{6193}{23}$	$\frac{235601}{62}$	$\frac{4181}{15}$	$\frac{223}{53}$	$\frac{317}{43}$	$\frac{171}{25}$
$\frac{7263}{59}$	$\frac{718}{25}$	$\frac{1858}{63}$	$\frac{4978}{27}$	$\frac{37838}{99}$	$\frac{1257}{20}$	$\frac{742}{37}$	$\frac{4181}{15}$	$\frac{737}{35}$	$\frac{15}{29}$	$\frac{17}{33}$	$\frac{8}{17}$
$\frac{451}{129}$	$\frac{19}{27}$	$\frac{13}{18}$	$\frac{584}{117}$	$\frac{453}{49}$	$\frac{69}{44}$	$\frac{7}{16}$	$\frac{223}{33}$	$\frac{15}{29}$	$\frac{2}{15}$	$\frac{2}{37}$	$\frac{1}{18}$
$\frac{73}{24}$	$\frac{9}{13}$	$\frac{14}{19}$	$\frac{77}{17}$	$\frac{388}{39}$	$\frac{30}{19}$	$\frac{66}{133}$	$\frac{317}{43}$	$\frac{17}{33}$	$\frac{2}{37}$	$\frac{3}{25}$	$\frac{2}{37}$
$\frac{58}{19}$	$\frac{19}{26}$	$\frac{19}{27}$	$\frac{139}{30}$	$\frac{293}{31}$	$\frac{35}{22}$	$\frac{1}{2}$	$\frac{171}{23}$	$\frac{8}{17}$	$\frac{1}{18}$	$\frac{2}{37}$	$\frac{1}{8}$

Fig. 19 $[\mathcal{K}_{rr}^{(2,2)}]$: Nodal element stiffness matrix

$\frac{3273535}{61}$	$\frac{1015}{18}$	$\frac{1510}{39}$	$\frac{189}{95}$	$\frac{31}{32}$	$\frac{5}{6}$
$\frac{9}{11}$	$\frac{8}{13}$	$\frac{40}{67}$	$\frac{21}{46}$	$\frac{25}{62}$	$\frac{7}{18}$
$\frac{17}{52}$	$\frac{7}{24}$	$\frac{5}{28}$	$\frac{7}{43}$	$\frac{2}{27}$	$\frac{1}{15}$
0	0	0	0	0	0

Fig. 20 Eigenvalues of nodal stiffness matrix

References

1. Ivo Babuška and Mani Suri. Locking effects in the finite element approximation of elasticity problems, December 1990. Technical Note BN-1119.
2. J. T. Baldwin, A. Razzaque, and B. M. Irons. Shape function subroutine for an isoparametric thin plate element shape function subroutine for an isoparametric thin plate element. *International Journal for Numerical Methods in Engineering*, 7:431–440, 1973. DOI: 10.1002/nme.1620070403.
3. M. Born. Zur Raumgittertheorie des Diamanten. *Annalen der Physik*, 44:605–642, 1914.
4. E. Buckingham. On physically similar systems; illustrations of the use of dimensional equations. *Physical Review*, 4, October, 1914.
5. Anil K. Chopra, Partha S. Chakrabarti, and G. Dasgupta. Frequency dependent stiffness matrices for viscoelastic halfplane foundations. Report EERC 75-22, University of California, Berkeley, California, 1975.
6. Ray W. Clough. The finite element method after twenty-five years: a personal view. *Computers & Structures*, 12:361 – 370, 1980.
7. Ray W. Clough. The finite element method in plane stress analysis. In *Proceedings, 2nd Conference on Electronic Computation, A.S.C.E. Structural Division*, pages 345 – 378, Pittsburgh, PA, September 8 and 9, 1960.
8. R. Courant. Variational methods for the solution of problems of equilibrium and vibration. *Bulletin of the American Mathematical Society*, 49:1–29, 1943.
9. H.S.M. Coxeter. *Projective Geometry*. Springer, New York, NY, 2000. First 1964 edition published by Blaisdell Publishing Company, Second 1974 edition published by Toronto University Press.
10. G. Dasgupta. Sommerfeld radiation conditions and cloning algorithm. *New Concepts in Finite Element Analysis*, 44:47–66, 1981. ASME Special issue.
11. G. Dasgupta. A finite element formulation for unbounded homogeneous continua. *Journal of Applied Mechanics*, 104:136 – 140, 3 1982.
12. G. Dasgupta. Integration within polygonal finite elements. *Journal of Aerospace Engineering, ASCE*, 16(1):9–18, January 2003.
13. G. Dasgupta. Closed-form isoparametric shape functions of four-node convex finite elements. *Journal of Aerospace Engineering, ASCE*, 21:10 – 18, January 2008.
14. G. Dasgupta. Stiffness matrices of isoparametric four-node finite elements by exact analytical integration. *Journal of Aerospace Engineering, ASCE*, 21(2):45 – 50, April 2008.
15. G. Dasgupta. Integration within polyhedral finite elements. *Journal of Aerospace Engineering, ASCE*, June 2013.
16. G. Dasgupta. Incompressible and locking-free finite elements from Rayleigh mode vectors. *Acta Mechanica*, 223:1645 – 1656, August 2012.
17. G. Dasgupta. Locking-free quadrilateral finite elements: Poisson’s ratio-dependent vector interpolants. *Acta Mechanica*, June 2013 (accepted). DOI: 10.1007/s00707-013-0927-x, ACME-D-12-00437.2.
18. G. Dasgupta and A. K. Chopra. Dynamic stiffness matrices for viscoelastic half planes. *Journal Engineering Mechanics Division*, 105(EM5):729 – 745, 10 1979.
19. Gautam Dasgupta. Stress analysis using a defect-free four-node finite element technique. Patent Number: 6101450, Aug 08, 2000. U.S. Patent owned by Columbia University, New York, NY, USA.
20. I. Ergatoudis, B. M. Irons, and O. C. Zienkiewicz. Curved, isoparametric, ‘quadrilateral’ elements for finite element analysis. *International Journal of Solids and Structures*, 4, 1968.
21. Peter Fritzson, Vadim Engelson, and Krishnamurthy Sheshadri. *MathCode: A system for C++ or Fortran code generation from Mathematica*. *The Mathematica Journal*, 10(4):740–777, 2008.
22. P. Fritzson. *Principles of Object-Oriented Modeling and Simulation with Modelica 2.1*. John Wiley & Sons, 2004.
23. Peter Fritzson, Vadim Engelson, and Krishnamurthy Sheshadri. *MathCode: A system for C++ or Fortran code generation from Mathematica*. *The Mathematica Journal*, 10(4):740 – 776, 2008.

24. William G.Gray and Martinus Th. Van Genuchten. Economical alternatives to gaussian quadrature over isoparametric quadrilaterals. *International Journal of Numerical Methods in Engineering*, 12, 1978. Short Communication.
25. E. Golub and C. Van Loan. *Matrix Computations*. Johns Hopkins Press, 1988.
26. J. L. Gout. Construction of a hermite rational interpolation Wachspress type finite element. *Computational Mathematical Applications*, pages 337–347, May 1979.
27. B. Hassani and S.M. Tavakkoli. Derivation of incompatible modes in nonconforming finite elements using hierarchical shape functions. *Asian Journal of Civil Engineering (Building and Housing)*, 6(3), 2005.
28. B. M. Irons. Quadrature rules for brick based finite elements. *International Journal of Numerical Methods in Engineering*, 3, April/June 1971.
29. B. M. Irons and A. Razzaque. Experience with the patch test for convergence of finite elements method. In A.K. Aziz, editor, *Mathematical Foundations of the Finite Element Method with Application to Partial Differential Equations*, pages 557–587. Academic Press, New York, 1972.
30. B. M. Irons and O. C. Zienkiewicz. The isoparametric finite element system a new concept in finite element analysis. In *Proc. Conf. Recent Advances in Stress Analysis*. Royal Aeronautical Society, 1968.
31. Bruce Irons and Sohrab Ahmad. *Techniques of Finite Elements*. John Wiley, 1980.
32. Nam-Sua Lee and Klaus-Jurgen Bathe. Effects of element distortions on the performance of isoparametric elements. *IJNME*, 36, 1993.
33. M. J. Loikkanen and B. M. Irons. An 8-node brick finite element. *International Journal for Numerical Methods in Engineering*, 20(3):523–528, 1984.
34. Jacob Lubliner. *Plasticity Theory*. Dover, New York, 2nd edition, 2008. (paperback).
35. R. H. MacNeal. *Finite Elements: Their Design and Performance*. Marcel Dekker, 1994.
36. Richard H. MacNeal. A theorem regarding the locking of tapered four-noded membrane elements. *International Journal for Numerical Methods in Engineering*, 24(9):1793 — 1799, 1987.
37. Richard H. MacNeal. Toward a defect-free four-noded membrane element. *Finite Elements in Analysis and Design*, 5(1):31 – 37, 1989.
38. E. A. Malsch and G. Dasgupta. Shape functions for concave quadrilaterals. In Bathe, editor, *First Mit Conference*. Massachusetts Institute of Technology, Elsevier, June 2001.
39. Univ. of Tennessee, Berkeley Univ. of California, Univ. of Colorado Denver, and NAG Ltd. Lapack linear algebra package, 2013. <http://www.netlib.org/lapack/>.
40. H. Padé. *Sur la représentation approchée d’une fonction par des fractions rationnelles*. Ph.d. thesis, École Normal, 1892.
41. G. Pelosi. The finite-element method, part i: R. l. courant [historical corner]. *Antennas and Propagation Magazine, IEEE*, 49, April 2007.
42. W. Ritz. Über eine neue methode zur lösung gewisser variationalprobleme der mathematischen physik. *Journal Reine Angew. Math.*, 135:1– 61, 1908.
43. J. Robinson. New fem user project: Single element test for aspect ratio sensitivity. Part L Finite Element News, Issue 1, February.
44. J. Robinson. A single element test. *International Journalfor Computer Meth. Appl. Mech. Engng*, 7:191—200, 1976.
45. Sandia National Laboratories. *A Comparison of All-Hexahedral and All-Tetrahedral Finite Element Meshes for Elastic and Elasto-Plastic Analysis*. Sandia National Laboratories, October 1995.
46. Jian Shen. Mixed finite element methods on distorted rectangular grids. Technical report, Institute for Scientific Computation Texas A & M University, College Station, TX 77843-3404, U.S.A., 1994. AMS(MOS) sub ject classifications: 65N12, 65N30; Communicated by R. E. Ewing, R. D. Lazarov and J. M. Thomas.
47. I. C. Taig. Structural analysis by the matrix displacement method. Technical report, British Aircraft Corporation, Warton Aerodrome : English Electric Aviation Limited, April, 1962. Report Number SO 17 based on work performed ca. 1957.
48. R. L. Tayllor. Feappv - - a finite element analysis program. <http://www.ce.berkeley.edu/projects/feap/feappv/manual.pdf>.

49. R. L. Taylor. A mixed-enhanced formulation for tetrahedral finite. Report no. ucb/sem-99/02, University of California at Berkeley, Department of Civil and Environmental Engineering, 1999. (In English: Human posture study using 3D optical profilometry techniques).
50. R. L. Taylor. Isogeometric analysis of nearly incompressible solids. *International Journal for Numerical Methods in Engineering*, 87, 2011. Published online 28 October 2010 in Wiley Online Library (wileyonlinelibrary.com). DOI: 10.1002/nme.3048.
51. R.L. Taylor, J.C. Simo, O.C. Zienkiewicz, and A.C.H. Chen. The patch test – a condition for assessing FEM convergence. *International Journal for Numerical Methods in Engineering*, 22:39–62, 1986.
52. Michael M. Tiller. *Introduction to Physical Modeling with Modelica*, volume 615 of *Engineering and Computer Science*. Kluwer Academic, Boston, M. A., 2001.
53. K. J. Versprille. *Computer-Aided Design Applications of the Rational B-spline Approximation Form*. PhD thesis, Syracuse University, February 1975.
54. E Wachspress. Algebraic geometry foundations for finite element computation. *Mathematical Modelling*, 1, 1980.
55. E. L. Wachspress. *A Rational Basis for Function Approximation*, volume 228 of *Lecture Notes in Mathematics*. Springer Verlag, 1971.
56. E. L. Wachspress. *A Rational Finite Element Basis*. Academic Press, 1975.
57. E. L. Wachspress. The case of the vanishing denominator. *Mathematical Modelling*, 1(4):395 – 399, 1980.
58. J.H. Weiner. *Statistical Mechanics of Elasticity*. J. Wiley, 1983. Dover, NY, NY, October 22, 2002, New York, NY.
59. E. L. Wilson, R. L. Taylor, W. P. Doherty, and J. Ghaboussi. *Incompatible displacement models*, pages 43 – 57. Academic Press, 1973. editors: S. J. Fenves and N. Perrone and A. R. Robinson and W. C. Schnobrich.
60. Edward L. Wilson. *Static and Dynamic Analysis of Structures*. Computers & Structures, Inc., 1995 University Avenue, Berkeley, CA, 94704, 2003.
61. Edward L. Wilson and Adnan Ibrahimbegovic. Use of incompatible displacement modes for the calculation of element stiffnesses or stresses. *Finite Elements in Analysis and Design*, 7(3):229 – 241, 1990.

Contents

1	Introduction	4
1.1	Exact volume integration	5
1.2	Computer algebra implementation	6
1.3	The <i>locking-free</i> ‘brick’ : a 3-D extension of four-node compressible/incompressible and convex/concave finite elements	7
1.4	Field equations	8
1.4.1	Tensors and lists	8
1.4.2	The body force vector	8
1.5	Rayleigh modal vis-à-vis the <i>isoparametric</i> formulation	9
1.5.1	Unconditional possibility of analytical integration	9
1.6	Rayleigh modes with cubic (x, y, z) polynomials	10
1.6.1	Incompressible cases	11
1.7	Shape functions from Rayleigh modes: compressible solid $\nu \neq \frac{1}{2}$	11
1.7.1	Finite elements from Rayleigh modes	12
1.7.2	Relationship between modal and nodal strain-displacement matrices	12
1.7.3	Relationship between modal and nodal element stiffness matrices	13
1.7.4	General elements admitting volume change	13
1.8	Poisson’s ratio(s): a <i>persistent</i> nondimensional system parameter(s) to enforce <i>point-wise</i> the zero body force requirement in a <i>patch test</i>	14
1.8.1	Poisson’s ratios for the generalized case	14
1.8.2	Isotropic constitutive equation: an important special case	14
2	Derivation of Rayleigh modes	15
2.1	Cubic interpolants in the physical (x, y, z) frame	15
2.2	Compressible elements: Poisson’s ratio $\nu \neq \frac{1}{2}$	17
2.2.1	Extension of Courant’s triangulation	17
2.2.2	Rejection of shear locking modes	17
2.2.3	The three-dimensional element — additional stipulated modes	19
2.2.4	The modal strain-displacement transformation matrix	20
2.3	Incompressible solids	21
3	<i>Closed-form</i> development: compressible isotropic solid	23
3.1	Numerical Example: $\mu = 1, \nu = \frac{1}{4}$	23
3.1.1	The $[G]$ Matrix	24
4	Conclusions: what is a ‘high accuracy’ finite element	24
4.1	The single element test and limitations of the present formulation	25
4.2	Embellishing existing finite element programs	26
4.3	Sommerfeld problems motivated ‘high accuracy’ finite elements	26
4.4	Incompressibility and concavity	26

4.5	Generalization for <i>linear</i> partial differential equations	27
4.6	Generalization for structural elements	27
Appendix	28
	Rayleigh modes	28
	Modal to nodal transformation matrix: $[G]$	32
	Element shape functions	35
	A <i>Mathematica</i> function: Calculation for a given Poisson's ratio ν	35
	Modal and nodal <i>element stiffness</i> matrices	43

List of Figures

1	A hexahedral finite element	5
2	Modes 1 through 12: Simplex modes	29
3	Modes 13 through 18: shear-free flexure modes	30
4	Modes 19 through 24: shear-free flexure modes	31
5	G-Matrix	32
6	G-inverse matrix	33
7	Shape functions # 1 to 4	37
8	Shape functions # 5 to 8	38
9	Shape functions # 9 to 12	39
10	Shape functions # 13 to 16	40
11	Shape functions # 17 to 20	41
12	Shape functions # 21 to 24	42
13	$[\mathcal{K}_{qq}^{(1,1)}]$: Modal element stiffness matrix	43
14	$[\mathcal{K}_{qq}^{(1,2)}]$: Modal element stiffness matrix	44
15	$[\mathcal{K}_{qq}^{(2,2)}]$: Modal element stiffness matrix	45
16	Eigenvalues of modal stiffness matrix	46
17	$[\mathcal{K}_{rr}^{(1,1)}]$: Nodal element stiffness matrix	47
18	$[\mathcal{K}_{rr}^{(1,2)}]$: Nodal element stiffness matrix	48
19	$[\mathcal{K}_{rr}^{(2,2)}]$: Nodal element stiffness matrix	49
20	Eigenvalues of nodal stiffness matrix	50

List of Tables

1	nodal values for a brick element	6
---	--	---

High Accuracy three-dimensional Finite Elements

Gautam Dasgupta¹

Abstract

The numerical technique of finite element method motivated this discovery. Therein, evaluations of (*stiffness*-like) system matrices in three-dimensional viscoplastic analysis of thermo-mechanical has been done exactly with the computer program² written by the author.

Finite element approximations, which pertain to both scalar and vector solution fields, are addressed. Instead of resorting to numerical quadrature, the divergence theorem, which yielded high accuracy results, is employed where indefinite integrals are calculated algebraically. Instead of isoparametric mapping, Poisson's ratio dependent shape functions, which satisfy equilibrium throughout the element, are derived from Rayleigh modes that satisfy tensorial invariance. All operations leading to element formulation are carried out in closed analytic form.

The two-dimensional analog of the present discovery is in the patent [?]. In this document, only the three-dimensional treatments, which have no prior reference, are summarized.

keywords: computer algebra, divergence theorem, element level integration, exact integration, Rayleigh modes

What are new:

1. Rayleigh modes for incompressibility
2. Rayleigh modes for compressibility and procedure to determine full anisotropic case with 21 constants
3. Exact volume integration algorithm
4. Rule application to implement accurate and efficient volume integration to calculate the element stiffness matrix.

¹Dept. of Civil Engineering and Engineering Mechanics, School of Engineering and Applied Sciences, Columbia University, 500 West 120 St., New York, NY 10027. E-mail: dasgupta@columbia.edu

²in Appendix-I

Contents

1	Introduction	4
1.1	Scalar field <i>high accuracy</i> finite elements	5
1.1.1	Limitation	6
2	Formulation for polyhedral finite elements	6
2.1	<i>Exact Integration</i>	6
2.1.1	<i>Convex</i> polyhedra	6
3	An optimized form of the divergence theorem	7
3.1	Convex polyhedra	7
3.2	<i>Exact Integration</i>	7
4	Numerical Examples	8
4.1	Volume integration on a 3D-Brick finite element	8
4.2	<i>Locking-free</i> interpolants	9
4.2.1	Notation	9
4.2.2	Polynomial shape functions	9
4.2.3	Incompressible Rayleigh modes	9
4.2.4	Incompressible solution	11
4.2.5	The Compressible Rayleigh modes	11
4.2.6	Modal stiffness matrix	13
4.2.7	Nodal stiffness matrix	13
4.2.8	The shape functions	13
5	Appendices	18
5.1	Appendix-I: <i>Mathematica</i> Package for Volume integration	19
5.1.1	Auxiliary functions for volume integration	22
5.2	Appendix-II: <i>Mathematica</i> Package and Example	23
5.2.1	Developing the rules	23
5.2.2	Example of developing the rules	24

References

- [1] Adi Ben-Israel and Thomas N.E. Greville. *Generalized Inverses: Theory and Applications*. Springer Verlag, 2000. Second Edition: Canadian Mathematical Society: ISBN, 0 8058 1525 2.
- [2] Claude Brezinski. *History of Continued Fractions and Padé Approximants*. Springer Verlag, October 2012. Springer Series in Computational Mathematics.
- [3] Bernard Chazelle and David P. Dobkin. Optimal convex decompositions. Elsevier Science, 1985.
- [4] G. Dasgupta. Convex polygonal finite/boundary element. In V. Demidov and V. Keränen, editors, *International Arctic Seminar (Physics and Mathematics)*, pages 1–8. State Pedagogic Institute, Murmansk University of Technology, May 1998.
- [5] G. Dasgupta. Incompressible and locking-free finite elements from Rayleigh mode vectors. *Acta Mechanica*, 223:1645 – 1656, August 2012.
- [6] G. Dasgupta. Locking-free quadrilateral finite elements. *Acta Mechanica*, June 2013 (accepted).
- [7] P. Fritzson. *Principles of Object-Oriented Modeling and Simulation with Modelica 2.1*. John Wiley & Sons, 2004.
- [8] P. Fritzson. *MathCode*. MathCore Engineering AB, 2011.
- [9] R. H. MacNeal. *Finite Elements: Their Design and Performance*. Marcel Dekker, 1994.
- [10] Karin Nachbagauer, Astrid Pechstein, Hans Irschik, and Johannes Gerstmayr. A new locking-free formulation for planar, shear deformable, linear and quadratic beam finite elements based on the absolute nodal coordinate formulation. *Multibody System Dynamics*, 26:245 — 263, 2011. 10.1007/s11044-011-9249-8.
- [11] E. L. Wachspress. *A Rational Basis for Function Approximation*, volume 228 of *Lecture Notes in Mathematics*. Springer Verlag, 1971.
- [12] E. L. Wachspress. *A Rational Finite Element Basis*. Academic Press, 1975.
- [13] H. Werner and H. J. Bünger, editors. *Padé Approximation and its Applications*, number 1071 in *Lecture Notes in Mathematics*, Bad Honnef, Germany, 1983. Springer-Verlag, New York.

1 Introduction

The scope of Columbia University's patent: U.S. Patent No. 6,101,450 — Gautam Dasgupta — “Stress Analysis Using a Defect-Free Four Node Finite Element Technique” - has been extended here to device solutions for its three-dimensional counterpart. Applications to locking-free solid, plate and shell elements can be developed devoid of errors from element shape distortion and Poisson's effect.

The finite element shown in Figure 1 is demonstrated as a sample problem throughout this discourse.

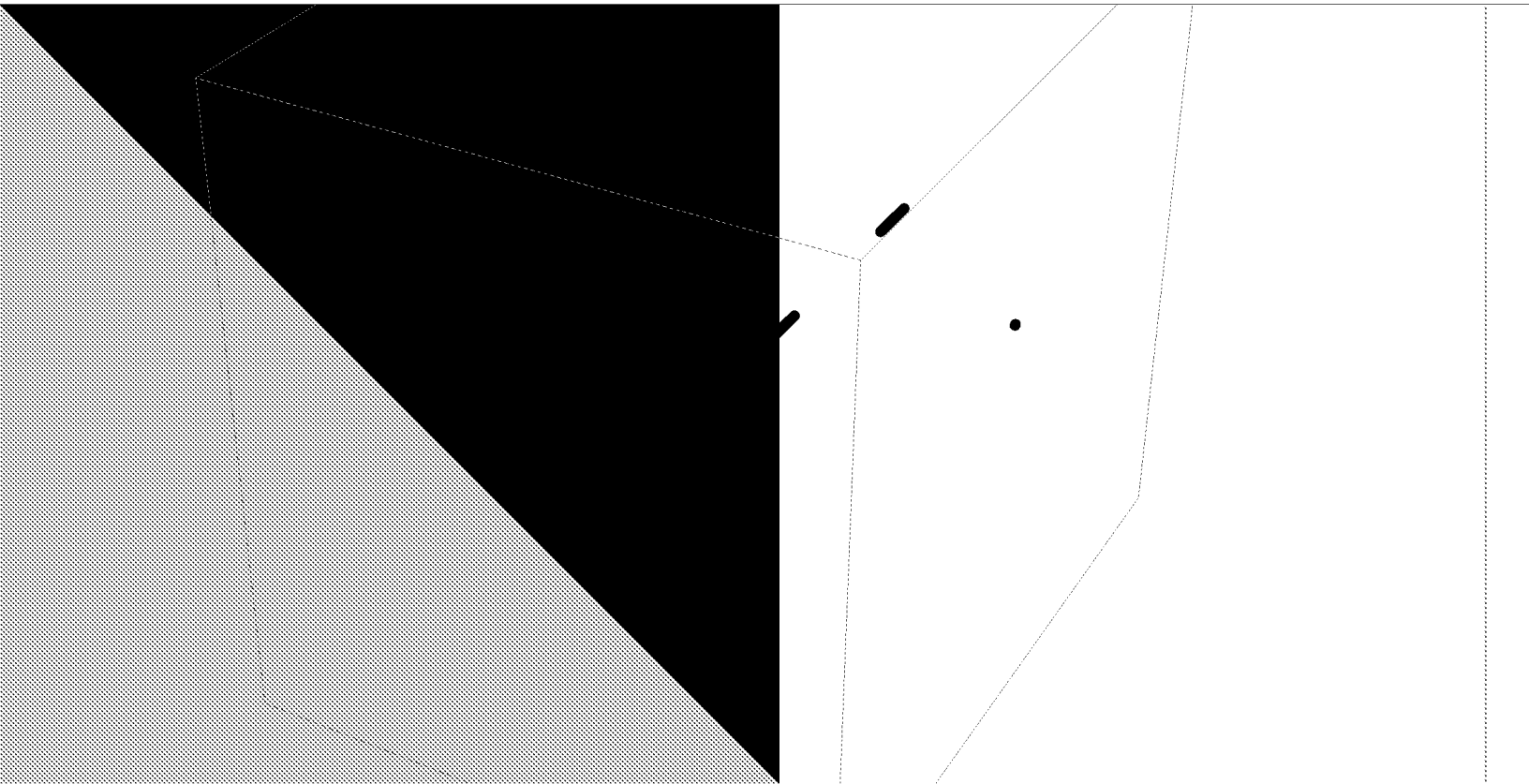


Figure 1: A hexahedral finite element

For example, in order to construct *locking-free*, *vide* [9], three-dimensional brick elements, cubic polynomials, which explicitly depend upon Poisson's ratio(s), in the physical (x, y, z) coordinates were derived for twenty four Rayleigh modes. Their linear combinations yield twenty four shape functions that are associated with the degrees-of-freedom located on the vertices.

To maintain the high accuracy consistently, especially the *locking-free* features, numerical quadrature has been completely avoided in evaluating the stiffness-like system matrices. This analytical strategy, which is based on the divergence theorem, is computationally more efficient than any quadrature scheme.

The *locking-free* interpolants (for a eight node hexahedral brick element) in the physical (x, y, z) co-ordinates are cubic functions, hence the *linear elastic* stresses are quadratic in (x, y, z) . Hence, the energy density expressions comprise of the terms in the expanded expression of $(1 + x + y + z)^4$. Its each term, within the brick shown in Figure 1 can be *exactly integrated* by the computer program presented here without resorting to any numerical quadrature.

Restrictions of convex elements do not apply and concavity, as it develops during elasto-plastic deformation, can be considered. For general vector field problems, e.g., those of continuum mechanics, the computer algebra systems can be incorporated seamlessly within a UNIX environment. The Modelica Language, *vide*[7], can achieve the same for all platforms. Therein, general numerics can be optimized for efficiency and accuracy by utilizing C++ routines [8].

1.1 Scalar field *high accuracy* finite elements

The Chazelle discretization of any region into minimum number of convex subsets [3] minimizes *incompatibility* errors along the interior boundaries due to tessellation. The Wachspress rational polynomial interpolants [11, 12] on each subset ensure C^0 inter-element compatibility.

In general, in the (x, y, z) frame energy terms like:

$$\frac{p_i(x, y, z) q_j(x, y, z)}{(r_k(x, y, z))^2}; \quad p, q, r : \text{polynomials in } (x, y, z) \quad (1)$$

are decomposed into partial fractions:

$$\frac{p_i(x, y, z) q_j(x, y, z)}{(r_k(x, y, z))^2} = \sum_{\alpha} \left(\frac{A_{\alpha}(x, y)}{(z - C_{\alpha}(x, y))} + \frac{B_{\alpha}(x, y)}{((z - C_{\alpha}(x, y)))^2} \right) \quad (2)$$

$$\text{where } A, B, C : \text{are in general complex functions of } (x, y) \quad (3)$$

so that an indefinite integral of a generic energy term :

$$\int \left(\frac{p_i(x, y, z) q_j(x, y, z)}{(r_k(x, y, z))^2} \right) dz = \sum_{\alpha} A_{\alpha}(x, y) \log(z - C_{\alpha}(x, y)) + \frac{B_{\alpha}(x, y)}{C_{\alpha}(x, y) - z} \quad (4)$$

can be obtained in the *closed-form*.

For large number of faces, the degrees of polynomials in equation (1) are high, and this will not permit analytical decomposition in the form of equation (2). Padé approximation [13, 2] is used to estimate \mathcal{P} , \mathcal{Q} and \mathcal{R} , in:

$$\frac{p_i(x, y, z) - q_j(x, y, z)}{(r_k(x, y, z))^2} \simeq \frac{\mathcal{P}_i(x, y, z) - \mathcal{Q}_j(x, y, z)}{(\mathcal{R}_k(x, y, z))^2}; \quad \mathcal{R}_k : \text{quadratic in } z \quad (5)$$

1.1.1 Limitation

For vector field problems, the constraints from the Wachspress interpolants on element boundary surfaces will prevent success in *patch tests* hence the element cannot be prevented from locking [10]. In order to resolve this, polynomial test function in (x, y, z) must be employed.

2 Formulation for polyhedral finite elements

2.1 Exact Integration

The divergence theorem:

$$\iiint_{\Omega} (\vec{\nabla} \odot \vec{g}(x, y, z)) d\Omega = \iint_{\Gamma} (\hat{n} \odot \vec{g}(x, y, z)) d\Gamma = \iint_{\Gamma} \vec{g}(x, y, z) \odot d\hat{\Gamma} \quad (6)$$

where the dot product is indicated by \odot

converts a volume integral in Ω to its surface Γ . Within the context of a polyhedron defined by Ω , the surface Γ is a collection of planes $\wp_i(x, y, z)$:

$$\text{where the equation for a } \wp_i(x, y, z) : d_i = a_i x + b_i y + c_i z \quad (7)$$

2.1.1 Convex polyhedra

For a convex³ element Ω , any interior point can be selected as the origin. Since no plane \wp_i of equation (7) passes through the origin, d_i in equation (7) is always non-zero. Hence it is possible to select for all faces on Γ :

$$\text{select: } d_i > 0 \text{ and} \quad (8)$$

$$\text{obtain: } \frac{\{a, b, c\}}{\sqrt{a^2 + b^2 + c^2}} = \hat{n} : \text{outer normal vector} \quad (9)$$

$$\text{notation : a vector is encased within curly braces: } \hat{n} = \{n_x, n_y, n_z\} \quad (10)$$

³To verify convexity from vertices defined by the matrix **nodes**, the *Mathematica* code:

And @@ (MemberQ[nodes, #] & /@
(ComputationalGeometry`Methods`ConvexHull13D[nodes]))[[1, 1]])
is written as a part of this document

3 An optimized form of the divergence theorem

For an arbitrary function $h(x, y, z)$:

$$\text{define: } g_z(x, y, z) = \int h(x, y, z) dz : \text{an indefinite integral in } z \quad (11)$$

$$\text{and then } \vec{g}(x, y, z) = \{0, 0, g_z(x, y, z)\} \quad (12)$$

$$\vec{g}(x, y, z) \odot d\hat{\Gamma} = \vec{g}(x, y, z) \odot \hat{n} d\Gamma = g_z(x, y, z) d\Gamma_{xy} \quad (13)$$

$$\Gamma_{xy} : \text{the projection of } \Gamma \text{ on the } x - y \text{ plane} \quad (14)$$

3.1 Convex polyhedra

It is important to realize that $d\Gamma_{xy}$ is a vector quantity whose magnitude is to be multiplied by the sign of n_z in equation (12). It is identical to the sign of c_i for plane number i in equation (9). For a surface plane perpendicular to z - axis:

$$n_z = 0 : \vec{z} \perp \wp_i \quad (15)$$

In the case of a non-convex polyhedra such a determination is not possible because at least one surface plane will pass through the interior of Ω .

3.2 Exact Integration

Area integrations in equations (6) and (13) are to be carried out using the following *Mathematica* program :

```
areaIntegrate[z_, {x_, y_}, nodes_, proc_ :> Integrate] :=
Module[{t, segments, lineIntegrate},

  lineIntegrate[int_, zz_, {xx_, yy_, tt_},
    {{x1_, y1_}, {x2_, y2_}}] :=
int[ ((y2 - y1) zz) /. {xx -> x1 + tt (x2 - x1),
  yy -> y1 + tt (y2 - y1)}, {tt, 0, 1}];

  segments = Partition[Append[nodes, nodes[[1]]], 2, 1];
  Plus @@ Map[lineIntegrate[proc,
    Integrate[z, x], {x, y, t}, #] &, segments] ]

areaIntegrate[{z_, {x_, y_}, nodes_}] :=
areaIntegrate[z, {x, y}, nodes]
```

For a face, if the nodal numbering on the $z = 0$ plane is *counterclockwise* then the *sign* of n_z in equation (12) will be $+1$ that is consistent with the tensorial approach implemented throughout. The *Mathematica* code of **Appendix-II** ensures this precautionary step for convex polyhedra.

By combining equation (6) and equations (11) through (13) the volume integral is expressed as a sum on the polyhedron faces that are not orthogonal to the z -axis (i.e., $c_i \neq 0$):

$$\iiint_{\Omega} h(x, y, z) d\Omega = \sum_i \iint_{\mathcal{A}_i} \left(g_z(x, y, z) \Big|_{z=\frac{d_i - a_i x - b_i y}{c_i}} \right) d\mathcal{A}_i \quad (16)$$

$$\text{non-zero } \mathcal{A}_i : \text{projection of face } i \text{ on } x - y \text{ plane} \quad (17)$$

$$g_z \text{ on the plane } \wp_i, \text{ can be reduced to a function of } x, y : g^*(x, y) \quad (18)$$

$$\text{then: } \iiint_{\Omega} h(x, y, z) d\Omega = \sum_i \iint_{\mathcal{A}_i} g^*(x, y) d\mathcal{A}_i \quad (19)$$

each integrals in equation (19) is evaluated using the computer algebra program furnished in **Appendix-II**.

4 Numerical Examples

Here, printing of 24 by 24 matrices is avoided.

4.1 Volume integration on a 3D-Brick finite element

For a typical finite element, as shown in Figure 1, in stiffness integration, with quadratic distribution of the stress profiles, the full quartic functions appear in the energy density terms. The nodal coordinates of Figure 1 are presented in Table 1:

node:	1	2	3	4	5	6	7	8
x	0	0	1	1.20272	0	0	1.21608	1.59793
y	1	0	0	1.31422	1.36807	0	0	1.90818
z	0	0	0	0	1.30599	1	1.23926	1.74118

(20)

Table 1: nodal values for a convex brick element

The stiffness integration can be carried out using the present formulation. The calculated volume integrals using computer programs of **Appendix-I** of the polynomial terms are shown in equation (21):

1	x	x^2	x^3	x^4		2.22344	1.53912	1.37624	1.37572	1.46922	
y	xy	x^2y	x^3y	y^2		1.71844	1.29807	1.23539	1.30083	1.73422	
xy^2	x^2y^2	y^3	xy^3	y^4		1.39974	1.39106	1.97293	1.68464	2.4153	
z	xz	x^2z	x^3z	yz	\rightarrow	1.63007	1.22254	1.15959	1.21846	1.39539	(21)
xyz	x^2yz	y^2z	xy^2z	y^3z		1.13712	1.14255	1.5175	1.31454	1.83679	
z^2	xz^2	x^2z^2	yz^2	xyz^2		1.54731	1.23191	1.21622	1.42495	1.22679	
y^2z^2	z^3	xz^3	yz^3	z^4		1.62714	1.64678	1.37935	1.61085	1.87798	

These high accuracy results, which are devoid of contamination due to quadrature, are indispensable on order to constructing the three-dimensional *locking-free* brick elements as an extension of *locking-free* quadrilateral elements developed in [4, 5, 6].

4.2 Locking-free interpolants

4.2.1 Notation

The nodal and Rayleigh modal variables are respectively indicated with roman and Greek symbols:

$$\{r\} : \text{list of nodal displacements}; \quad \{R\} : \text{list of nodal forces} \quad (22)$$

$$\{\psi\} : \text{list of modal participation factors}; \quad (23)$$

$$\{\Psi\} : \text{list of modal generalized forces: conjugate of } \{\psi\} \quad (24)$$

$$\text{vector-valued shape function: } \varpi(x, y, z) = \{u(x, y, z), v(x, y, z), w(x, y, z)\} \quad (25)$$

a vector (in the tensorial sense) is encased in curly braces

4.2.2 Polynomial shape functions

The full cubic polynomial displacement fields $\{u(x, y, z), v(x, y, z), w(x, y, z)\}$ are:

$$\begin{aligned}
u(x, y, z) = & a[1] + x * a[2] + y * a[3] + z * a[4] \\
& + x^2 * a[5] + x * y * a[6] + y^2 * a[7] \\
& + x * z * a[8] + y * z * a[9] + z^2 * a[10] \\
& + x^3 * a[11] + x^2 * y * a[12] + x * y^2 * a[13] + y^3 * a[14] \\
& + x^2 * z * a[15] + x * y * z * a[16] + y^2 * z * a[17] \\
& + x * z^2 * a[18] + y * z^2 * a[19] + z^3 * a[20]
\end{aligned} \quad (26)$$

The other two displacement components v, w along x, y respectively, are obtained by cyclic replacment; to obtain v from u replace a by b and then x by y , y by z and z by x . Similarly, w is obtained from v with coefficient $c[i]$.

4.2.3 Incompressible Rayleigh modes

Starting with the form of equation (26), there are 60 unknown parameters in the vector-valued shape function $\varpi(x, y, z) = \{u(x, y, z), v(x, y, z), w(x, y, z)\}$:

$$a[1] \dots a[20], b[1] \dots b[20], c[1] \dots c[20] \quad (27)$$

Incompressibility demands:

$$\frac{\partial u}{\partial x} + \frac{\partial v}{\partial y} + \frac{\partial w}{\partial z} = 0, \quad \text{for all } x, y, z \quad (28)$$

that leads to the following possible interrelations between the parameters:

$$\begin{aligned} a[2] &\rightarrow -b[2] - c[2], a[8] \rightarrow -b[6] - 2c[5], a[5] \rightarrow -\frac{b[8]}{2} - \frac{c[6]}{2}, \\ a[6] &\rightarrow -2b[5] - c[8], a[18] \rightarrow -b[13] - 3c[11], a[15] \rightarrow -\frac{b[16]}{2} - c[12], \\ a[11] &\rightarrow -\frac{b[18]}{3} - \frac{c[13]}{3}, a[16] \rightarrow -2b[12] - 2c[15], \\ a[12] &\rightarrow -b[15] - \frac{c[16]}{2}, a[13] \rightarrow -3b[11] - c[18] \end{aligned} \quad (29)$$

These ten substitutions make the incompressible shape functions $\varpi^o(x, y, z)$, which contain 50 constants, in the following three parts:

$$\varpi^o(x, y, z) = \varpi_1^o(x, y, z) + \varpi_2^o(x, y, z) + \varpi_3^o(x, y, z) \quad (30)$$

$$\varpi_1^o(x, y, z) : \text{“triangulation” modes} \quad (31)$$

$$\varpi_2^o(x, y, z) : \text{“flexural” modes} \quad (32)$$

$$\varpi_3^o(x, y, z) : \text{“quadratic stress” modes} \quad (33)$$

in particular:

$$\varpi_1^o(x, y, z) = \begin{Bmatrix} a[3]y + a[4]z + a[1] + x(-b[2] - c[2]) \\ b[4]x + b[2]y + b[3]z + b[1] \\ c[3]x + c[4]y + c[2]z + c[1] \end{Bmatrix} \quad (34)$$

therein, the 11 parameters are associated with 6 rigid body modes and 5 deviatoric modes. These eleven modes are evaluated by setting one parameter to unity and rest to zero, at a time leading to:

1	y	z	0	$-x$	0	0	0	$-x$	0	0	0
0	0	0	1	y	z	x	0	0	0	0	0
0	0	0	0	0	0	0	1	z	x	y	0

(35)

Throughout, the vector displacement field is listed as a column encased in curly braces:

$$\text{a column represents: } \begin{Bmatrix} x - displacement \\ y - displacement \\ z - displacement \end{Bmatrix} \text{ as in equation (35)} \quad (36)$$

The flexural modes contain quadratic terms in x, y, z and free from shear strains:

$$0 = \frac{\partial u}{\partial y} + \frac{\partial v}{\partial x} = \frac{\partial v}{\partial z} + \frac{\partial w}{\partial y} = \frac{\partial w}{\partial x} + \frac{\partial u}{\partial z}, \quad \text{for all } x, y, z \quad (37)$$

and yields the following possible interrelations between the parameters:

$$\begin{aligned} a[7]- &> -(b[8]/2), a[9]- > 0, b[9]- > 0, a[10]- > -(c[6]/2), \\ b[6]- &> -2c[10], c[5]- > c[7] + c[10], b[5]- > b[7] + b[10], \\ c[8]- &> -2b[7], c[9]- > 0 \end{aligned} \quad (38)$$

the six terms:

$$b[7], b[8], b[10], c[6], c[7], c[10] \quad (39)$$

are responsible for pure bending in two orthogonal planes on each of three orthogonal directions. Thus the six incompressible flextural modes are:

$$\begin{array}{c|c|c|c|c|c} \frac{xy}{2} & \frac{xz}{2} & -\frac{xz}{2} & \frac{z^2}{4} - \frac{y^2}{4} & \frac{y^2}{4} - \frac{z^2}{4} & -\frac{xy}{2} \\ \frac{z^2}{4} - \frac{x^2}{4} & -\frac{yz}{2} & \frac{yz}{2} & \frac{xy}{2} & -\frac{xy}{2} & \frac{x^2}{4} - \frac{z^2}{4} \\ -\frac{yz}{2} & \frac{y^2}{4} - \frac{x^2}{4} & \frac{x^2}{4} - \frac{y^2}{4} & -\frac{xz}{2} & \frac{xz}{2} & \frac{yz}{2} \end{array} \quad (40)$$

The six cubic displacement modes are:

$$\begin{array}{c|c|c|c|c|c} \frac{x^2y}{4} - \frac{y^3}{12} & \frac{x^2z}{4} - \frac{z^3}{12} & 0 & \frac{1}{2}y \left(\frac{z^2}{2} - \frac{x^2}{2} \right) & \frac{1}{2}z \left(\frac{y^2}{2} - \frac{x^2}{2} \right) & 0 \\ \frac{1}{2}x \left(\frac{z^2}{2} - \frac{y^2}{2} \right) & 0 & \frac{y^2z}{4} - \frac{z^3}{12} & \frac{xy^2}{4} - \frac{x^3}{12} & 0 & \frac{1}{2}z \left(\frac{x^2}{2} - \frac{y^2}{2} \right) \\ 0 & \frac{1}{2}x \left(\frac{y^2}{2} - \frac{z^2}{2} \right) & \frac{1}{2}y \left(\frac{x^2}{2} - \frac{z^2}{2} \right) & 0 & \frac{xz^2}{4} - \frac{x^3}{12} & \frac{yz^2}{4} - \frac{y^3}{12} \end{array} \quad (41)$$

4.2.4 Incompressible solution

There are twenty three *independent* Rayleigh modes, eleven, six and six, respectively, in equations (35), (40) and (41). The corresponding twenty three modal participation factors of equation (23) and a uniform element pressure \mathbf{p} constitute the twenty unknowns per brick element. Their *unique* solution for boundary value problems can be found in [5].

The *modal* participation factors in $\{\psi\}$ are the *independent* variables. The matrix $[G_{r\psi}]$ transformations $\{\phi\}$ to the nodal displacements $\{r\}$:

$$\{r\} = [G_{r\psi}] \{\psi\} \text{ or } \{r\} = [G] \{\psi\} \rightarrow \{\psi\} = [G]^{-1} \{r\} \quad (42)$$

$$[G]^{-1} : \text{in the sense of Moore-Penrose } [G]^+ \text{ vide [1]} \quad (43)$$

4.2.5 The Compressible Rayleigh modes

Following the procedure of systematic elimination, whose result is shown in equation (29), the twenty four Rayleigh modes are solved as follows.

The simplex modes are:

$$\left(\begin{array}{c|c|c|c|c|c|c|c|c|c|c|c|c|c} 1 & x & y & z & 0 & 0 & 0 & 0 & 0 & 0 & 0 & 0 & 0 & 0 \\ 0 & 0 & 0 & 0 & 1 & y & z & x & 0 & 0 & 0 & 0 & 0 & 0 \\ 0 & 0 & 0 & 0 & 0 & 0 & 0 & 0 & 1 & z & x & y & 0 & 0 \end{array} \right) \quad (44)$$

The six quadratic displacement modes are:

$$\begin{pmatrix} x^2 + \frac{y^2(1-\nu)}{\nu} \\ xy \left(4(\nu-1) + \frac{(1-\nu)(4\nu-2)}{\nu} \right) \\ 0 \end{pmatrix} \begin{vmatrix} z^2 - y^2 \\ 2xy \\ -2xz \end{vmatrix} \quad (45)$$

$$\begin{pmatrix} xy \left(-\frac{2(1-\nu)}{\nu} + 4(1-\nu) + 4(\nu-1) \right) \\ \frac{(1-\nu)x^2}{\nu} + y^2 \\ 0 \end{pmatrix} \begin{vmatrix} 2xy \\ z^2 - x^2 \\ -2yz \end{vmatrix} \quad (46)$$

$$\begin{pmatrix} -2xz \left(-2(\nu-1) - \frac{(1-\nu)(2\nu-1)}{\nu} \right) \\ 0 \\ \frac{(1-\nu)x^2}{\nu} + z^2 \end{pmatrix} \begin{vmatrix} 2xz \\ -2yz \\ y^2 - x^2 \end{vmatrix} \quad (47)$$

The six cubic displacement modes are:

$$\begin{pmatrix} \begin{pmatrix} \frac{x^2y}{4} - \frac{y^3}{12} \\ 0 \\ -\frac{1}{2}xyz \end{pmatrix} & \begin{pmatrix} -\frac{1}{2}xyz \\ \frac{y^2z}{4} - \frac{z^3}{12} \\ 0 \end{pmatrix} & \begin{pmatrix} 0 \\ -\frac{1}{2}xyz \\ \frac{xz^2}{4} - \frac{x^3}{12} \end{pmatrix} \\ \begin{pmatrix} \frac{x^2z}{4} - \frac{z^3}{12} \\ -\frac{1}{2}xyz \\ 0 \end{pmatrix} & \begin{pmatrix} 0 \\ \frac{xy^2}{4} - \frac{x^3}{12} \\ -\frac{1}{2}xyz \end{pmatrix} & \begin{pmatrix} -\frac{1}{2}xyz \\ 0 \\ \frac{yz^2}{4} - \frac{y^3}{12} \end{pmatrix} \end{pmatrix} \quad (48)$$

4.2.6 Modal stiffness matrix

The strain-displacement transformation matrix $[b]$ is separated in three parts:

$$[b] = \{[b1], [b2], [b3]\} \quad (49)$$

$$[b1] = \begin{pmatrix} 0 & 1 & 0 & 0 & 0 & 0 & 0 & 0 & 0 & 0 & 0 & 0 \\ 0 & 0 & 0 & 0 & 0 & 1 & 0 & 0 & 0 & 0 & 0 & 0 \\ 0 & 0 & 0 & 0 & 0 & 0 & 0 & 0 & 0 & 1 & 0 & 0 \\ 0 & 0 & 1 & 0 & 0 & 0 & 0 & 1 & 0 & 0 & 0 & 0 \\ 0 & 0 & 0 & 0 & 0 & 0 & 1 & 0 & 0 & 0 & 0 & 1 \\ 0 & 0 & 0 & 1 & 0 & 0 & 0 & 0 & 0 & 0 & 1 & 0 \end{pmatrix} \quad (50)$$

$$[b2] = \begin{pmatrix} \begin{array}{c|c|c} 2x & 0 & \frac{2y(\nu-1)}{\nu} \\ \frac{2x(\nu-1)}{\nu} & 2x & 2y \\ 0 & -2x & 0 \end{array} & 2x\left(\frac{1}{\nu}-1\right) + \frac{2x(\nu-1)}{\nu} & \begin{array}{c|c|c} 2y & \frac{2z(\nu-1)}{\nu} & 2z \\ 0 & 0 & -2z \\ -2y & 2z & 0 \end{array} \\ \begin{array}{c} 0 \\ 0 \\ 0 \\ 0 \end{array} & 0 & \begin{array}{c} 0 \\ 0 \\ 0 \\ 0 \end{array} \end{pmatrix} \quad (51)$$

$$[b3] = \begin{pmatrix} \begin{array}{c|c|c} \frac{xy}{2} & \frac{xz}{2} & -\frac{yz}{2} \\ 0 & -\frac{xz}{2} & \frac{yz}{2} \\ -\frac{xy}{2} & 0 & 0 \end{array} & \begin{array}{c} 0 \\ \frac{xy}{2} \\ -\frac{xy}{2} \end{array} & \begin{array}{c|c|c} 0 & 0 & -\frac{yz}{2} \\ -\frac{xz}{2} & -\frac{xz}{2} & 0 \\ \frac{yz}{2} & \frac{yz}{2} & \frac{yz}{2} \end{array} \\ \begin{array}{c} \frac{x^2}{4} - \frac{y^2}{4} \\ -\frac{xz}{2} \\ -\frac{yz}{2} \end{array} & \begin{array}{c} \frac{y^2}{4} - \frac{x^2}{4} \\ -\frac{yz}{2} \\ \frac{z^2}{4} - \frac{y^2}{4} \end{array} & \begin{array}{c} \frac{yz}{2} \\ -\frac{xz}{2} \\ -\frac{xy}{2} \end{array} \end{pmatrix} \quad (52)$$

4.2.7 Nodal stiffness matrix

The *energy balance principle* connects modal variables $\{\phi\}$ and $\{\Phi\}$ with their nodal counterparts:

$$\{R\}^T \{r\} = \{\Psi\}^T \{\psi\} \rightarrow \{R\} = [G^T]^{-1} \{\Psi\} : \text{the force transformation rule} \quad (53)$$

$$\text{and } [k_{rr}] = [G^T]^{-1} [k_{\phi\phi}] [G]^{-1}; \quad k : \text{stiffness matrix} \quad (54)$$

4.2.8 The shape functions

The $[G]$ matrix in equation (42) associated with the element nodes presented in equation (20) for the Rayleigh modes in equations (44) through (48), *vide* [6] for details.

Appendix-I: *Mathematica* Package

main functions

```

conexPolyhedronVolumeIntegrate::usage =
  "conexPolyhedronVolumeIntegrate[g,{x,y,z},allFaceNodes]
  returns the volume integral of g a function in {x,y,z}
  within the convex polyhedron defined by allFaceNodes."

polyhedronVolumeIntegrate::usage =
  "polyhedronVolumeIntegrate[g,{x,y,z},allFaceNodes,
  signZOutwardNormalList]
  returns the volume integral of g a function in {x,y,z}
  within the polyhedron defined by allFaceNodes.
  The signs of the normal to the z-axis are prescribed in
  signZOutwardNormalList."

conexPolyhedronVolumeIntegrate[g_, {x_, y_, z_}, allFaceNodes_] :=
  Module[{signZOutwardNormalList, signCorrectionList, i, funcList},
    signZOutwardNormalList =
      Sign[#[[3]] & /@ outwardNormalsConvexPolyhedron[allFaceNodes]];
    polyhedronVolumeIntegrate[g, {x, y, z}, allFaceNodes, signZOutwardNormalList]

polyhedronVolumeIntegrate[g_, {x_, y_, z_}, allFaceNodes_,
  signZOutwardNormalList_] := Module[{signCorrectionList, i, funcList},
  signCorrectionList = (
    (Sign[areaIntegrate[1, {x, y}, #] & /@ (extractXY /@ allFaceNodes)])
    signZOutwardNormalList);
  funcList = Integrate[g, z] /. ((Solve[# == 0, z] // Flatten) & /@
    (LhsEquationOfAPlane[#, {x, y, z}] & /@ allFaceNodes));
  Sum[signCorrectionList[[i]] * areaIntegrate[funcList[[i]], {x, y},
    Part[extractXY /@ allFaceNodes, i]], {i, funcList // Length}]

```

example

```

In[22]:= fourNodes = RandomReal[{RandomReal[], RandomReal[]}, {4, 3}]
Out[22]:= {{0.532308, 0.475947, 0.579055}, {0.389285, 0.386792, 0.431123},
  {0.468785, 0.477351, 0.444661}, {0.602696, 0.461231, 0.595927}}

In[23]:= allFaceNodes = Partition[Join[fourNodes, {fourNodes[[1]],
  fourNodes[[2]]}], 3, 1]
Out[23]:= {{{0.532308, 0.475947, 0.579055}, {0.389285, 0.386792, 0.431123},
  {0.468785, 0.477351, 0.444661}}, {{0.389285, 0.386792, 0.431123},
  {0.468785, 0.477351, 0.444661}, {0.602696, 0.461231, 0.595927}},
  {{0.468785, 0.477351, 0.444661}, {0.602696, 0.461231, 0.595927},
  {0.532308, 0.475947, 0.579055}}, {{0.602696, 0.461231, 0.595927},
  {0.532308, 0.475947, 0.579055}, {0.389285, 0.386792, 0.431123}}}

In[24]:= error = Abs[conexPolyhedronVolumeIntegrate[1,
  {x, y, z}, allFaceNodes] - Abs[Det[Append[#, 1] & /@ fourNodes] / 6]]
Out[24]:= 8.86335 × 10-18

```

auxiliary functions

extractXY

```
extractXY[xyz_] := ({#[[1]], #[[2]]}) & /@ Partition[Flatten[xyz], 3];
```

normalToPlane

```
normalToPlane[h_, {x_, y_, z_}] :=
  Module[{m}, m = D[h, #] & /@ {x, y, z}; m / Sqrt[m.m]];
outwardNormal[p_?MatrixQ, interiorPoint_] :=
  Module[{x, y, z, draftNormal, directionOfOutwardRay, av},
    av[x_] := Plus @@ x / Length[x];
    draftNormal = normalToPlane[LhsEquationOfAPlane[p, {x, y, z}], {x, y, z}];
    directionOfOutwardRay = av[p] - interiorPoint;
    If[directionOfOutwardRay.draftNormal < 0, -draftNormal, draftNormal]
  ]
```

outwardNormalsConvexPolyhedron[nodesOfFaces_] :=

```
Module[{interiorPoint, allNodes, av},

  av[x_] := Plus @@ x / Length[x];
  allNodes = Partition[Flatten[nodesOfFaces], 3] // Union;
  interiorPoint = av[allNodes];
  outwardNormal[#, interiorPoint] & /@ nodesOfFaces
]
```

inPlaneQ

```
inPlaneQ[x_] := Module[{bs},
  If[Length[x] == 3, True, (bs = Prepend[#, 1] & /@ x; Max[Abs[Det /@
    (Prepend[#, First[bs]] & /@
      Partition[Rest[bs], 3, 1])]] < 10^-6) ]]
```

normalToPlane

```
normalToPlane[h_, {x_, y_, z_}] := Module[{m}, m = D[h, #] & /@ {x, y, z}; m / Sqrt[m.m]]
```

LHSequationOfAPlane

```
LhsEquationOfAPlane[p_, {x_, y_, z_}] :=
  If[inPlaneQ[p], Expand[
    Det[Append[#, 1] & /@ Append[Take[p, 3], {x, y, z}]]],
    Print["points ", p, "are not co-planar"]]
```

Appendix-III: *Mathematica* Package

Example-I: Integration rule

June 27

Author: Gautam Dasgupta

four parts for terms

code: solidToVolumeIntegral

```
Clear[solidToVolumeIntegral];
solidToVolumeIntegral[f_, {x_, y_, z_}, {nodes_, faceIndices_}] :=
Module[{faceNodes},
  faceNodes =
    Partition[nodes[[#]] & /@ Flatten[faceIndices], Length[faceIndices[[1]]]];
  volumeIntegrate[f, {x, y, z}, faceNodes]
]
```

code: integrator

```
Clear[integrator];
integrator[func_, {x_, y_, z_}, {p1Terms_, p2Terms_, p3Terms_, p4Terms_},
  {valueP4Terms_, valueP3Terms_, valueP2Terms_, valueP1Terms_}] :=
Module[{elmVol = valueP1Terms[[1]]},
  elmVol * (((((Expand[func] /. Thread[
    p4Terms → (valueP4Terms / elmVol)])
    /. Thread[ p3Terms → (valueP3Terms / elmVol)]) /.
    Thread[ p2Terms → (valueP2Terms / elmVol)])
    ) /. Thread[ p1Terms → (valueP1Terms / elmVol)])
]
```

polynomial data

```
p1Terms = {1, x, y, z}; p2Terms = {x2, x y, y2, x z, y z, z2};
p3Terms = {x3, x2 y, x y2, y3, x2 z, x y z, y2 z, x z2, y z2, z3}; p4Terms =
  {x4, x3 y, x2 y2, x y3, y4, x3 z, x2 y z, x y2 z, y3 z, x2 z2, x y z2, y2 z2, x z3, y z3, z4};
{valueP4Terms, valueP3Terms, valueP2Terms, valueP1Terms} =
solidToVolumeIntegral[{p4Terms, p3Terms, p2Terms, p1Terms},
  {x, y, z}, {nodes, faceIndices}]
```

2 | *fourParts-3.nb*

Example

element data

```

In[6]:= nodes = {{0, 1, 0}, {0, 0, 0}, {1, 0, 0}, {1.202715965606913`, 1.314215366298273`, 0},
  {0, 1.368066309144244`, 1.305989793327691`},
  {0, 0, 1}, {1.216079880285841`, 0, 1.23925741120344`},
  {1.597930989278036`, 1.90818293399255`, 1.7411801057262242`}}

In[6]:= faceIndices =
  {{1, 4, 3, 2}, {5, 8, 7, 6}, {6, 5, 1, 2}, {7, 3, 4, 8}, {2, 3, 7, 6}, {5, 8, 4, 1}}

```

calculated results

```

In[7]:= valueP4Terms = {1.4692184020676273`, 1.3008258816213933`, 1.391055637976948`,
  1.684639189614494`, 2.4153018320293618`, 1.2184569407424475`,
  1.1425465853282244`, 1.3145355635675942`, 1.836793786704385`,
  1.2162187222826766`, 1.2267934933996645`, 1.6271444555393084`,
  1.3793529251241945`, 1.6108494493895607`, 1.8779826716598929`}

In[8]:= valueP3Terms = {1.375724277679978`, 1.2353866617421558`, 1.3997396270453801`,
  1.9729269721181257`, 1.1595858030999338`, 1.13712469543483`, 1.517503755878869`,
  1.2319095628467431`, 1.4249475541728107`, 1.6467759711183976`}

valueP2Terms = {1.3762442046785648`, 1.298072609873346`, 1.7342150490206258`,
  1.2225410787060726`, 1.3953906401333516`, 1.5473082043008088`}

In[9]:= valueP1Terms = {2.2234367654359333`,
  1.539118468423933`, 1.7184382389677864`, 1.6300687226378585`}

```

verification

```

In[10]:= selfTest = integrator[Flatten[{p4Terms, p3Terms, p2Terms, p1Terms}],
  {x, y, z}, {p1Terms, p2Terms, p3Terms, p4Terms},
  {valueP4Terms, valueP3Terms, valueP2Terms, valueP1Terms}] ==
  Flatten[{valueP4Terms, valueP3Terms, valueP2Terms, valueP1Terms}]

Out[10]:= True

```

5 Appendices

Mathematica program segments furnished here. All calculations presented can be verified by executing these modules.

Appendix-I: *Exact* Three-dimensional volume integration

Appendix-II: In order to ensure the locking free condition *exact* integration of the energy density function is unavoidable. To attain fast calculation, the substitution of polynomial terms, as in equation (21), recommended. One of the main parts of this discovery is to ensure proper implementation of the substitution rule that appears here.

Appendix-III: An important part of the validation is that the rigid body modes are exactly reproduced. This can be verified from the minimum eigenvalues of the element stiffness matrix furnished below:

$$\begin{pmatrix} 146.716 & 67.7913 & 18.304 & 9.52665 & 2.88408 & 2.29533 \\ 2.19528 & 2.0452 & 1.08073 & 0.795941 & 0.510553 & 0.504974 \\ 0.389806 & 0.148966 & 0.132988 & 0.0728463 & 0.0619707 & 0.0514826 \\ 0 & 0 & 0 & 0 & 0 & 0 \end{pmatrix} \quad (55)$$

Appendix-IV: This discovery encompasses general anisotropy with twenty one Poisson's ratios. The method of calculation is with the proper constitutive relation but the steps to determine the Rayleigh modes are the same as that of the isotropic case. For this purpose a complete and detailed program is enclosed here.

5.1 Appendix-I: *Mathematica* Package for Volume integration

main functions

```

conexPolyhedronVolumeIntegrate::usage =
  "conexPolyhedronVolumeIntegrate[g,{x,y,z},allFaceNodes]
returns the volume integral of g a function in {x,y,z}
within the convex polyhedron defined by allFaceNodes."

polyhedronVolumeIntegrate::usage =
  "polyhedronVolumeIntegrate[g,{x,y,z},allFaceNodes,
signZOutwardNormalList]
returns the volume integral of g a function in {x,y,z}
within the polyhedron defined by allFaceNodes.
The signs of the normal to the z-axis are prescribed in
signZOutwardNormalList."

conexPolyhedronVolumeIntegrate[g_, {x_, y_, z_}, allFaceNodes_] :=
  Module[{signZOutwardNormalList, signCorrectionList, i, funcList},
    signZOutwardNormalList =
      Sign[#[[3]] & /@ outwardNormalsConvexPolyhedron[allFaceNodes]];
    polyhedronVolumeIntegrate[g, {x, y, z}, allFaceNodes, signZOutwardNormalList]]

polyhedronVolumeIntegrate[g_, {x_, y_, z_}, allFaceNodes_,
signZOutwardNormalList_] := Module[{signCorrectionList, i, funcList},
  signCorrectionList = (
    (Sign[areaIntegrate[1, {x, y}, #] & /@ (extractXY /@ allFaceNodes)])
    signZOutwardNormalList);
  funcList = Integrate[g, z] /. ((Solve[# == 0, z] // Flatten) & /@
    (LhsEquationOfAPlane[#, {x, y, z}] & /@ allFaceNodes));
  Sum[signCorrectionList[[i]] * areaIntegrate[funcList[[i]], {x, y},
    Part[extractXY /@ allFaceNodes, i]], {i, funcList // Length}]]

```

example

```

fourNodes = RandomReal[{RandomReal[], RandomReal[]}, {4, 3}]
{{0.532308, 0.475947, 0.579055}, {0.389285, 0.386792, 0.431123},
 {0.468785, 0.477351, 0.444661}, {0.602696, 0.461231, 0.595927}}

allFaceNodes = Partition[Join[fourNodes, {fourNodes[[1]],
fourNodes[[2]]}], 3, 1]
{{{0.532308, 0.475947, 0.579055}, {0.389285, 0.386792, 0.431123},
 {0.468785, 0.477351, 0.444661}}, {{0.389285, 0.386792, 0.431123},
 {0.468785, 0.477351, 0.444661}, {0.602696, 0.461231, 0.595927}},
 {{0.468785, 0.477351, 0.444661}, {0.602696, 0.461231, 0.595927},
 {0.532308, 0.475947, 0.579055}}, {{0.602696, 0.461231, 0.595927},
 {0.532308, 0.475947, 0.579055}, {0.389285, 0.386792, 0.431123}}}

error = Abs[conexPolyhedronVolumeIntegrate[1,
 {x, y, z}, allFaceNodes] - Abs[Det[Append[#, 1] & /@ fourNodes] / 6]]
8.86335 × 10-18

```

5.1.1 Auxiliary functions for volume integration

auxiliary functions

extractXY

```
extractXY[xyz_] := ({#[[1]], #[[2]]}) & /@ Partition[Flatten[xyz], 3];
```

normalToPlane

```
normalToPlane[h_, {x_, y_, z_}] :=  
  Module[{m}, m = D[h, #] & /@ {x, y, z}; m / Sqrt[m.m]];  
outwardNormal[p_?MatrixQ, interiorPoint_] :=  
  Module[{x, y, z, draftNormal, directionOfOutwardRay, av},  
    av[x_] := Plus @@ x / Length[x];  
    draftNormal = normalToPlane[LhsEquationOfAPlane[p, {x, y, z}], {x, y, z}];  
    directionOfOutwardRay = av[p] - interiorPoint;  
    If[directionOfOutwardRay.draftNormal < 0, -draftNormal, draftNormal]  
  ]
```

outwardNormalsConvexPolyhedron[nodesOfFaces_] :=

```
  Module[{interiorPoint, allNodes, av},  
  
    av[x_] := Plus @@ x / Length[x];  
    allNodes = Partition[Flatten[nodesOfFaces], 3] // Union;  
    interiorPoint = av[allNodes];  
    outwardNormal[#, interiorPoint] & /@ nodesOfFaces  
  ]
```

inPlaneQ

```
inPlaneQ[x_] := Module[{bs},  
  If[Length[x] === 3, True, (bs = Prepend[#, 1] & /@ x; Max[Abs[Det /@  
    (Prepend[#, First[bs]] & /@  
      Partition[Rest[bs], 3, 1])] < 10^-6) ]]
```

normalToPlane

```
normalToPlane[h_, {x_, y_, z_}] := Module[{m}, m = D[h, #] & /@ {x, y, z}; m / Sqrt[m.m]]
```

LHSequationOfAPlane

```
LhsEquationOfAPlane[p_, {x_, y_, z_}] :=  
  If[inPlaneQ[p], Expand[  
    Det[Append[#, 1] & /@ Append[Take[p, 3], {x, y, z}]]],  
    Print["points ", p, "are not co-planar"]]
```

5.2 Appendix-II: *Mathematica* Package and Example

5.2.1 Developing the rules

Example-I: Integration rule

June 27

Author: Gautam Dasgupta

four parts for terms

code: solidToVolumeIntegral

```
Clear[solidToVolumeIntegral];
solidToVolumeIntegral[f_, {x_, y_, z_}, {nodes_, faceIndices_}] :=
Module[{faceNodes},

faceNodes =
Partition[nodes[[#]] & /@ Flatten[faceIndices], Length[faceIndices[[1]]]];
volumeIntegrate[f, {x, y, z}, faceNodes]
]
```

code: integrator

```
Clear[integrator];
integrator[func_, {x_, y_, z_}, {p1Terms_, p2Terms_, p3Terms_, p4Terms_},
{valueP4Terms_, valueP3Terms_, valueP2Terms_, valueP1Terms_}] :=
Module[{elmVol = valueP1Terms[[1]]},

elmVol * (((((Expand[func] /. Thread[
p4Terms → (valueP4Terms / elmVol)])
/. Thread[ p3Terms → (valueP3Terms / elmVol)]) /.
Thread[ p2Terms → (valueP2Terms / elmVol)])
) /. Thread[ p1Terms → (valueP1Terms / elmVol)])
]
```

polynomial data

```
p1Terms = {1, x, y, z}; p2Terms = {x2, x y, y2, x z, y z, z2};
p3Terms = {x3, x2 y, x y2, y3, x2 z, x y z, y2 z, x z2, y z2, z3}; p4Terms =
{x4, x3 y, x2 y2, x y3, y4, x3 z, x2 y z, x y2 z, y3 z, x2 z2, x y z2, y2 z2, x z3, y z3, z4};
{valueP4Terms, valueP3Terms, valueP2Terms, valueP1Terms} =
solidToVolumeIntegral[{p4Terms, p3Terms, p2Terms, p1Terms},
{x, y, z}, {nodes, faceIndices}]
```

2 | *fourParts-3.nb*

5.2.2 Example of developing the rules

Example

element data

```
nodes = {{0, 1, 0}, {0, 0, 0}, {1, 0, 0}, {1.202715965606913`, 1.314215366298273`, 0},
         {0, 1.368066309144244`, 1.305989793327691`},
         {0, 0, 1}, {1.216079880285841`, 0, 1.23925741120344`},
         {1.597930989278036`, 1.90818293399255`, 1.7411801057262242`}}
```

```
faceIndices =
  {{1, 4, 3, 2}, {5, 8, 7, 6}, {6, 5, 1, 2}, {7, 3, 4, 8}, {2, 3, 7, 6}, {5, 8, 4, 1}}
```

calculated results

```
valueP4Terms = {1.4692184020676273`, 1.3008258816213933`, 1.391055637976948`,
                1.684639189614494`, 2.4153018320293618`, 1.2184569407424475`,
                1.1425465853282244`, 1.3145355635675942`, 1.836793786704385`,
                1.2162187222826766`, 1.2267934933996645`, 1.6271444555393084`,
                1.3793529251241945`, 1.6108494493895607`, 1.8779826716598929`}
```

```
valueP3Terms = {1.375724277679978`, 1.2353866617421558`, 1.3997396270453801`,
                1.9729269721181257`, 1.1595858030999338`, 1.13712469543483`, 1.517503755878869`,
                1.2319095628467431`, 1.4249475541728107`, 1.6467759711183976`}
```

```
valueP2Terms = {1.3762442046785648`, 1.298072609873346`, 1.7342150490206258`,
                1.2225410787060726`, 1.3953906401333516`, 1.5473082043008088`}
```

```
valueP1Terms = {2.2234367654359333`,
                1.539118468423933`, 1.7184382389677864`, 1.6300687226378585`}
```

verification

```
selfTest = integrator[Flatten[{p4Terms, p3Terms, p2Terms, p1Terms}],
                      {x, y, z}, {p1Terms, p2Terms, p3Terms, p4Terms},
                      {valueP4Terms, valueP3Terms, valueP2Terms, valueP1Terms}] ==
  Flatten[{valueP4Terms, valueP3Terms, valueP2Terms, valueP1Terms}]
```

```
True
```

Appendix-IV

June 26, 2013

Author: Gautam Dasgupta

Auxiliary functions

```
Global`x; Global`y; Global`z; xyz = {x, y, z}
{x, y, z}
```

*γ*FromUVW

```
γFromUVW[{u_, v_, w_}, {x_, y_, z_}] :=
{D[u, y] + D[v, x], D[v, z] + D[w, y], D[w, x] + D[u, z]}
```

nextMode

```
Clear[nextMode];
nextMode::usage =
"nextMode[thisMode,xyz] generates the mode by rotating left the
coordinate system xyz from the given thisModes."
nextMode[thisMode_?VectorQ, xyz_] := RotateRight[
thisMode /. Thread[xyz → RotateLeft[xyz]]]

nextMode[theseModes_?MatrixQ, xyz_] := nextMode[#, xyz] & /@ theseModes
```

nextMode[thisMode,xyz] generates the mode by rotating
left the coordinate system xyz from the given thisModes.

```
nextMode[theseModes_?MatrixQ] := nextMode[theseModes, xyz]
```

dilatation

```
Clear[dilatation];
dilatation::usage = "dilatation[s_List,{x, y, z}]
returns ilatation for s in x,y,z."
dilatation[s_List,{x, y, z}]
returns ilatation for s in x,y,z.
```

```
dilatation[s_List, xyz_] :=
(D[#[[1]], xyz[[1]]] + D[#[[2]], xyz[[2]]] + D[#[[3]], xyz[[3]]]) &[s]
```

```

dilatation[s_?MatrixQ, {x_, y_, z_}] := Flatten[dilatation[#, {x, y, z}] & s]
dilatation[s_List] := dilatation[s, {x, y, z}]
dilatation[s_] := dilatation[Partition[Flatten[s], 3]] // Flatten

```

shearStrainsFromUVW

```

Clear[shearStrainsFromUVW];

shearStrainsFromUVW::usage = "shearStrainsFromUVW[{u,v,w}, {x,y,z}]
returns the shear strain tensor
    components for the coupled displacement field {u,v,w},
in {x, y, z} coordinates."
shearStrainsFromUVW[{u,v,w}, {x,y,z}]
returns the shear strain tensor
    components for the coupled displacement field {u,v,w},
in {x, y, z} coordinates.

shearStrainsFromUVW[{u_, v_, w_}, {x_, y_, z_}] :=
  {D[u, y] + D[v, x], D[v, z] + D[w, y], D[w, x] + D[u, z]} / 2

```

equilibriumPart

```

Clear[equilibriumPart];
equilibriumPart::usage = "equilibriumPart[uvw, {x,y,z}, v]
return the part of uvw in x,y,z that
    satisfies equilibrium equation for Poisson's ratio v."

equilibriumPart[uvw, {x,y,z}, v]
return the part of uvw in x,y,z that
    satisfies equilibrium equation for Poisson's ratio v.

equilibriumPart[uvw_, {x_, y_, z_}, v_ : v] := Module[{sol},
  sol = Select[SolveAlways[Thread[
    (D[#[[1]], x] + D[#[[2]], y] + D[#[[3]], z]) & /@ stressesFromUVW[uvw,
    {x, y, z}, v] == 0], xyz], Not[MemberQ[#, v -> aaa_]] &] // Flatten;
  Simplify[uvw /. sol]
]

equilibriumPart[uvw_] := equilibriumPart[uvw, {x, y, z}]

```

shearStrainsFromUVW

```

shearStrainsFromUVW[uvw_List, {x_, y_, z_}] := Simplify[{D[#[[1]], y] + D[#[[2]], x],
  D[#[[2]], z] + D[#[[3]], y],
  D[#[[3]], x] + D[#[[1]], z]} & uvw]

shearStrainsFromUVW[uvw_] := shearStrainsFromUVW[uvw, {x, y, z}]

shearStrainsFromUVW[uvw_?MatrixQ] := shearStrainsFromUVW[#, {x, y, z}] & /@ uvw

```

strainsFromUVW

```

Clear[strainsFromUVW];
strainsFromUVW::usage = "strainsFromUVW[uvw, xyz]
returns the strain tensor
    associated with the coupled displacement field {u,v,w},
in {x, y, z} coordinates."
strainsFromUVW[uvw_?VectorQ, xyz_?VectorQ] := Module[{deformationGradient},
    deformationGradient = Outer[D, uvw, xyz];
    Simplify[(deformationGradient + Transpose[deformationGradient]) / 2]
]
strainsFromUVWUVW[uvw, xyz]
returns the strain tensor
    associated with the coupled displacement field {u,v,w},
in {x, y, z} coordinates.

strainsFromUVW[uvw_] := strainsFromUVW[uvw, xyz]

strainsFromUVW[uvws_?MatrixQ, xyz_?VectorQ] := strainsFromUVW[#, xyz] & /@uvws

```

stressesFromUVW

```

Clear[stressesFromUVW];

stressesFromUVW::usage = "stressesFromUVW[uvw, xyz, v, mu]
returns the stress tensor for shear modulus  $\mu$  (optional parameter unity) and
    Poisson's ratio  $\nu$  associated with the coupled displacement field {u,v,w},
in {x, y, z} coordinates."

stressesFromUVW[uvw_, xyz_, v_, mu_: 1] := Module[ $\left\{\lambda = 2 \mu * \frac{\nu}{(1 - 2 \nu)}\right.$ , strainTensor},

    strainTensor = strainsFromUVW[uvw, xyz];

    Simplify[ $\left((\text{Sum}[\text{strainTensor}[[i, i]], \{i, 3\}]) * \lambda * \text{IdentityMatrix}[3] + 2 \mu \text{strainTensor}\right)$ 
]

stressesFromUVW[uvw, xyz, v, mu]
returns the stress tensor for shear modulus  $\mu$  (optional parameter unity) and
    Poisson's ratio  $\nu$  associated with the coupled displacement field {u,v,w},
in {x, y, z} coordinates.

stressesFromUVW[uvw_, xyz_] := stressesFromUVW[uvw, xyz, v]

stressesFromUVW[uvw_?VectorQ] := stressesFromUVW[uvw, {x, y, z}]

stressesFromUVW[uvw_?MatrixQ] := stressesFromUVW /@ uvw

stressesFromUVW[uvw_] := stressesFromUVW /@ Partition[Flatten[uvw], 3]

```

equilibriumQ

```
Clear[equilibriumQ];
equilibriumQ::usage = "equilibriumQ[{u,v,w}, {x, y, z}, v] returns True if the coupled displacement field {u,v,w}, in {x, y, z} coordinates satisfy equilibrium for (optional parameter) Poisson's ratio v."

equilibriumQ[uvw_?VectorQ, {x_, y_, z_}, v_:v] := And@@Thread[
  (D[#[[1]], x] + D[#[[2]], y] + D[#[[3]], z]) & /@
  stressesFromUVW[uvw, {x, y, z}, v] == 0]
equilibriumQ[{u,v,w}, {x, y, z}, v]
  returns True if the coupled displacement field {u,v,w},
  in {x, y, z} coordinates satisfy equilibrium for
  (optional parameter) Poisson's ratio v.

equilibriumQ[uvw_?VectorQ] := equilibriumQ[uvw, {x, y, z}]

equilibriumQ[uvw_?MatrixQ] := And@@(equilibriumQ[#, {x, y, z}] & /@ uvw)
equilibriumQ[uvw_] := equilibriumQ[Partition[Flatten[uvw], 3]]
```

termCount

```
Clear[termList];
termList::usage = "termList[x]
  returns the list of parameters in x."
termList[x_] := Cases[
  Flatten[
    x /. Thread[{Power, Times, Plus} → List]], a_[b_] // Union
termList[x]
  returns the list of parameters in x.

Clear[termCount];
termCount::usage = "termCount[x] returns the number of parameters in x."
termCount[x_] := termList[x] // Length
termCount[x] returns the number of parameters in x.
```

Calculations

polynomials

```
linearTerms = Flatten[{1, xyz}]
{1, x, y, z}
```

```

poly2 = (List @@ Expand[ (Plus @@ linearTerms) ^ 2] ) /. c_Integer *  $\alpha$ _  $\rightarrow$   $\alpha$ 
{1, x, x2, y, x y, y2, z, x z, y z, z2}

quadraticTerms = Complement[poly2, linearTerms]
{x2, x y, y2, x z, y z, z2}

poly3 = (List @@ Expand[ (Plus @@ linearTerms) ^ 3] ) /. c_Integer *  $\alpha$ _  $\rightarrow$   $\alpha$ 
{1, x, x2, x3, y, x y, x2 y, y2, x y2, y3, z, x z, x2 z, y z, x y z, y2 z, z2, x z2, y z2, z3}

cubicTerms = Complement[poly3, poly2]
{x3, x2 y, x y2, y3, x2 z, x y z, y2 z, x z2, y z2, z3}

poly = Flatten[{linearTerms, quadraticTerms, cubicTerms}]
{1, x, y, z, x2, x y, y2, x z, y z, z2, x3, x2 y, x y2, y3, x2 z, x y z, y2 z, x z2, y z2, z3}

u = poly.Array[a, Length[poly]]; TeXForm[u]
Full cubic representation:

v = u /. {a  $\rightarrow$  b, x  $\rightarrow$  y, y  $\rightarrow$  z, z  $\rightarrow$  x};
w = v /. {b  $\rightarrow$  c, x  $\rightarrow$  y, y  $\rightarrow$  z, z  $\rightarrow$  x};
uvw = {u, v, w};
vxyz = {v, x, y, z};

linearModes

uvwLinearTerms = uvw /. a_[b_ /; b > 4]  $\rightarrow$  0
{a[1] + x a[2] + y a[3] + z a[4], b[1] + y b[2] + z b[3] + x b[4], c[1] + z c[2] + x c[3] + y c[4]}

all terms are significant

varLinear = uvwLinearTerms // termList
{a[1], a[2], a[3], a[4], b[1], b[2], b[3], b[4], c[1], c[2], c[3], c[4]}

linearModes = Evaluate[ToExpression[StringJoin["mode", #]] & /@
  (ToString /@ Range[Length[varLinear]])] = (uvwLinearTerms /. #) & /@
  (Thread[varLinear  $\rightarrow$  #] & /@ IdentityMatrix[Length[varLinear]])
TeXForm[linearModes // Transpose]

quadraticModes

uvwQuadratic = uvw /. a_[b_ /; (b < 5 || b > 10)]  $\rightarrow$  0
uvwQuadraticEquilibrium = equilibriumPart[uvwQuadratic]

```

```

{ $x^2 a[5] + y^2 a[7] + y z a[9] + z^2 a[10] +$ 
 $x y (4 (-1 + \nu) b[5] + (-2 + 4 \nu) b[7] - 2 b[10] + 4 \nu b[10] - c[8]) -$ 
 $x z (b[6] + 2 (-2 (-1 + \nu) c[5] - (-1 + 2 \nu) (c[7] + c[10]))) + y^2 b[5] + y z b[6] + z^2 b[7] +$ 
 $x z b[9] + x^2 b[10] + x y (4 (-1 + \nu) a[5] + (-2 + 4 \nu) a[7] - 2 a[10] + 4 \nu a[10] - c[6]),$ 
 $z^2 c[5] + x z c[6] + x^2 c[7] + y z c[8] + x y c[9] + y^2 c[10]$ }

(uvwQuadraticEquilibrium[[1]] // Expand) // TeXForm

(uvwQuadraticEquilibrium[[2]] // Expand) // TeXForm

(uvwQuadraticEquilibrium[[3]] // Expand) // TeXForm

oQuadratic = stressesFromUVW[uvwQuadraticEquilibrium, xyz,  $\nu$ ]

```

shear free terms

impose zero shear

```

zeroShearQuadraticSol = Select[
  SolveAlways[Thread[shearStrainsFromUVW[uvwQuadraticEquilibrium] == 0], xyz],
  Not[MemberQ[#,  $\nu \rightarrow$  aaa_]] &] // Flatten

zeroShearQuadraticTerms = uvwQuadraticEquilibrium //. zeroShearQuadraticSol

vars = termList[zeroShearQuadraticTerms]
{a[5], a[10], b[5], b[7], c[5], c[10]}

quadraticModes = Simplify[
  Evaluate[ToExpression[StringJoin["mode", #]] & /@ (ToString /@ Range[13, 18])] =
    (zeroShearQuadraticTerms //. #) & /@
    (Thread[vars  $\rightarrow$  #] & /@ IdentityMatrix[Length[vars]])
]

equilibriumQ[quadraticModes]

True

shearStrainsFromUVW[quadraticModes] // Simplify
{{0, 0, 0}, {0, 0, 0}, {0, 0, 0}, {0, 0, 0}, {0, 0, 0}, {0, 0, 0}}

MatrixForm /@ (strainsFromUVW[quadraticModes] // Simplify)

```

cubicModes

```

cubic
Modes

uvwCubic = uvw /. a_[b_ /; (b < 11)]  $\rightarrow$  0

uvwCubicEquilibrium = uvwCubic // equilibriumPart

```

```

σCubicEquilibrium = uvwCubicEquilibrium // stressesFromUVW

xx = σCubicEquilibrium[[1, 1]]

var = termList[Coefficient[xx, x * y]] // First
a[12]

rule1 =
  Solve[Coefficient[xx, x * y] == 1, termList[Coefficient[xx, x * y]] // First] // Flatten

$$\left\{ a[12] \rightarrow \frac{1}{4} (1 + 4 \vee b[15] + 4 \vee b[17] + 12 \vee b[20]) \right\}$$


rule2 = Thread[(FullSimplify[xx //. rule1] // termList) → 0]
Simplify[xx //. rule1 //. rule2]
x y

rule3 = Thread[(Simplify[σCubicEquilibrium //. rule1 //. rule2] // termList) → 0]
σCubicEquilibrium //. rule1 //. rule2 //. rule3
sf1 = uvwCubicEquilibrium //. rule1 //. rule2 //. rule3
mode19 = sf1
mode20 = {#[[1]], #[[3]], #[[2]]} &[mode19 /. {y → z, z → y}]
equilibriumQ[{mode19, mode20}]
True

{mode21, mode22} = {mode19, mode20} // nextMode
{mode23, mode24} = {mode21, mode22} // nextMode
shearForceModes = {{mode19, mode20}, {mode21, mode22}, {mode23, mode24}}
MatrixForm /@ stressesFromUVW[shearForceModes]
shearForceModes // dilatation // Flatten
allModes = ToExpression[StringJoin["mode", ToString[#]]] & /@ Range[24]
pureBendingModes = Take[Drop[allModes, 12], 6]
TeXForm[MatrixForm /@ (Transpose /@ Partition[pureBendingModes, 2])]
shearForceModes // Transpose // MatrixForm // TeXForm
cubicModes = Flatten[shearForceModes, 1]
allModes

```

Element

```
nodes = {{0, 1, 0}, {0, 0, 0}, {1, 0, 0}, {1.202715965606913`, 1.314215366298273`, 0},
{0, 1.368066309144244`, 1.305989793327691`},
{0, 0, 1}, {1.216079880285841`, 0, 1.23925741120344`},
{1.597930989278036`, 1.90818293399255`, 1.7411801057262242`}}
```

bMatrix

```
bMatrix = BMatrix3D[allModes, xyz]
```

$$\left\{ \left\{ 0, 1, 0, 0, 0, 0, 0, 0, 0, 0, 0, 0, 0, 2x, 0, y \left(4(1-\nu) + 4(-1+\nu) - \frac{2(1-\nu)}{\nu} \right), \right. \right.$$

$$2y, -2z \left(-2(-1+\nu) - \frac{(1-\nu)(-1+2\nu)}{\nu} \right), 2z, \frac{xy}{2}, \frac{xz}{2}, -\frac{yz}{2}, 0, 0, -\frac{yz}{2} \left. \right\},$$

$$\left\{ 0, 0, 0, 0, 0, 0, 1, 0, 0, 0, 0, 0, 0, 0, x \left(4(-1+\nu) + \frac{(1-\nu)(-2+4\nu)}{\nu} \right), \right.$$

$$2x, 2y, 0, 0, -2z, 0, -\frac{xz}{2}, \frac{yz}{2}, \frac{xy}{2}, -\frac{xz}{2}, 0 \left. \right\},$$

$$\left\{ 0, 0, 0, 0, 0, 0, 0, 0, 0, 0, 1, 0, 0, 0, -2x, 0, -2y, 2z, 0, -\frac{xy}{2}, 0, 0, -\frac{xy}{2}, \frac{xz}{2}, \frac{yz}{2} \right\},$$

$$\left\{ 0, 0, 1, 0, 0, 0, 0, 0, 1, 0, 0, 0, 0, 0, \frac{2y(1-\nu)}{\nu} + y \left(4(-1+\nu) + \frac{(1-\nu)(-2+4\nu)}{\nu} \right), \right.$$

$$0, x \left(4(1-\nu) + 4(-1+\nu) - \frac{2(1-\nu)}{\nu} \right) + \frac{2x(1-\nu)}{\nu}, 0, 0, 0, \frac{x^2}{4} - \frac{y^2}{4}, -\frac{yz}{2},$$

$$-\frac{xz}{2}, -\frac{x^2}{4} + \frac{y^2}{4}, -\frac{yz}{2}, -\frac{xz}{2} \left. \right\}, \left\{ 0, 0, 0, 0, 0, 0, 1, 0, 0, 0, 0, 1, 0, 0, 0, \right.$$

$$0, 0, 0, -\frac{xz}{2}, -\frac{xy}{2}, \frac{y^2}{4} - \frac{z^2}{4}, -\frac{xz}{2}, -\frac{xy}{2}, -\frac{y^2}{4} + \frac{z^2}{4} \left. \right\}, \left\{ 0, 0, 0, 1, 0, 0, 0, \right.$$

$$0, 0, 0, 1, 0, 0, 0, 0, 0, \frac{2x(1-\nu)}{\nu} - 2x \left(-2(-1+\nu) - \frac{(1-\nu)(-1+2\nu)}{\nu} \right),$$

$$0, -\frac{yz}{2}, \frac{x^2}{4} - \frac{z^2}{4}, -\frac{xy}{2}, -\frac{yz}{2}, -\frac{x^2}{4} + \frac{z^2}{4}, -\frac{xy}{2} \left. \right\} \left. \right\}$$

```
bMatrix1 = BMatrix3D[linearModes, xyz]
```

```
bMatrix2 = BMatrix3D[quadraticModes, xyz]
```

```
bMatrix3 = BMatrix3D[cubicModes, xyz]
```

```
TeXForm[bMatrix1]
```

```
TeXForm[bMatrix2]
```

```
TeXForm[bMatrix3]
```

```
d = DMatrix3D[\nu]
```

```
TeXForm[d]
```

```
bTdb = Expand[Transpose[bMatrix].(d.bMatrix)];
```

develop stiffness integration

```
bTdb[[24, 24]]
```

$$\frac{x^2 y^2}{4} + \frac{y^4}{16} + \frac{x^2 z^2}{4} - \frac{y^2 z^2}{8} + \frac{z^4}{16} - \frac{y^2 z^2 \sqrt{v}}{1-2\sqrt{v}} - \frac{y^2 z^2}{-1+2\sqrt{v}} + \frac{y^2 z^2 \sqrt{v}}{-1+2\sqrt{v}}$$

```
elementVolume = 2.2234367654359333`
```

```
2.22344
```

```
quarticRule = Thread[
```

```
{x^4, x^3 y, x^2 y^2, x y^3, y^4, x^3 z, x^2 y z, x y^2 z, y^3 z, x^2 z^2, x y z^2, y^2 z^2, x z^3, y z^3, z^4} ->
{1.4692184020676273`, 1.3008258816213933`, 1.391055637976948`,
1.684639189614494`, 2.4153018320293618`, 1.2184569407424475`,
1.1425465853282244`, 1.3145355635675942`, 1.836793786704385`,
1.2162187222826766`, 1.2267934933996645`, 1.6271444555393084`,
1.3793529251241945`, 1.6108494493895607`, 1.8779826716598929`} / elementVolume]
```

```
cubicRule =
```

```
Thread[{x^3, x^2 y, x y^2, y^3, x^2 z, x y z, y^2 z, x z^2, y z^2, z^3} -> {1.375724277679978`,
1.2353866617421558`, 1.3997396270453801`, 1.9729269721181257`,
1.1595858030999338`, 1.13712469543483`, 1.517503755878869`,
1.2319095628467431`, 1.4249475541728107`, 1.6467759711183976`} / elementVolume]
```

```
quadraticRule = Thread[{x^2, x y, y^2, x z, y z, z^2} ->
```

```
{1.3762442046785648`, 1.298072609873346`, 1.7342150490206258`,
1.2225410787060726`, 1.3953906401333516`, 1.5473082043008088`} / elementVolume]
```

```
{x^2 -> 0.618972, x y -> 0.583814, y^2 -> 0.77997,
x z -> 0.549843, y z -> 0.627583, z^2 -> 0.695908}
```

```
linearRule = Thread[{1, x, y, z} -> {2.2234367654359333`, 1.539118468423933`,
1.7184382389677864`, 1.6300687226378585`} / elementVolume]
```

```
{1 -> 1., x -> 0.692225, y -> 0.772875, z -> 0.73313}
```

```
elementStiffnessMatrix =
```

```
((bTdb /. {v -> .25}) /. quarticRule) /. cubicRule) /. quadraticRule) /. linearRule
```

```
Eigenvalues[elementStiffnessMatrix] // Chop
```

```

\qss\ Partition[
  {146.7163746154547`, 67.79126237448892`, 18.30397222748412`, 9.526653215400222`,
    2.884077252692104`, 2.2953305015127063`, 2.1952773520088753`,
    2.045200439968091`, 1.0807298108717698`, 0.7959409439230846`,
    0.5105533728254921`, 0.504974298301407`, 0.3898058307950653`,
    0.1489659214262449`, 0.1329884704859719`, 0.07284627783297316`,
    0.06197070216079959`, 0.05148260334446004`, 0, 0, 0, 0, 0, 0}, 6] // TeXForm
\qss\TeXForm
\left(
\begin{array}{cccccc}
146.716 & \& 67.7913 & \& 18.304 & \& \\
9.52665 & \& 2.88408 & \& 2.29533 & & \\
\\
2.19528 & \& 2.0452 & \& 1.08073 & \& \\
0.795941 & \& 0.510553 & \& & & \\
0.504974 & & & & & & \\
0.389806 & \& 0.148966 & \& 0.132988 & & \\
& \& 0.0728463 & \& 0.0619707 & \& \\
0.0514826 & & & & & & \\
0 & \& 0 & \& 0 & \& 0 & \& 0 & \& 0 & \& 0 & \& 0 & \& 0 & \\
\end{array}
\right)

```

WHAT IS CLAIMED IS:

1. A computer-implemented method comprising:
performing three-dimensional mechanical analysis for finite element analysis based on indefinite integral determined algebraically, and based on Poisson's ratio dependent shape functions satisfying equilibrium throughout a finite element.
2. The method of claim 1, wherein the finite element includes a three-dimensional brick element.
3. The method of claim 1, wherein performing the three-dimensional mechanical analysis comprises:
constructing locking-free, three-dimensional brick elements, including deriving cubic polynomials dependent upon Poisson's ratio(s) in the physical (x, y, z) coordinates for a plurality of twenty four Rayleigh modes.

ABSTRACT

disclosed herein are methods, procedures, systems, devices, products, and other implementations, including a computer-implemented method that includes performing three-dimensional mechanical analysis for finite element analysis based on indefinite integral determined algebraically, and based on Poisson's ratio dependent shape functions satisfying equilibrium throughout a finite element. In some embodiments, the finite element includes a three-dimensional brick element.

Electronic Patent Application Fee Transmittal

Application Number:

Filing Date:

Title of Invention:

MECHANICAL ANALYSIS WITH HIGH ACCURACY THREE-DIMENSIONAL FINITE ELEMENTS

First Named Inventor/Applicant Name:

Gautam Dasgupta

Filer:

Ido Rabinovitch./Leslie Miller

Attorney Docket Number:

10065-509P01US

Filed as Large Entity

Provisional Filing Fees

Description

Fee Code

Quantity

Amount

**Sub-Total in
USD(\$)**

Basic Filing:

Provisional Application Filing

1005

1

260

260

Pages:

Claims:

Miscellaneous-Filing:

Petition:

Patent-Appeals-and-Interference:

Post-Allowance-and-Post-Issuance:

Extension-of-Time:

Description	Fee Code	Quantity	Amount	Sub-Total in USD(\$)
Miscellaneous:				
Total in USD (\$)				260

Electronic Acknowledgement Receipt

EFS ID:	16829491
Application Number:	61876658
International Application Number:	
Confirmation Number:	4908
Title of Invention:	MECHANICAL ANALYSIS WITH HIGH ACCURACY THREE-DIMENSIONAL FINITE ELEMENTS
First Named Inventor/Applicant Name:	Gautam Dasgupta
Customer Number:	97218
Filer:	Ido Rabinovitch./Leslie Miller
Filer Authorized By:	Ido Rabinovitch.
Attorney Docket Number:	10065-509P01US
Receipt Date:	11-SEP-2013
Filing Date:	
Time Stamp:	19:06:52
Application Type:	Provisional

Payment information:

Submitted with Payment	yes
Payment Type	Credit Card
Payment was successfully received in RAM	\$260
RAM confirmation Number	6315
Deposit Account	
Authorized User	

File Listing:

Document Number	Document Description	File Name	File Size(Bytes)/ Message Digest	Multi Part /.zip	Pages (if appl.)
-----------------	----------------------	-----------	----------------------------------	------------------	------------------

1	Application Data Sheet	10065-509P01US_ADS.pdf	1504893 fa369a58732bbe84b92f82962ed6e3ce6e25f253	no	6
Warnings:					
Information:					
2	Specification	10065-509P01US_APPL.pdf	967550 6e74847564380ec919da91ddd7f4eb4a53cfc8bd	no	96
Warnings:					
Information:					
3	Fee Worksheet (SB06)	fee-info.pdf	29808 24bfeb21bfe4388cfb7f24530f8e27d658e65615	no	2
Warnings:					
Information:					
Total Files Size (in bytes):			2502251		
<p>This Acknowledgement Receipt evidences receipt on the noted date by the USPTO of the indicated documents, characterized by the applicant, and including page counts, where applicable. It serves as evidence of receipt similar to a Post Card, as described in MPEP 503.</p> <p><u>New Applications Under 35 U.S.C. 111</u> If a new application is being filed and the application includes the necessary components for a filing date (see 37 CFR 1.53(b)-(d) and MPEP 506), a Filing Receipt (37 CFR 1.54) will be issued in due course and the date shown on this Acknowledgement Receipt will establish the filing date of the application.</p> <p><u>National Stage of an International Application under 35 U.S.C. 371</u> If a timely submission to enter the national stage of an international application is compliant with the conditions of 35 U.S.C. 371 and other applicable requirements a Form PCT/DO/EO/903 indicating acceptance of the application as a national stage submission under 35 U.S.C. 371 will be issued in addition to the Filing Receipt, in due course.</p> <p><u>New International Application Filed with the USPTO as a Receiving Office</u> If a new international application is being filed and the international application includes the necessary components for an international filing date (see PCT Article 11 and MPEP 1810), a Notification of the International Application Number and of the International Filing Date (Form PCT/RO/105) will be issued in due course, subject to prescriptions concerning national security, and the date shown on this Acknowledgement Receipt will establish the international filing date of the application.</p>					

Document code: WFEE

United States Patent and Trademark Office
Sales Receipt for Accounting Date: 10/01/2013

CCETIN	SALE	#00000016	Mailroom Dt:	09/11/2013	61876658
		01	FC : 2005	130.00	OP

Document code: WFEE

United States Patent and Trademark Office
Sales Receipt for Accounting Date: 10/01/2013

CCETIN	ADJ #00000003	Mailroom Dt: 09/11/2013	
	Seq No: 6315	Sales Acctg Dt: 09/12/2013	61876658
	01 FC : 1005	-260.00	OP